

DEVELOPMENT OF SOY-BASED BIODEGRADABLE FIBERS AND RESINS
FOR SOIL STABILIZATION AND CROP PROTECTION

A Thesis

Presented to the Faculty of the Graduate School
of Cornell University

In Partial Fulfillment of the Requirements for the Degree of
Master of Science

by

Senthil Kumar Lingamoorthy

May 2010

© 2010 Senthil Kumar Lingamoorthy

ABSTRACT

The primary objective of this research was to develop fully biodegradable and environment-friendly fibers from soy flour (SF), a by-product of the soy bean crushing process, for soil stabilization and crop protection. Soybean crop is grown abundantly in USA and other parts of the world. SF is biodegradable and during degradation it also fertilizes the soil naturally. In this research extruded SF fibers containing desired chemicals were used to form a mat that will protect the crops, prevent soil erosion and fertilize the soil, thus creating a novel 'green' technology.

Unmodified SF-based fibers showed tensile stress of 2.25 MPa, tensile strain of 2.4% and Young's modulus of 172.69 MPa. Various types of cross-linking agents like glyoxal, glutaraldehyde, rutin and quercetin (a polyphenol occurring in plants), thickening agents like agar agar and guar gum and forms of cellulose like Cellulo[®], micro-fibrillated cellulose and micro-crystalline cellulose were added to SF fibers to improve their mechanical properties, reduce moisture sensitivity and improve durability under normal environmental conditions such as rain. SF fibers biodegrade naturally to provide nutrients to the soil helping plant growth. The physical and mechanical properties of the SF fibers were characterized using appropriate ASTM standards. Field trials indicate that the SF-based fibers are completely biodegradable and SF-based resins performed satisfactorily in comparison with commercially available hydromulch for soil stabilization. One of the main objectives was to find cross linking agents which are environment-friendly and to use them in improving the mechanical characteristics of SF fibers. Compost studies, FTIR spectroscopy and SDS-PAGE analysis indicate that cross-linking has taken place due to reaction of rutin and quercetin with polypeptide chains in soy protein.

BIOGRAPHICAL SKETCH

Senthil Kumar Lingamoorthy was born on November 11th 1985, in Fertilizer City (Karimnagar district) in Andhra Pradesh, India. After completing his high school he enrolled in University of Mumbai Institute of Chemical Technology (UICET) and he graduated with Bachelor of Technology in Chemical Technology of Fiber and Textile in May 2007. After completing his Bachelor of Technology degree he was admitted to Cornell University in Fiber Science program in August 2007 under the guidance of Professor Anil Netravali.

Dedicated to my family and friends

ACKNOWLEDGMENTS

First of all I would like to thank Professor Anil N. Netravali for his constant inspiration and guidance towards completing my graduate study at Cornell University. I would also like to thank Professor Michael Hoffmann for his valuable support during my research work.

I am also grateful to Jeffrey Gardner, Sylvie Pitcher and Kyle Dumont for their effort and support during this research project. I would like to thank all my colleagues at Fiber Science and Apparel Design for providing friendly atmosphere during my stay. I would like to thank the staff of Fiber Science and Apparel Design for their administrative help throughout my studies. Special thanks to Dr. Jagdish Tewari for training me on various instruments for my research. I would like to acknowledge Simona Despa and Shamil Sadigov for their help in statistical analysis. I would also like to thank Dr. Cynthia Kinsland for help in SDS-PAGE analysis and Dr. Ann Piombino for help in nitrogen content analysis.

TABLE OF CONTENTS

Biographical Sketch.....	iii
Dedication.....	iv
Acknowledgements.....	v
List of Figures.....	ix
List of Tables.....	xiii
Chapter 1. Introduction.....	1
1.1 Biodegradable Fibers for Crop Protection and Prevention of Soil Erosion.....	1
1.2 Objective and Potential Applications.....	4
Chapter 2. Literature Review.....	6
2.1 Soy Protein.....	6
2.2 Structure and Composition.....	8
2.3 Modification of Soy Protein.....	10
2.4 Use of Plant Phenolics as Eco-friendly Cross-linking Agents.....	15
2.5 Use of Fibers and Textiles for Soil Stabilization.....	18
Chapter 3. Experimental Procedures.....	22
3.1 Materials.....	22
3.2 Soy Protein Pre-curing Process.....	23
3.3 Extrusion Setup and Process.....	23
3.4 Processing of Soy Protein Resin Films.....	27
3.5 Characterization of Soy Flour Fibers.....	27
3.6 Characterization of Soy Protein Film.....	29
3.7 Evaluation of Biodegradability of Soy Flour.....	30

3.7.1 Resin Preparation.....	32
3.7.2 Resin Composting Studies.....	32
3.7.3 Attenuated Total Reflectance-Fourier Transform Infra Red (ATR-FTIR) Characterization.....	33
3.8 Field Trials.....	33
3.8.1 Preliminary Field Trials to Evaluate Soil Stabilization Effect of SF Fiber Mats.....	33
3.8.2 Greenhouse Trials for Evaluation of Shrinkage Characteristics of SF Fiber Mats.....	35
3.8.3 Field Trials for Evaluation of SF Resin on Seed Germination and Weed Suppression.....	36
3.8.4 Greenhouse Trials for Evaluation of SF Resin on Seed Germination....	39
3.9 Soy Protein Resin Film Production Process with Eco-Friendly Cross-linking Agents.....	41
3.10 Characterization of Cross-linked Resin with Eco-Friendly Cross-linking Agents.....	43
3.10.1 Characterization of Tensile Properties.....	43
3.10.2 SDS-PAGE Analysis.....	43
Chapter 4. Results and Discussion.....	46
4.1 Fiber Characterization.....	46
4.1.1 Effect of Glycerol Content on SF-based Fibers.....	46
4.1.2 Effect of Cellulo [®] Content on SF-based Fibers.....	48
4.1.3 Effect of Fitz Milled Grand Prairie (FMGP) Content on SF-based Fibers.....	50

4.1.4 Effect of Micro-crystalline cellulose (MCC) Content on SF-based Fibers.....	52
4.1.5 Effect of Micro-fibrillated Cellulose (MFC) Content on SF-based Fibers.....	54
4.1.6 Effect of NB416 Fitz Milled Fiberized Cellulose Derivative (NB416) Content on SF-based Fibers.....	57
4.1.7 Effect of Phytigel, Agar agar and Guar gum on SF-based Fibers.....	58
4.2 Field Trials Evaluation.....	60
4.2.1 Preliminary Field Trials to Evaluate Soil Stabilization Effect of SF Fiber Mats	60
4.2.2 Greenhouse Trials for Evaluation of Shrinkage of SF-based Fiber Mats.....	62
4.2.3 Field Trials for Evaluation of SF-based Resin on Seed Germination and Soil Stabilization.....	69
4.2.4 Greenhouse Trials for Evaluation of SF Resin on Seed Germination.....	77
4.3 Characterization of Cross-linked Resin with Eco-Friendly Cross-linking agents.....	81
4.3.1 Tensile Properties.....	81
4.3.2 SDS-PAGE Analysis.....	82
4.4 Evaluation of Biodegradability of Soy Flour Resins.....	87
4.4.1 Weight Loss of SF-based Resin Films	87
4.4.2 ATR-FTIR Characterization	90
Chapter 5. Conclusions.....	93
References.....	95

LIST OF FIGURES

Figure 2.1 Reactions of a phenolic acid with amino side chains of polypeptides.....	17
Figure 3.1 Lab scale extrusion gun.....	24
Figure 3.2 Extrusion plate with pipette tips.....	25
Figure 3.3 SEM images of (a) MCC particle; (b) MFC fibrils in aggregated form; (c) FMGP fibrils and (d) NB416 fibrils.....	26
Figure 3.4 Paper tab for Instron testing of SF-based fibers.....	28
Figure 3.5 Typical stress-strain plot of SF-based fiber.....	29
Figure 3.6 Experimental setup for rutin and quercetin cross-linked resin preparation.....	31
Figure 3.7 Design of field trials.....	38
Figure 3.8 Design of greenhouse trials.....	40
Figure 4.1 Mean and standard deviation of tensile stress, tensile strain and Young's modulus values of SF-based fibers modified with glycerol.....	47
Figure 4.2 Mean and standard deviation of tensile stress, tensile strain and Young's modulus values of SF-based fibers modified with Cellulo [®]	49
Figure 4.3 Mean and standard deviation of tensile stress, tensile strain and Young's modulus values of SF-based fibers modified with FMGP.....	51
Figure 4.4 Mean and standard deviation of tensile stress, tensile strain and modulus values of SF-based fibers modified with MCC.....	53
Figure 4.5 Mean and standard deviation of tensile stress and tensile strain values of SF-based fibers with MFC.....	56
Figure 4.6 Mean and standard deviation of modulus values of SF-based fibers modified with MFC.....	56
Figure 4.7 Mean and standard deviation of tensile stress, tensile strain and Young's modulus values of SF-based fibers modified with NB416.....	57

Figure 4.8 Mean and standard deviation of tensile stress, tensile strain and Young's modulus values of SF-based fibers modified with Phytigel [®] , agar agar and guar gum.....	59
Figure 4.9 Results of Tukey-Kramer test for comparison of treatment means of ryegrass count.....	61
Figure 4.10 Results of Tukey-Kramer test for comparison of shrinkage means.....	62
Figure 4.11 Photographic images of micro-plots of Control treatment on (a) day 1 just after extrusion; (b) week 1, dry condition; (c) week 4, dry condition; (d) week 5, wet condition; (e) week 6, wet condition and (f) week 7, wet condition.....	64
Figure 4.12 Photographic images of micro-plots with GA formulation on (a) day 1 just after extrusion; (b) week 1, dry condition; (c) week 4, dry condition; (d) week 5, wet condition; (e) week 6, wet condition and (f) week 7, wet condition.....	65
Figure 4.13 Photographic images of micro-plots with GL formulation on (a) day 1 just after extrusion; (b) week 1, dry condition; (c) week 4, dry condition; (d) week 5, wet condition; (e) week 6, wet condition and (f) week 7, wet condition.....	66
Figure 4.14 'Shrinkage' x 'days' graph of SF-based fibers during field trials	67
Figure 4.15 Arrangement of micro-plots for field trials described in section 3.8.3....	69
Figure 4.16 Photographic images of micro-plots for CONTROL on (a) day 1; (b) day 9 and (c) day 43.....	70
Figure 4.17 Photographic images of micro-plots for soy light (SL) treatment on (a) day 1; (b) day 9 and (c) day 43.....	70
Figure 4.18 Photographic images of micro-plots for hydromulch (HYDRO) treatment on (a) day 1; (b) day 9 and (c) day 43.....	70

Figure 4.19 Photographic images of micro-plots for soy heavy (SH) treatment on (a) day 1; (b) day 9 and (c) day 43.....	71
Figure 4.20 Photographic images of micro-plots for soy seed (SS) treatment on (a) day 1; (b) day 9 and (c) day 43.....	71
Figure 4.21 Plot showing 'shoot count' x 'days' for field trials in section 4.2.3.....	72
Figure 4.22 Tukey HSD results for nitrogen content of grass in field trials	77
Figure 4.23 Image of a greenhouse tray (a typical block) on (a) day 1; (b) day 3 and (c) day 7.....	78
Figure 4.24 Graph showing 'shoot count' x 'days' grouped for each 'treatment' for greenhouse trials in section 4.2.4.....	78
Figure 4.25 Mean and standard deviation of tensile stress, tensile strain and Young's modulus values of cross-linked SF resin using different process conditions	82
Figure 4.26 SDS-PAGE of unmodified soy protein showing molecular weight markers and soy protein profile.....	83
Figure 4.27 SDS-PAGE of unmodified and reacted soy proteins.....	86
Figure 4.28 SDS-PAGE of unmodified and reacted soy proteins.....	86
Figure 4.29 'Weight loss' x 'days' plot of compost specimens.....	87
Figure 4.30 Photographic images of control specimen on (a) day 1; (b) day 30 and (c) day 60 of compost study	88
Figure 4.31 Photographic images of GA specimen on (a) day 1; (b) day 30 and (c) day 60 of compost study	88
Figure 4.32 Photographic images of rutin specimen on (a) day 1; (b) day 30 and (c) day 60 of compost study	88
Figure 4.33 FTIR spectra of control specimens.....	90
Figure 4.34 FTIR spectra of glutaraldehyde cross-linked soy protein resin	

specimens.....91

Figure 4.35 FTIR spectra of rutin cross-linked soy protein resin

specimens.....91

LIST OF TABLES

Table 2.1 Amino acid composition of soybeans.....	10
Table 3.1 Composition of resin used for field trials in 3.8.1.....	34
Table 3.2 Composition of resin used for greenhouse trials in 3.8.2.....	35
Table 3.3 Composition of treatments used for field trials in 3.8.3.....	38
Table 4.1 Moisture contents of SF-based fibers with varying glycerol content	47
Table 4.2 Moisture contents of SF-based fibers with varying Cellulose [®] content	49
Table 4.3 Moisture contents of SF-based fibers with varying FMGP content	51
Table 4.4 Moisture contents of SF-based fibers with varying MCC content	52
Table 4.5 Moisture contents of SF-based fibers with MFC (cured and uncured).....	55
Table 4.6 Moisture contents of SF-based fibers with varying NB416 content.....	58
Table 4.7 Moisture contents of SF-based fibers modified with Phytigel [®] , agar agar and guar gum	59
Table 4.8 Ryegrass seedling establishment as a percentage of number of seeds planted.....	61
Table 4.9 SF-based fiber mat shrinkage as a percent of initial area covered by fibers.....	62
Table 4.10 Fixed effect test from generalized mixed model for field trials	71
Table 4.11 Tukey HSD test results for shoot count difference among treatments	73
Table 4.12 Tukey HSD results for biomass means	74
Table 4.13 Biomass weight data for Field Trials	75
Table 4.14 Carbon %, Nitrogen % and adjusted nitrogen % of grasses from different treatments in field trials.....	76
Table 4.15 Fixed effects result for greenhouse trials.....	79
Table 4.16 Tukey HSD for shoot count among treatments.....	79
Table 4.17 Contents corresponding to lane numbers in Figures 4.26, 4.27 and 4.28...84	

CHAPTER 1

INTRODUCTION

1.1 Biodegradable Fibers for Crop Protection and Prevention of Soil Erosion

The use of petroleum-based polymers, most of which are not biodegradable, has increased significantly in the past few decades. These polymers do not readily degrade in the normal environment and most end up in landfills and marine environment at the end of their life, polluting both land and water ^[1]. The growing concerns about sustainability and environmental pollution have resulted in increased efforts to develop environment-friendly, biodegradable ‘green’ alternatives, in particular, those based on yearly renewable plants ^[2]. Biodegradable polymers, thus, have attracted much attention in recent years. Natural polymers such as cellulose, protein and starch are fully biodegradable, sustainable and environment-friendly, available worldwide and have been used in many applications ^[3-11]. Fully biodegradable composites have been fabricated from soy protein isolate/soy protein concentrate based resins reinforced by natural fibers ^[5, 12].

One of the biggest manifestations of human activity within the biosphere has been the conversion of natural landscapes to highly managed ecosystems like croplands, pastures and urban areas ^[13]. At present, 12% of the total land surface on earth (18 million km²) is under some form of cultivation ^[14]. A significant amount of the land has been over-cultivated, making it unsuitable for further cultivation, e.g., marginal land. About 14 to 15 million km² of global land is in some form of cultivation and about 70 million km² of additional land is in pasture and grassland ^[13]. Enhancement and maintenance of soil productivity is necessary, particularly for the marginal lands, for sustainability of agriculture to meet food needs of the growing population ^[15].

Soil on earth is finite and is slowly losing its fertility. Most of the potential cultivable land has already been brought under cultivation ^[13]. The remaining land is either in inaccessible areas or in ecologically-sensitive areas. In addition, a significant amount of land is lost to urbanization, which is fast expanding. As a result, increase in food production in the future has to come through intensification of cultivation on existing land or by increasing the use of marginal lands. It is also speculated that there may be a decline in cultivable land due to soil degradation and erosion in the future ^[13, 15]. Fertile soils with good physical properties are required for sustainable agriculture, but since 1945, approximately 17% of the vegetated land on earth has undergone soil degradation and loss in productivity, often from poor fertilizer and water management, soil erosion and shortened fallow periods ^[16]. Fallow period is defined as the length of time between short cultivation periods which allows the soil nutrient status to be restored in the field. Continuous cropping and inadequate replacement of nutrients removed in harvested materials result in reduction of soil fertility. That, in turn, reduces the crop yield. Nutrients lost through erosion, leaching or gaseous emissions cause soil organic matter levels to decrease ^[17]. Erosion can be severe on steep slopes where windbreaks are absent or have been cleared, land where vegetative cover is absent during the rainy season and where heavy machinery is involved in land preparation. In some cases, the effects of land degradation on productivity can be compensated for by increased fertilization and irrigation, which increases production costs ^[18].

Soil stabilization, soil rehabilitation and food production are topics of prime importance for the survival of the entire mankind. These topics can be addressed in part by using techniques that involve biodegradable materials rather than petroleum-based non-biodegradable materials that pollute the environment. Plant-based biodegradable fibers and polymers have distinctive advantages in avoiding

environmental pollution as compared to synthetic non-biodegradable materials. However, they also have their drawbacks. Some advantages and disadvantages are listed below:

Advantages:

- Plant-based materials are yearly renewable and provide new avenues for agriculture.
- Most of the plant-based materials are non-toxic and show good moisture regulation and noise and thermal damping ^[19].
- These materials show good mechanical properties on a per weight basis to synthetic non-biodegradable materials and can be improved using further treatments.

Drawbacks:

- The properties of these materials vary from batch to batch leading to high variability in quality which need to be controlled using available technologies.
- The availability of the plant-based materials is based on climate and other factors.
- Plant-based materials exhibit characteristic odors as compared to synthetic materials which can be masked using available technologies.
- For certain plant-based materials, the demand for it as a food material will compete against its use for non-food purposes.

The plant-based materials are still not as cost effective as the traditional petroleum-based materials, but they have gained importance in recent years due to their biodegradable and environment-friendly nature ^[2, 12]. Among various plant-based

materials, use of soy protein has increased as biodegradable resin due to its easy availability and low cost ^[5, 9, 19-24].

Biodegradable fibers like natural and regenerated cellulose fibers, protein fibers, poly (hydroxyalkanoate) (PHA) and poly (lactic acid) fibers have been used to replace petroleum-based non-biodegradable fibers used in today's world ^[25-28]. These fibers provide moderate physical and mechanical properties suitable for various applications. Cellulose fibers have attracted special attention since it is the most abundant biomass material available in nature. Cellulose is a linear molecule and plants organize them into oriented fibrils/fibers that provide excellent mechanical properties. Plant-based fibers are biodegradable, inexpensive and have high mechanical properties and low density ^[12].

Many natural and synthetic biodegradable resins are commercially available at present for fabricating green materials. Some of the common biodegradable polymers available are poly (lactic acid), proteins, starches, polyhydroxyalkanoates and their copolymers, etc. Most of these polymers are obtained either from plant sources or from bacterial fermentation processes and are fully sustainable ^[29].

1.2 Objective and Potential Applications

The primary objective of this research was to develop fully biodegradable and environment-friendly fibers from defatted soy flour (SF), a by-product of the soy bean crushing process, for soil stabilization and crop protection. The soybean crop is grown abundantly in USA and other parts of the world. SF is biodegradable and during degradation it also fertilizes the soil, naturally. SF is obtained after extraction of biodiesel from soybean and not all SF can be used for cattle feed. SF can be used for crop protection and soil stabilization which will in turn help rehabilitate marginal lands thus indirectly contributing to agriculture and food production in future. In the

present research extruded SF-based fibers containing desired additives such as cellulose-based materials in fibrillar form and cross-linking agents have been used to form a fibrous mat with an aim to protect the crops, prevent soil erosion and fertilize the soil, thus creating a novel 'green' technology for such applications. The fiber mats are aimed to be used for weed suppression and crop protection similar to non-biodegradable fibers used currently to protect the crops. Non-biodegradable fibers are difficult to remove once the crops grow as they get entangled with the crops and can cause pollution if not removed. The prospect of using biodegradable fibers for crop protection and weed suppression is attractive as it eliminated the need for removal of these fibers. In fact, as they degrade they provide excellent nutrition to the soil.

Soy protein is extrudable and moldable and therefore, is very convenient for industrial production. However before using soy protein for applications, it has to be modified for improved mechanical and thermal properties and reduced moisture sensitivity. Soy protein itself is brittle with very low toughness. Plasticizers have been used to increase the fracture strain of soy protein, but they decrease the Young's modulus (stiffness) and increase moisture sensitivity. Further research needs to be conducted to improve the mechanical and physical performance of soy protein plastics.

CHAPTER 2

LITERATURE REVIEW

Soybeans and soybean products have been used as the chief source of protein and as a medicine by millions of people for centuries. The food use of soybeans goes back to ancient times, but their history in the western world dates from the 20th century. The demand for soybeans has increased in recent years as markets developed for oil and later for the high-quality soybean meal used as cattle feed ^[30].

2.1 Soy Protein

Soy protein has been used as nutritional ingredient in almost every food category available to the consumer. Soy proteins are more versatile than many other food proteins in various worldwide nutrition programs at present. Advances in technology have resulted in development of soy protein products that can perform functions like emulsification, binding, and giving texture. Acceptance of soy protein has grown because of such functional properties, abundance and low cost ^[30].

Soybean is a legume. The protein content of the seed is around 40%. Defatted soy flakes, obtained after the removal of hulls and oil, contains about 50% protein, and is used as the starting material for most of the commercial protein ingredients. Soy protein products are divided into three major groups. They are defatted soy flour (SF), soy protein concentrate (SPC) and soy protein isolate (SPI). Defatted soy flours are soybeans from which hulls and oils are removed. SPC is defatted flour from which parts of sugars, water and alcohol have been removed. SPI is defatted soy flour from which sugars, other water-soluble materials and cotyledon fibers have been removed ^[30]. SPI contains 90-93% of protein and SPC contains about 70% protein ^[31]. The rest is carbohydrates, minerals, soluble fibers, ash, etc. SF consists of 52-54% protein, 30-

32% carbohydrates, 0.5-1.0% crude free lipid, 2.5-3.5% crude fiber, 2.5-6.0% ash and 6-8% moisture ^[30, 32].

The manufacturing processes for various soy protein fractions are as follows ^[30]. Soybeans entering the processing plant are screened to remove damaged beans and other foreign matter. The oil is then extracted from the flakes by a solvent (hexane) in one of several types of countercurrent extraction systems. Any residual solvent, after the defatted flakes leave the extractor, is removed by heat and vacuum. Soy flours and grits are made by grinding and screening soybean flakes either before or after removal of the oil. SF is the least refined form of soy protein products used for human consumption and vary in fat content, particle size and degree of heat processing. The degree of heat treatment results in varying levels of water dispersibility and enzyme activity qualities that can be useful in tailoring functionality in many applications ^[30].

SPC is prepared from dehulled and defatted soybeans by removing the water-soluble non-protein contents. They contain at least 65% protein (N x 6.25) on a moisture-free basis. The protein content is determined on the basis of nitrogen content and Kjeldahl method is almost universally applied to calculate total nitrogen content. On the basis of early determinations, proteins contained on an average, 16 percent nitrogen which led to use of the calculation $N \times 6.25$ ($1/0.16=6.25$) to convert nitrogen content into protein content ^[33]. SPC is produced by three basic processes; acid leaching (at pH 4.5), extracting with aqueous alcohol (60-90%) and denaturing soy protein with moist heat before extraction with water. SPC with low water-solubility is subjected to heat (jet cooking or steam injection) and mechanical working (homogenization) to increase solubility and functionality ^[30].

SPI is the most highly refined soy protein product available commercially. It represents the major protein fraction of the soybean. SPI is prepared from dehulled and defatted soybeans by removing most of the non-protein content. The protein is

extracted from unheated defatted soy flakes with water or mild alkali at a pH range of 8-9, followed by centrifuging to remove insoluble fibrous residue. The pH of the resulting extract is adjusted to 4.5 where most of the protein precipitates as a curd. The curd is separated by centrifugation from the soluble oligosaccharides, followed by multiple washes. The curd is then spray dried to yield an 'isoelectric' isolate. The isolate is neutralized (Na or K proteinates) to make it more soluble and functional. About 33% of the starting flake weight is recovered in the form of an isolate ^[30].

2.2 Structure and Composition

Soy protein contains 18 different amino acids with some containing carboxyl groups (glutamic acid and aspartic acid) and some containing amino groups (lysine and arginine). The composition of different amino acids in soy protein is listed in Table 2.1. There are other amino acids that contain polar hydroxyl groups (serine, threonine and tyrosine). The amino acids are linked by peptide (amide) bonds to form polypeptide chains. The reactive groups on the amino acids can be exploited to modify soy proteins chemically and improve their tensile properties and moisture resistance. Soy protein has an isoelectric point between pH of 4.5 to 5 and is insoluble in water at the isoelectric point. However, away from the isoelectric point, either in acidic or alkaline direction, the soy protein molecules open up and become more soluble in water. This opening of the molecules allows the reactive groups to be exposed making it easier to access them and chemically modify them ^[29].

Soy protein has mainly four polymer weight fractions called 2S (S stands for Svedberg units), 7S, 11S and 15S which are based on their sedimentation constants. The 7S fraction is also called conglycinin and comprises important enzymes and storage proteins. The 7S fraction is about 30% (w/w) of the total soy protein ^[34]. The 11S fraction comprises about 35% (w/w) of the total soy protein and is usually called

glycinin^[34]. The polar groups in soy protein can be modified to alter its properties^[34]. The soy protein fractions (7 S and 11 S) cross-link through covalent sulfur bonds under oxidative conditions in cysteine residues^[35]. Dehydroalanine, formed from alanine by loss of side chain also react with lysine and cysteine to form lysinoalanine and lanthionine cross-links, respectively^[35, 36]. Asparagines and lysine can also react together to form an amide-type of cross-link. The above mentioned reactions occur during the curing process of soy protein forming a resin of moderate strength^[37, 38]. The soy protein polymer is highly moisture sensitive in nature due to presence of polar groups like amine, amide, carboxyl and hydroxyl groups^[36].

The native proteins have disordered conformations which are caused by tight folding due to covalent bonding such as disulfide bonds. The proteins can be denatured wherein the secondary, tertiary, or quaternary structure of the protein can be dissociated and associated without breaking covalent bonds by allowing disulfide interchange among protein molecules. Protein denaturation can be brought about through changes in pH or heat treatment and is required along with plasticization to provide soy protein-based materials with desired chemical and physical properties^[21, 39].

The resin obtained from pure SPI is very brittle and is inconvenient to process. As a result, external plasticizers such as glycerol and sorbitol have been used to improve the toughness and to make resin more flexible. Glycerol is bound to the protein molecules via weak hydrogen bonds^[4, 5, 40].

Table 2.1 Amino acid composition of soybeans ^[41]

Amino Acid	Composition (g/16 g nitrogen)
Isoleucine	4.54
Leucine	7.78
Lysine	6.38
Methionine	1.26
Cysteine	1.33
Phenylalanine	4.94
Tyrosine	3.14
Threonine	3.86
Tryptophan	1.28
Valine	4.8
Arginine	7.23
Histidine	2.53
Alanine	4.26
Aspartic acid	11.70
Glutamic acid	18.70
Glycine	4.18
Proline	5.49
Serine	5.12

2.3 Modification of Soy Protein

Soy protein has been used as resin for production of biodegradable fibers due to its low cost, environment-friendly manufacturing process and easy availability. As stated earlier soy protein has a highly hygroscopic nature as it contains polar groups

such as amino, hydroxyl and carboxyl groups. During the curing process, polypeptide chains in soy protein can form several types of cross-links such as the disulfide bonds between two cysteine residues, lysinoalanine and lanthionine cross-links by linking lysine with cysteine and the amide type linkage formed by asparagines and lysine ^[19].

Dried pure or modified SPI is, however, very brittle because of its low fracture strain, which makes it inconvenient for further processing. Attempts have been made to overcome the problem of brittleness by adding plasticizers to soy protein resins. Mo and Sun ^[42] used polyol-based plasticizers like glycerol, propylene glycol, 1,2-butanediol and 1,3-butanediol to plasticize the resin. The thermal and mechanical properties and morphology of the plasticized resin were evaluated. It was reported that both glycerol and propylene glycol effectively lowered the glass transition temperature by increasing the free volume in the system. These plasticizers were found to have good compatibility with soy protein because of their small structure and hydrophilic nature ^[42].

Wang *et al.* ^[43] evaluated the plasticizing effects of polyhydric alcohols such as glycerol, ethylene glycol, propylene glycol, 1,3-propanediol and polyethylene glycol. It was concluded that glycerol is the most suitable plasticizer for soy protein resins considering the toxicity of other plasticizing agents ^[43]. Ethylene glycol is classified as a hazardous chemical, while propylene glycol has a low order of toxicity but is volatile ^[44]. Glycerol is non-toxic and was chosen as the plasticizing agent to reduce the brittleness of soy protein resin and improve its toughness, in this study.

Several methods have been developed to improve the mechanical properties and minimize the moisture sensitivity of the soy protein-based materials ^[3, 4, 6, 7, 10, 45-48]. Cross-linking agents, such as glutaraldehyde, glyoxal and formaldehyde, have been used to increase the Young's modulus and fracture stress of soy protein ^[49, 50]. Nano-clay has also been used to fabricate soy protein nano-composites with higher modulus

[50, 51]. Commonly, the toughness decreases with the addition of nano-clay [46, 49]. Enzyme modifications (such as transglutaminase) have shown slight increase in mechanical properties and increase in moisture resistance [52-54]. Soy protein can also be modified by blending it with other biodegradable polymers like polyvinyl alcohol (PVA), starch and gellan and these blends also have shown significant improvements in tensile properties [3, 10, 20, 47, 49].

Rhim *et al.* [11] effectively used the affinity of aldehyde groups towards the amine group of soy protein by producing 'green' plastics from SPI and dialdehyde starch. It was reported that the total soluble matter of the final film reduced by 50% thereby increasing its moisture resistance. Its potential use in packaging and mulching was also stated by authors [11].

Xi *et al.* [55] grafted SPI with styrene to increase the hydrophobicity of the molecule. The resulting polymer has a potential use in drug delivery. The FTIR analysis showed strong absorption peaks at 1113, 696, 618 cm^{-1} wavenumbers, which correspond to polystyrene. Characterization using differential scanning calorimetry (DSC) confirmed the grafting of polystyrene due to resemblance of the glass transition temperature to that of polystyrene [55].

Phytigel[®] has been previously used to modify properties of soy protein [49, 50]. Phytigel[®], also known as Gellan, is an exocellular heteropolysaccharide produced by fermentation [56]. It is produced by the bacterium species known as *Pseudomonas* [56, 57]. Gellan produced from *Sphingomonas paucimobilis* is composed of a linear repeating tetrasaccharide sequence of D-glucose, D-glucuronic acid, and L-rhamnose in the ratio of 2:1:2 [57]. Phytigel[®] forms weak gels in water in the absence of salts, but forms a strong gel in presence of monovalent or divalent ions. Appropriate cations screen the electrostatic repulsion between the carboxylate groups and serve as cross-linking points to cross-link the polysaccharide helix [58, 59]. Intra- and intermolecular

hydrogen bonding can also be formed through the carboxyl and hydroxyl groups. The carboxyl groups on glucuronic acid can also react with the hydroxyl, amine and carboxyl groups present in soy protein under specific conditions. The hydroxyl and carboxyl groups in Phytigel[®] can also form H-bonding with hydrophilic groups in soy protein^[3]. In this research, the solution of Phytigel[®] in water was blended with water-based soy protein resin to form an interpenetrating polymer network (IPN) like structure, a cross-linked complex^[3]. Sperling^[60] has defined IPNs as a combination of two or more polymer networks that are synthesized. IPNs can be formed by several types of multi-component polymer materials, such as a graft copolymer, a block copolymer and a simple polymer blend without any bonding between chains^[60].

Many plant-based fibers possess very good mechanical properties and have been used as reinforcement for composites^[61, 62]. Plant-based cellulose fibers have a fibrillar structure and the cellulose nano-fibrils have excellent mechanical properties due to their high molecular orientation and high amount of crystallinity. Nano-fibrillated cellulose (NFC) has been estimated to have strength between 2 and 10 GPa and Young's modulus of about 140 GPa^[8, 63, 64]. Micro-fibrillated cellulose (MFC) which is made up of NFC also has high strength and modulus. MFC is most commonly obtained by mechanical shearing of cellulose fibers^[63-65]. Composites fabricated using MFC and phenolic resin has showed Young's modulus of 19 GPa^[63]. MFC has also been shown to improve the interfacial adhesion in bamboo composites by preventing the growth of micro-cracks^[65].

Micro-crystalline cellulose (MCC) can be used as a reinforcing agent to increase the strength of soy protein resin. MCC is manufactured from wood and cotton cellulose in large scale quantities^[66]. Capadona *et al.*^[67] have successfully developed polymer nano-composites incorporated with nano-whiskers isolated from MCC. The nano-whiskers obtained from MCC show elastic modulus in the range of 120 to 150

GPa. Due to strong interactive nature of the hydroxyl groups on the surface of MCC, they have a tendency for self association ^[67]. MCC used for experiments in this research have particle dimensions of around 200 μm . Agar agar (agar) is also used as an additive in certain applications. Agar is a strong gelling component and is used as a thickening agent in foods. It consists of unbranched polysaccharides obtained from cell walls of some species of seaweed and red algae. Agar chains are believed to be arranged in the double helix structure and the chains are cross-linked to each other to form a double helix with pitch of 1.9 nm. This results in the formation of a 3D polymeric network which has a microscopic characteristic length of 0.2 μm ^[68].

Guar gum has been used commonly as a thickening agent in textile printing and imparts the required rheological properties for a textile print paste. It can be used to tailor the viscosity of the resin for extrusion of fiber. It is a polygalactomannan obtained from seeds of *Cyamopsis tetragonalobus*. It is a nonionic branched polymer with β -D-mannopyranosyl units forming 1-4 linkages with single membered α -D-galactopyranosyl units occurring as side chains ^[69]. It is a polysaccharide and can be dissolved in water. Guar gum can generate high viscosities at relatively low concentrations ^[70]. Zhu *et al.* ^[71] reported that addition of guar gum improved the thermal and functional properties of soybean β -conglycinin thermally induced gel.

Different methods including chemical cross-linking, chemical modification, enzymatic treatment, nano-particle reinforcing and physical blending have been used to improve the physical and mechanical properties of soy protein resins ^[20, 72-76]. Otaigbe and Adams ^[72] reported that addition of bioresorbable polyphosphate filler increased the stiffness, strength and moisture resistance of soy protein plastic. Jane *et al.* ^[73] reported that in the presence of two parts of zinc sulfate, water absorption of soy protein resin decreased by 30%. Epichlorohydrin was also used to increase mechanical properties through cross-linking. Zhong and Sun ^[74] blended SPI with

polycaprolactone (PCL) and modified the blend by adding methylene diphenyl diisocyanate (MDI). The addition of MDI increased the compatibility between SPI and PCL and also increased the mechanical properties and the water resistance of the blend [74]. The effect of microbial transglutaminase on glass transition temperature (T_g) of soy protein was studied by Mizuno *et al.* [75].

Rhim *et al.* [76] studied the effect of reinforcement of SPI with various clay minerals like montmorillonite (O-MMT), wamok clay (W-clay), talc powder, zeolite and bentonite. Tensile properties of the films increased significantly with addition of O-MMT and bentonite and water solubility of most of the nano-composite films decreased [76]. Lodha and Netravali [4] modified SPI using stearic acid. It was observed that the moisture content, fracture stress and fracture strain decreased on increasing the stearic acid content from 0 to 30% (by weight of SPI). Glutaraldehyde and glyoxal have also been used to modify (cross-link) soy protein resins for improved tensile properties and decreased moisture absorption [6, 7, 45, 77, 78]. Glutaraldehyde modified soy protein resins showed significant increase in Young's modulus. Cross-linking due to glyoxal decreased the weight loss of the modified soy protein in the degradation tests [6, 7, 45, 78]. Neither of these cross-linkers is environmentally benign and research is needed to find environment-friendly cross-linkers. Plant phenolics that are benign and eco-friendly have been used as cross-linking agents in this research.

2.4 Use of Plant Phenolics as Eco-friendly Cross-linking Agents

It is known that polyphenols can react with side chain amino groups of peptides under oxidizing conditions which can lead to formation of cross-links in the proteins [79]. Polyphenols are 'green', eco-friendly alternatives for aldehydes used in food processing. Polyphenols are widely distributed as minor, but functionally important part of the plant tissues. Examples of polyphenols include caffeic acid,

caftaric acid, quercetin and rutin. They have a 1-hydroxy-2-methoxy structure. Polyphenols are found in rigid tissues like cell wall of fruits, tubers, coffee beans and tea leaves ^[79].

Strauss and Gibson ^[79] used plant-derived phenolic acids and flavanoids to prepare cross-linked gelatin gels and cross-linked gelatin-pectin coacervates in the form of micro-particles for use as food ingredients. The reaction scheme proposed for the reaction of these plant phenolics with proteins is shown in Figure 2.1 ^[79]. The diphenol moiety of the polyphenol (compound 1 in figure 2.1) is oxidized to orthoquinone by molecular oxygen. The quinone may form a dimer, or react with amino or sulfhydryl groups present in the protein to form C-N or C-S bonds with the phenolic ring, with the regeneration of hydroquinone. The hydroquinone can be re-oxidized and bonded with a second polypeptide (compound 3 in figure 2.1). Two quinones, each carrying a chain, can react to form a cross-link (compound 4 in figure 2.1) ^[79]. This cross-linking mechanism is supported by the identification of phenolic acid dimers (compound 2 in figure 2.1) ^[80, 81].

Cross-linking of functional groups in soy protein will mask the polar groups and therefore, the moisture absorption will decrease increasing the moisture resistance of the resin. Moisture resistance is essential for increasing the life of the resin under normal conditions. Cross-linking results in the formation of intra-molecular and inter-molecular linkages which increases the strength of the resin and offers better dimensional stability. Cross-linking increases the Young's modulus and therefore the extent of deformation for a given amount of force decreases.

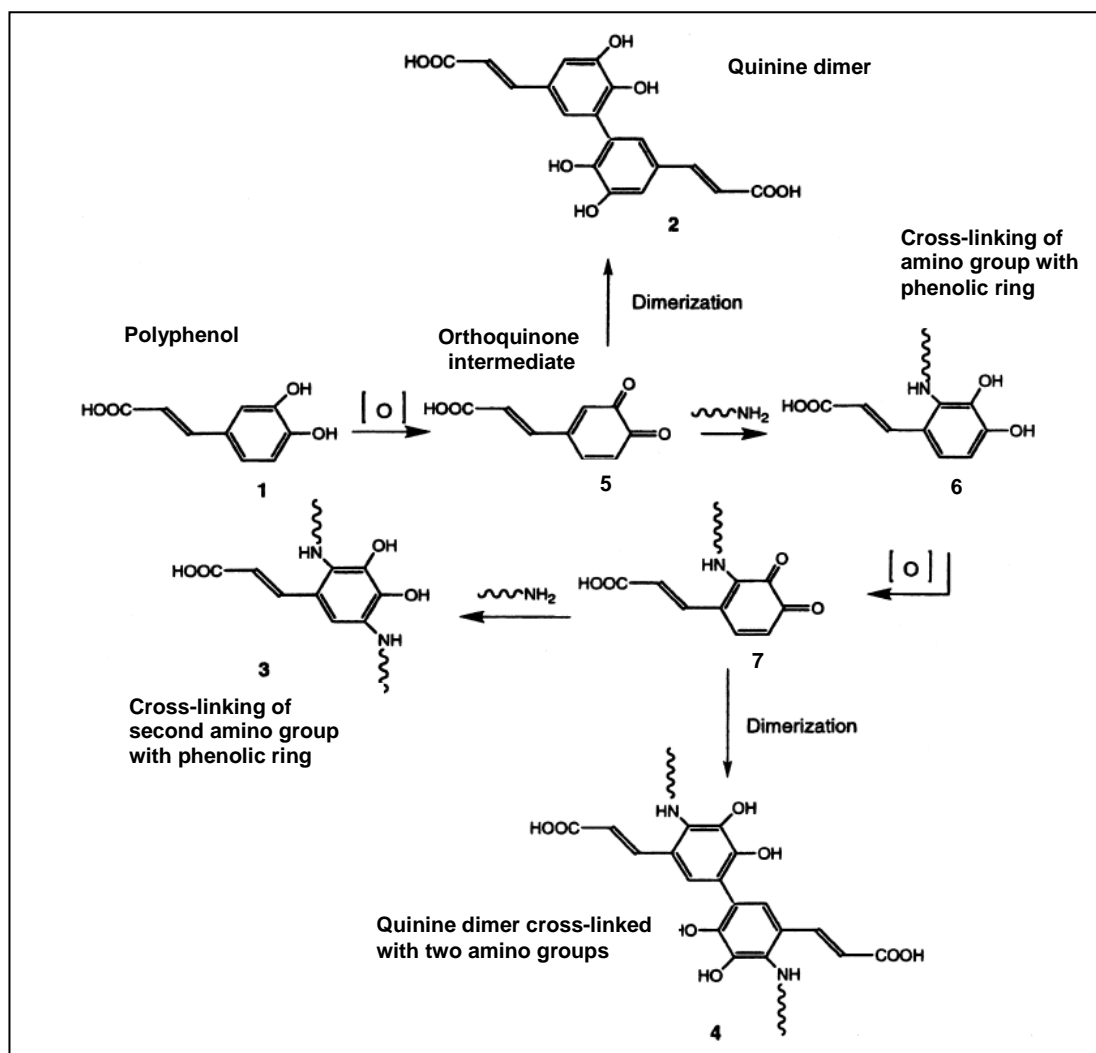


Figure 2.1 Reactions of a phenolic acid with amino side chains of polypeptides ^[79]

2.5 Use of Fibers and Textiles for Soil Stabilization

Soil consists of minerals, roots of plants, animal and microbial biomass, organic matter in various states of decay, as well as water and a gaseous component. The uneven distribution of these components provides a large combination of parameters resulting in different conditions at all levels from field to soil micro-pore. This represents a challenge for studying the composition and function of soil. A whole spectrum of various interacting physical and chemical factors contributes to the varied nature of the soil habitat ^[82]. A host of man-made changes like industrialization, expansion of cities have adversely affected land and rendered them infertile. The loss and abandonment of cultivable land in thirty one states of the eastern United States is widespread ^[83]. Urban expansion is a major cause for the permanent loss of cleared farm land, and despite its importance on the fringes of metropolitan areas, it is an important factor that influences loss and abandonment ^[83]. It is important that land is recovered and made cultivable; otherwise the decreasing availability of cultivable land could pose food problems in the near future. One of the important problems posing mankind is whether growth in agricultural production can keep pace with the increase in population and income driven demand for food ^[18].

Soil properties are a major factor in cultivation. Soils with low organic content or acidic or highly alkaline soils are unsuitable for cultivation. Organic matter indirectly enhances the quality of soils for growth of plants ^[13, 14]. New incentives and policies for ensuring the sustainability of agricultural system and ecosystem services will be crucial if people of the world are to meet the demands of improving yields without compromising public health or environmental integrity ^[16].

In wall and slope applications, geo-synthetic materials provide resistance to driving forces or moments caused by the self weight of soil and applied surcharges. The use of geo-synthetic materials for reinforcement of slopes and retaining walls has

increased significantly in the past two decades ^[84]. Chattopadhyay and Chakravarti ^[85] have studied the application of jute-based geotextiles as a facilitator in drainage. In their study, jute-based geotextiles were used in foundation soils that were soft and needed stabilization before loading. Remediation techniques can pose problems in soft clayey deposits and suitable reinforcements are required to reclaim the land. Once the target consolidation is achieved, one does not have to worry about the removal of the jute-based geotextile. Jute is biodegradable and rot resistant, and bitumen treated jute-based geotextiles can be used to lower degradation rates. Decomposition of jute does not produce toxic products and is therefore environment-friendly ^[85].

Jute-based geotextiles have also been used in the form of barrier for containment of sulfates that are harmful if they get mixed with water supplies. Chattopadhyay and Chakravarti ^[86] have investigated the use of jute-based geotextile impregnated with rot resistant bitumen to intercept the groundwater with pollutants like sulfates that otherwise can leach and damage concrete structures. The study reported that the modified jute-based geotextiles act as a barrier and might prevent the detrimental effects of sulfates on concrete during its 28 day curing period. The jute-based geotextiles can be used as a formwork in the field as it may yield improved performance of concrete structures during the initial curing period ^[86].

Soil erosion due to concentrated water flow can cause significant environmental damage. Geotextiles have shown great potential to reduce soil erosion. Smets *et al.* ^[87] studied the effect of borassus geotextiles, buriti geotextiles and bamboo geotextiles on soil detachment rate. It was reported that borassus geotextiles reduced soil detachment rate to 56%, buriti geotextiles to 59% and bamboo geotextiles to 66% as compared to the soil detachment rate of control bare soil surface. The Darcy-Weisbach friction coefficient (f) that indicated the flow-retarding effects of the tested geotextiles, was observed to be linearly correlated with geotextile thickness ^[87].

The Darcy-Weisbach friction coefficient (f) did not show any clear relation with geotextile cover or dry weight of the geotextile ^[87].

Vishnudas *et al.* ^[88] have studied the performance of coir-based geotextile with respect to the moisture content of soil, biomass production and protection against erosion. The coir-based geotextile retained 30% of its original strength after 7 months and 19% of the original strength after 9 months. However, the erosion control measures were not affected due to growth of vegetation during that period. Coir is inexpensive and coupled with potential for production using local labor makes it useful as reinforcement for sustainable development in watershed management ^[88].

Subaida *et al.* ^[89] studied the tensile and pullout behavior of geotextiles woven from different types of coir yarns (Anjengo, Vycome, Beach and Aratory yarns) in granular soils of different grain sizes. Beach fibers showed the highest breaking modulus while anjengo fibers showed higher breaking stress as well as breaking strain. The strength of the tested mesh mattings was reported in the range of 10-20 kN/m. It was reported that at lower normal stress values, the bond resistance of coir geotextile-sand interface was higher than the shear strength of the soil. At higher normal stresses, however, the values of the bond resistance were not found to be consistent. It was observed that closely woven geotextiles exhibited good pullout resistance from fine, medium and coarse sand and it was attributed to high interface friction. Open meshed geotextile showed better pullout resistance in fine-grained soil than in coarse-grained soil due to good bearing resistance and good interlocking ^[89].

Rawal and Anandjiwala ^[90] studied the effect of non-woven geotextiles produced from polyester and flax fibers. It was found that the variability in flax fineness and fiber length could result in loss of tensile stress. It could also result in variation in smallest detected pore diameter. High elastic recovery of polyester caused the polyester-based geotextile to be denser than flax-based geotextile. Flax-based

geotextiles were found to be compact and less anisotropic in nature. It was reported that flax fibers produced an open structure with higher permeability characteristics ^[90].

For agriculture to be sustainable the interconnections between farming and environment have to be explored and soil is an important part of it. Apart from geotextiles, mulching is one of the methods widely used to protect the soil. Mulches also enhance the productivity of the soil in addition to stabilizing it. Verdu and Mas ^[91] studied the effect of mulches for weed management. Mean species richness, an indicator of weed growth, ranged from 4.7 to 6.8 in mulches and reached 24.3 in control treatment. This indicates that mulches are effective in weed management. Verdu and Mas ^[91] concluded that organic mulches are effective alternatives to glyphosate (N-(phosphonomethyl) glycine) for managing weeds in citrus rows ^[91]. In another study, it was observed that in terms of soil run off, the cotton hydromulch performed better than mulches based on straw, wood and coconut ^[92]. The total runoff was measured for different treatments and the runoff consisted of both mulch and soil ingredients. The runoff was 7832 lbs/acre for straw hydromulch, 7474 lbs/acre for wood hydromulch, 3719 lbs/acre for coconut hydromulch; but only 222 lbs/acre for cotton gin hydromulch. The use of hydromulches reduces soil erosion and is an effective treatment for soil stabilization ^[92].

Synthetic fibers have also been used as geotextiles, but they are not biodegradable and are difficult to remove after their purpose is served. Use of biodegradable fibers for soil stabilization and crop protection is an attractive prospect, provided the process is economically feasible.

CHAPTER 3

EXPERIMENTAL PROCEDURES

The experimental procedures for production and characterization of soy protein resins and fibers are discussed in detail in this chapter. The SF-based fibers with different compositions were prepared and characterized for their tensile and moisture content properties. Field trials were carried out to study the behavior of the SF-based fiber mats in natural environment. Lab scale compost setup was used to study the degradation behavior of SF-based resins. Rutin and quercetin, plant polyphenols, were used as ‘green’ cross-linkers to cross-link SF. The field trials and greenhouse trials conducted to study the soil stabilization effects of SF-based resins are also described in this chapter.

3.1 Materials

The materials used in this research and their sources are listed in this section. SF and SPI powder, PRO FAM 970, and linseed oil (Toplin x-z grade) were obtained from Archer Daniels Midland Co., Decatur, IL. Glycerol and sodium hydroxide were obtained from Malinckdrodt Baker, Inc., Phillipsburg, NJ. Analytical grade rutin and quercetin hydrate were obtained from Sigma Aldrich, St. Louis, MO. MCC was obtained from FMC Corporation, Newark, DE. NB416 and FMGP were obtained from Weyerhaeuser, New Bern, NC. MFC was obtained from Daicel Chemical Industrial Lt., Japan, as a paste containing 10% micro-fibrils and 90% water. Agar agar was obtained from Seng Huad Limited Partnership, Bangkok, Thailand. Ultra-high pure oxygen was obtained from Airgas East, Elmira, NY. Glutaraldehyde (25 wt. % solution), glyoxal (40 wt. % solution) and Phytigel[®] were obtained from Sigma Aldrich, St. Louis, MO. Non-woven polypropylene Typar[®] sheets, of 0.30 mm

thickness and $9.35 \text{ cm}^3 \text{ sec}^{-1} \text{ cm}^{-2}$ air permeability, were obtained from DuPont (E.I.) de Nemours & Co., Typar[®] Nonwovens, DE. The 924 high thrust bulk extruder was bought from Newborn Brothers Co., Inc., Jessup, MD. A 10" x 15" Minco Kapton 13.5 Amp/7.8 Ohm laminar heater was bought from Minco, Minneapolis, MN. Sawdust (Kiln dried softwood) was obtained from Lanjay, Inc., Montreal, Canada. Pipette tips for the extruder were obtained from Thermo Scientific, Waltham, MA.

3.2 Soy Protein Pre-curing Process

This section describes pre-curing process of soy protein which was done to improve its mechanical and physical properties. SF was converted into the resin from which fibers could be extruded. To prepare the resin, SF powder was mixed with glycerol (5% w/w), a plasticizing agent that provided flexibility to the resin. Distilled water, 2.3 times SF (230% by weight), was added to this mixture. The SF mixture was then stirred using Kinematica[®] Polymix mechanical stirrer for 40 minutes in a water bath maintained at 80°C. To adjust the pH, 1 M NaOH solution was prepared by dissolving 4 g of NaOH in 25 ml of distilled water and then increasing the total volume of the solution to 100 ml by adding distilled water. The pH of the SF mixture was adjusted to 8.4 by addition of 1 M NaOH solution after 10 minutes of stirring. The pH was monitored using pH meter. The SF mixture was then loaded in the hand held extrusion gun.

3.3 Extrusion Setup and Process

This section describes the extrusion equipment needed for SF-based fiber production. A lab scale hand held extrusion gun was built around a Newborn brothers 924 high thrust bulk extruder as shown in Figure 3.1. A 10" x 15" Minco Kapton 13.5 amp/7.8 ohm laminar heater was wrapped around the extrusion chamber in order to

maintain the resin temperature at 120°C during the extrusion. Heater was controlled using a Minco CT325 controller coupled with a Minco S102406 sensor integrated into the cap piece. An extrusion plate with pipette tips attached to it was created to extrude fibers as shown in Figure 3.2. Teflon[®] coated boards were used for collection of SF-based fibers.

The SF-based mixture was loaded in the vertically held extrusion gun and the fibers were extruded using the levers of the extrusion gun on to Teflon[®] coated boards maintained on a horizontal platform. Uncured fibers were extruded at room temperature while the cured fibers were extruded with the extruder maintained at 120°C. The horizontal platform allowed the Teflon[®] coated boards to move along a horizontal axis. The Teflon[®] coated boards were moved horizontally to collect fibers during extrusion. The Teflon[®] coated boards were then kept at room temperature to allow the fibers to dry and were then transferred to the conditioning room maintained at ASTM conditions of 65% relative humidity (RH) and 21°C. The fiber diameters obtained in these experiments ranged between 250 μm and 350 μm.

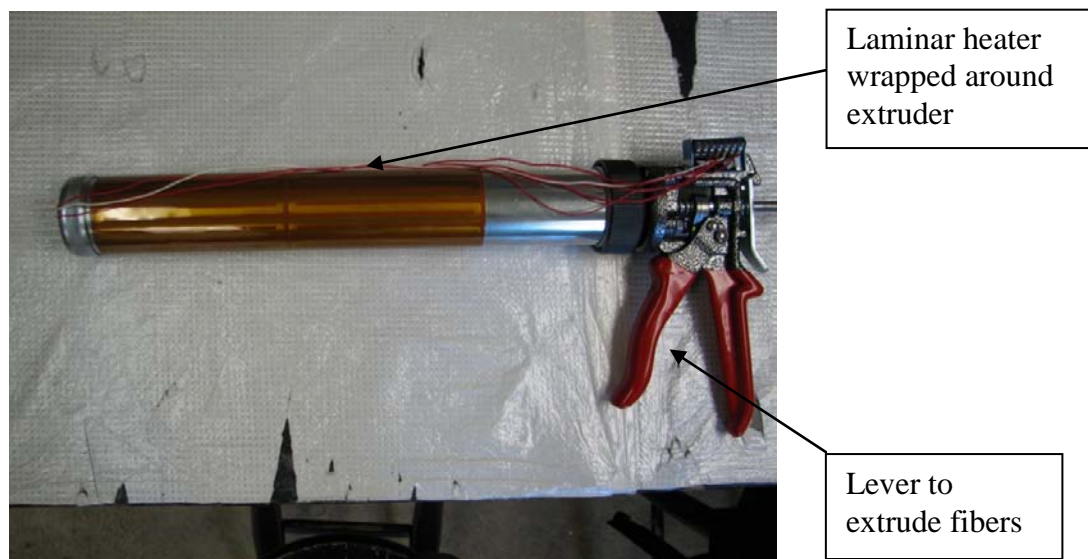


Figure 3.1 Lab scale extrusion gun



Figure 3.2 Extrusion plate showing pipette tips

Many types of additives were used to improve the properties of SF-based fibers as desired. Cellulo[®] which contains highly refined alpha cellulose fibers was used in SF-based fibers to increase the tensile strength. Fitz milled Grand Prairie (FMGP) is a finest softwood kraft pulp obtained from blend of spruce and pine from the forests of interior Canada. FMGP has increased hemicellulose content, which delivers high tensile strength. The FMGP fibrils were used to modify SF-based fibers and improve strength by orientating the fibrils in the SF-based fibers. FMGP consists of ribbon like structures as shown in Figure 3.3 with widths in the range of 30 to 60 μm and the length in the range of 2000 μm to 4500 μm . Micro-crystalline cellulose (MCC) is a cellulose-based derivative which contains nano-whiskers which can be isolated. The MCC used in this study had particle dimensions in the order of 200 μm . MCC was used to modify SF-based fibers and improve strength due to its highly crystalline nature in the fibers. Micro-fibrillated cellulose (MFC) is a cellulose-based derivative with fibrils in micro-scale and is shown in Figure 3.3. MFC is used to modify SF-based fibers and improve strength due to the orientation of the linear fibers

along the fiber axis during extrusion. NB416 Fitz mill fiberized (NB416) is a kraft fluff pulp containing high quality cellulose exhibiting excellent absorbency and wicking and contains fibrillar structures as shown in Figure 3.3. NB416 fibrils have widths in the range of 25 to 50 μm and lengths in the range of 2500 to 4500 μm . The morphology is different than FMGP with the fibrils showing a distinctive external layer. NB416 was used to modify SF-based fibers and improve their strength by orienting the NB416 fibers along the fiber axis during extrusion.

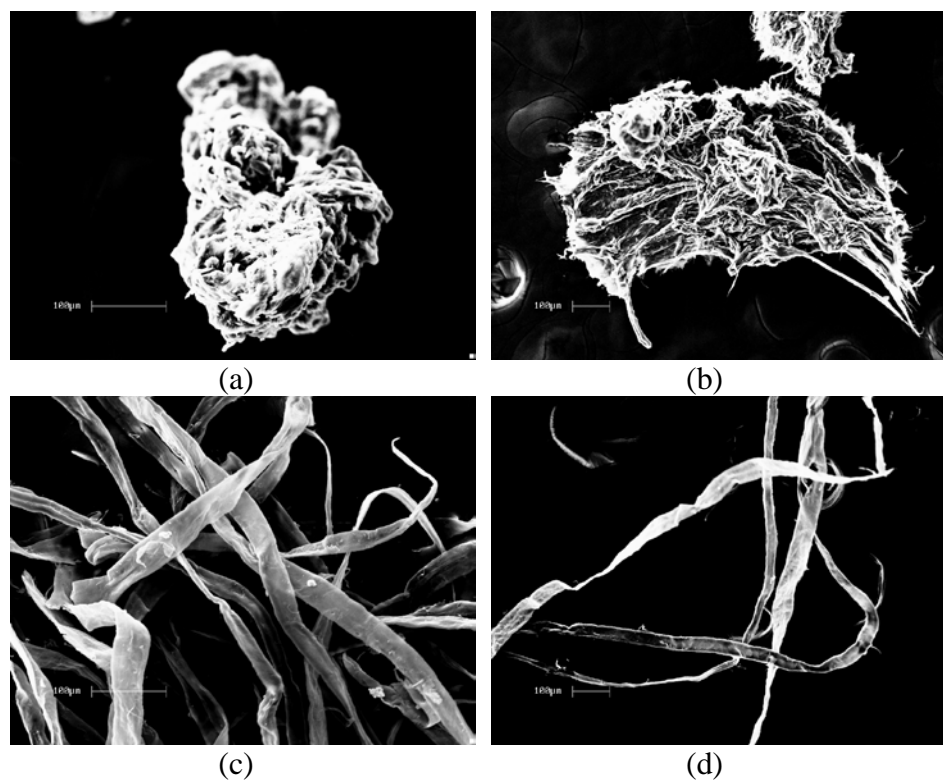


Figure 3.3 SEM images of (a) MCC particle; (b) MFC fibrils in aggregated form; (c) FMGP fibrils and (d) NB416 fibrils

3.4 Processing of Soy Protein Resin Films

SF was converted into films to study the effect of additives on the physical and mechanical properties of SF. This section lists the procedure for processing of soy protein to obtain films. SF was converted into the resin form, and processed into films, to characterize their properties. To process SF into resin form, it was mixed with glycerol (5% by weight of SF), a plasticizing agent which provided flexibility to the resin. Distilled water, 15 times the SF (1500% by weight of SF), was added to this mixture. The mixture was then stirred using magnetic stirrer for 40 minutes in a water bath maintained at 80°C. The pH of the mixture was adjusted to 8.4 by addition of 1 M NaOH after 10 minutes of stirring. The mixture was then poured on to Teflon[®] coated plates and allowed to dry to form a sheet. The dried sheets of SF-based resins were then hot pressed (cured) in a Carver hydraulic hot-press (model 3891-4PROA00, Fred S. Carver Inc., Wabash, IN, USA) at 120°C for 25 min at 38,000 lbs pressure. The cured resin sheets were then conditioned at ASTM conditions of 21°C and 65% RH for 72 hr prior to characterizing their properties.

3.5 Characterization of Soy Flour Fibers

SF-based fibers were characterized to study the effect of various additives on their mechanical properties. This section describes the procedure adopted for characterizing the SF-based fibers. The SF-based fibers were conditioned at 21°C and 65% RH for 72 hours prior to testing. Moisture content of SF-based fibers was measured at the end of 72 hours using a Brabender moisture/volatiles tester according to ASTM D 2654-89a. The moisture content was measured after drying the sample for 24 hours at 105°C. For analyzing moisture content, 10 g of SF-based fiber was tested and the reading on the moisture tester displayed the moisture content of the specimen.

No statistical analysis was performed for moisture content among treatments as it was a single measurement.

Fiber specimens were tensile tested on Instron (model 5566) universal testing machine. The gauge length used for tensile testing was 20 mm and the test was performed at a strain rate of 4.5% per minute. To perform the tests, fibers were glued onto a paper tab as shown in Figure 3.4. The fiber was laid on the paper tab and glued on the opposite ends. Two lines were marked perpendicular to the fiber axis 20 mm apart. This denotes the gauge length. The paper tab was mounted vertically on Instron and the paper was cut on the top end so that only the fiber was clamped between the jaws and then the tensile test was carried out. For each composition, 25 specimens were tested.

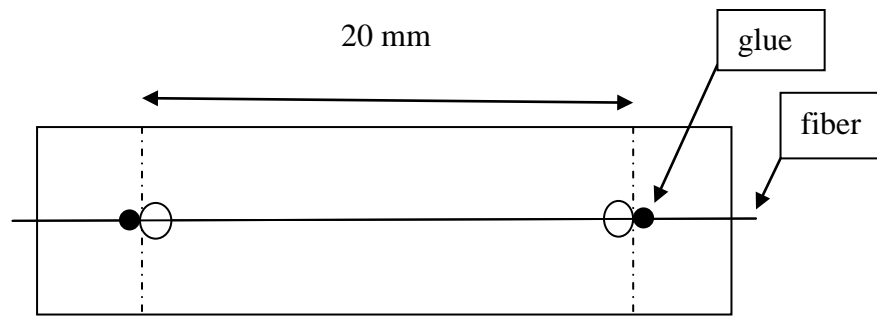


Figure 3.4 Paper tab for Instron testing of SF-based fibers

The tensile properties evaluated using Instron are tensile stress, tensile strain modulus (automatic) and/or Young's modulus. Tensile stress is defined as the force acting on specimen per unit area of its cross-section. Tensile stress at fracture is the tensile stress acting on the specimen at the point of break when strained. Tensile strain is defined as the increase in length of specimen relative to its original length along the axis in which elongation is taking place. Tensile strain at fracture is increase in length of specimen relative to its original length at point of break. Young's modulus is a measure of stiffness of the material and is defined as the ratio of tensile stress and

tensile strain in the range of stress where Hooke's law holds true. It is experimentally determined as the slope of a stress-strain curve created during tensile testing of a sample. A typical stress-strain plot of SF-based fiber is shown in Figure 3.5. Point of break is identified by the sudden drop of tensile stress to zero value. The tangent shown in the plot is used to calculate Young's modulus. Hooke's law holds true when tensile stress and tensile strain are directly proportional which is denoted by the initial straight line nature of the plot. Fracture stress is the tensile stress corresponding to the point of break and fracture strain is the tensile strain corresponding to the point of break. The tensile properties measured were analyzed for statistical significance ($\alpha=0.05$) using student's t-test (for comparing 2 means) or tukey HSD test (for comparing 3 or more means).

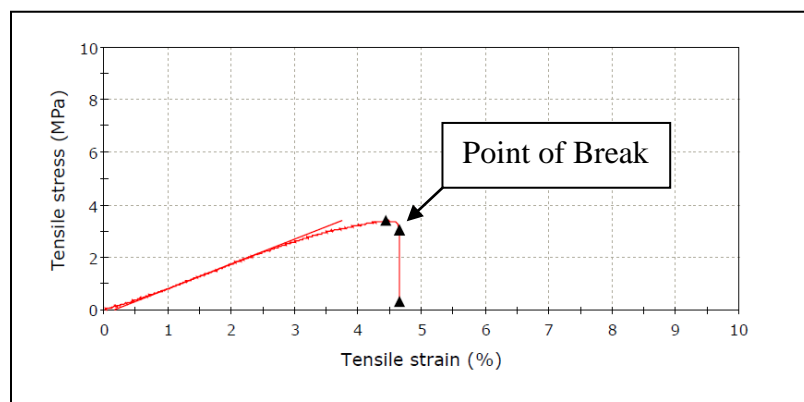


Figure 3.5 Typical stress-strain plot of SF-based fiber

3.6 Characterization of Soy Protein Film

For composting and cross-linking studies, SF-based films were studied instead of SF-based fibers as the fibers could not be recovered from the composting unit in intact state due to their biodegradability. The SF-based films were characterized for their mechanical properties and the procedures used are described in this section. The SF-based films were conditioned at 21°C and 65% RH for 72 hours prior to testing.

These tensile specimens were tested on same Instron testing machine according to ASTM D 3039-89. The gauge length used for these tests was 50 mm and the tests were performed at a strain rate of 100% per minute. The specimens were 10 mm wide and the thickness was measured individually for each specimen and input into the software before testing. The specimen thickness varied between 0.1 mm and 0.4 mm. For each composition, 7 specimens were tested to obtain average values for fracture stress, fracture strain and Young's modulus.

3.7 Evaluation of Biodegradability of Soy Flour-based Resin

3.7.1. Resin Preparation

SF was prepared in the form of films to study their degradation behavior in a compost environment. SF-based fibers could not be used as they would degrade fast due to higher surface area and it would be difficult to assess the biodegradation. This section describes the SF-based resin film preparation which is similar to process described in section 3.4. SF-based resin was prepared by mixing SF powder (10 g) with glycerol (5% by weight of SF) and distilled water (1500% by weight of SF). The pH of the solution was adjusted to 8.4 by addition of 1 M NaOH solution. In the precuring step, the SF solution was stirred in a water bath maintained at 80°C for 40 min. The pre-cured solution was then poured on to Teflon[®] coated glass plates and dried in an air circulating oven maintained at 35°C. For glutaraldehyde cross-linked resin (GA-SF), SF resin was prepared by mixing SF powder (10 g) with glycerol (5% by weight of SF) and distilled water (1500% by weight of SF) and glutaraldehyde (1:1 molar ratio based on lysine and arginine content in SF). The resin was pre-cured using the procedure described for SF resin in section 3.2.

Rutin cross-linked SF resin (R-SF) was prepared by mixing SF powder (10 g) with glycerol (5% by weight of SF) and distilled water (1500% by weight of SF) and

rutin (1:1 molar ratio based on lysine and arginine content in SF). The experimental setup is shown in Figure 3.6. The pH of the solution was adjusted to 8.4 by addition of 1 M NaOH. In the pre-curing step, the SF solution was stirred in a water bath maintained at 80°C for 40 min and ultra high pure oxygen was bubbled in the solution at a rate of 80 cc per minute. The pre-cured solution was then poured on to Teflon[®] coated glass plates and dried in an oven maintained at 35°C.

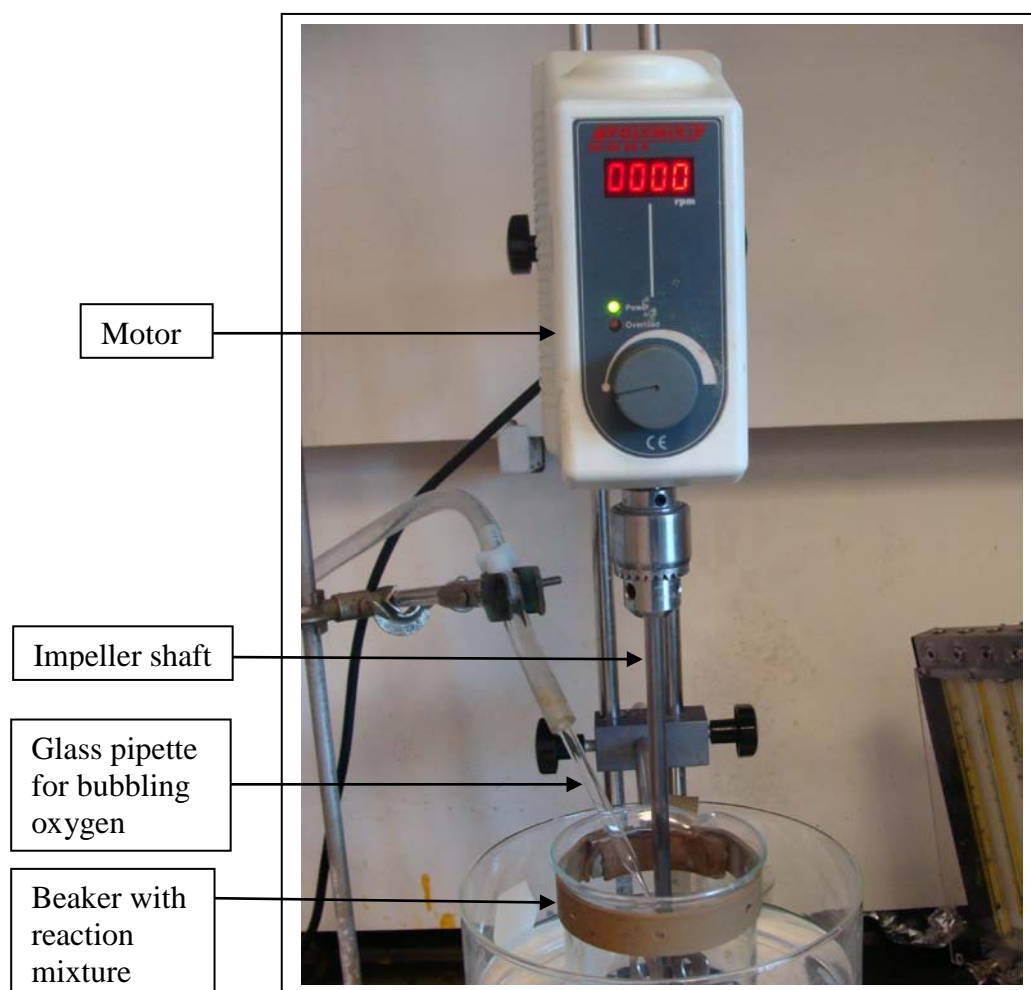


Figure 3.6 Experimental setup for rutin and quercetin cross-linked resin preparation

The dried sheets of SF, GA-SF and R-SF resins were then hot pressed (cured) in a Carver hydraulic hot-press (model 3891-4PROA00, Fred S. Carver Inc., Wabash, IN, USA) at 120°C for 25 min at 38,000 lbs pressure. The cured resin sheets were then conditioned at ASTM conditions of 21°C and 65% RH for 72 hr prior to characterizing them. Quercetin cross-linked SF resin was prepared using same procedure with quercetin used in place of rutin.

3.7.2 Resin Composting Studies

A composting medium was prepared to study the degradation behavior of the resins in the compost environment. The composting medium was prepared in a large plastic container so as to facilitate easy removal of samples when required. The composting medium was prepared by blending sawdust and chicken manure (droppings) in the ratio 1:1 (w/w) with a C/N ratio of 50/50^[93]. Sawdust, an organic matter was added to increase the C/N ratio to achieve the optimum degradation of organic C and retention of N through microbial biomass formation^[40, 93, 94]. One 94.5 liter plastic container was concentrically placed inside another 121 liter plastic container. Wooden spacers were used to maintain uniform spacing of about 75 mm between the two containers. The inside container had circular holes on its wall for air circulation. The walls of the outer plastic container were covered with 50 mm thick insulating plastic foam to reduce the heat loss from the surface which was required for maintaining the temperature inside the composting unit.

All three types of resin specimens in film form were individually placed in non-woven polypropylene Typar[®] bags (NPP) and these bags were then placed in the composting unit for microbial degradation. The NPP non-biodegradable bags were used to facilitate the retrieval of the buried sheet specimens and its open structure allowed circulation of moisture, air and microorganisms in the composting unit. The

composting setup parameters such as moisture, temperature, pH were monitored every day until the completion of the study. Moisture content was measured by weighing a predetermined amount of compost in an oven at 120°C for 24 hours and then the dry weight was measured. The pH was measured using pH paper to ensure it was acidic throughout the study. The moisture content of the composting medium was maintained at 50% by adding water initially and periodically during the study. Maintenance of moisture content of the composting unit at 50% resulted in the temperature of the composting medium being maintained at 32°C throughout the experiment. Weight loss of specimens was measured on days 10, 20, 30 and 60 of the composting study.

3.7.3 Attenuated Total Reflectance-Fourier Transform Infra Red (ATR-FTIR) Characterization

The surfaces of the resin sheets were analyzed for chemical changes, after composting, using the attenuated total reflectance (ATR) attachment (Harrick Scientific Co., Ossining, NY) on the Magna-IR 560 FTIR spectrometer (Thermo Electron Co., Madison, WI). A total of 128 scans were performed at a resolution of 4 cm^{-1} from 4000 cm^{-1} to 400 cm^{-1} wavenumbers. The surfaces of the specimens were washed and dried prior to characterization. Surface characterization was carried out for specimens after 0, 10 and 60 days of composting.

3.8 Field Trials

3.8.1 Preliminary Field Trials to Evaluate Soil Stabilization Effect of SF Fiber Mats

Field testing of the fibers potential for soil stabilization and re-vegetation was conducted. The procedure is described in this section. Promising formulations were applied to micro-plots of soil that were sown with 200 ryegrass seeds. There were 4 treatments used; control, fibers with micro-fibrillated cellulose (MFC), fibers with

micro-crystalline cellulose (MCC) and fibers with Cellulo[®]. The treatments and compositions are listed in Table 3.1.

Table 3.1 Composition of resins used for field trials in 3.8.1

Number	Treatment	Composition
1.	Control	No SF layer on micro-plot
2.	MCC	SF + 230% water + 5% glycerol + 10% MCC
3.	MFC	SF + 230% water + 5% glycerol + 10% MFC
4.	CELLULO	SF + 230% water + 5% glycerol + 5% Cellulo [®]

The micro-plots were prepared by filling plastic trays, having perforated walls, with soil. The plastic trays were filled with agricultural soil (dug up from the earth). The pH of the soil was slightly above 7 as reported by the greenhouse staff. The extrusion process was similar to the lab scale extrusion of SF-based fibers and the fibers were sprayed on an area of 20 cm x 20 cm. The micro-plots were positioned on a sloped surface and exposed to the environment. Seedling stand was measured for all micro-plots after 28 days (4 weeks). Differences in proportions of seed count for different treatments were tested using analysis of variance in SAS software. The response variable chosen was ‘asinpro’ (arcsine transformation of the ryegrass proportion to ensure underlying assumption of normal distribution of the response). Shrinkage was another variable of interest as the SF-based fiber mats shrink due to water evaporation and values of shrinkage. Differences in shrinkage percent for different treatments were tested using analysis of variance in SAS software.

3.8.2 Greenhouse Trials for Evaluation of Shrinkage Characteristics of SF Fiber Mats

Shrinkage of fiber mats was considered a hindrance in developing SF-based fiber mats and trials were conducted to determine the shrinkage characteristics of cross-linked formulations. These trials were conducted at a greenhouse in Kenneth Post lab using micro-plots to study the shrinkage characteristics of the SF-based fiber mats and the behavior of the SF-based fiber mats in dry and wet environments. The three treatments used for this study are listed in Table 3.2.

Table 3.2 Composition of resin used for greenhouse trials in 3.8.2

Number	Treatment	Composition
1.	Control	SF + 230% water + 5% glycerol
2.	GA	SF + 230% water + 5% glycerol + equi-molar glutaraldehyde
3.	GL	SF + 230% water + 5% glycerol + equi-molar glyoxal

Each treatment was assigned four replicates which resulted in total number of twelve micro-plots. The micro-plots were monitored over a period of seven weeks with the first four weeks in dry environment and the final three weeks in wet environment. The humidity was not regulated in the greenhouse. The micro-plots were prepared by filling plastic trays having perforated walls with soil. The plastic trays were filled with agricultural soil (dug up from the earth). The pH of the soil was slightly above 7 as reported by the greenhouse staff.

The fiber extrusion process was similar to the lab scale extrusion of SF-based fibers described in section 3.3, but the fibers were extruded on the micro-plot soil instead of the Teflon[®] coated board. The SF-based fibers were extruded to form a fiber mat and the original area was measured and was monitored thereafter to study its shrinkage. The temperature of the greenhouse housing the micro-plots was maintained

at 23.9°C (75°F). For the final three weeks of the study, the micro-plots were studied in wet environment by switching on the water mist outlets. Water mist was released for 12 seconds every 10 minutes during wet condition study. For evaluation of fiber mat behavior, the initial area covered by the fiber mat was recorded and the area was recorded each week. Dry condition was maintained from day 1 to day 28. Wet condition was employed from day 29 to day 49. The percent shrinkage of micro-plots was calculated from the area of soil covered by the fiber mats. Area of soil micro-plot covered by the SF-based fiber mat was recorded at the end of day 1, week 1, week 2, week 3, week 4, week 5, week 6 and week 7.

3.8.3 Field Trials for Evaluation of SF Resin on Seed Germination and Weed Suppression

Field trials were conducted to evaluate the effect of SF resin mixed with NB416 fibers (4.91% w/w) on seed germination and weed suppression. Ryegrass seeds were used for the study and since they were small and easily displaced by natural elements such as wind and rain, provided a proxy measure of soil erosion in the experiment. Field trials were conducted at Cornell Orchards at Dryden Rd, Ithaca, NY. The number of treatments studied was 5 and are listed in Table 3.3. Each treatment had 10 replicates, resulting in a total sample size of 50 plots. There were 10 blocks and each block contained one replicate of each treatment in a random order as shown in Figure 3.7. Each plot was 0.61 m x 0.61 m in dimension. Each plot was color coded to identify the treatment employed in that plot. Each plot was separated by at least 0.61 m from surrounding plots to ensure there was no migration of seeds which could result in bias in data. Completely randomized block design was used for the trials as it blocked any effect of slope on the trials as all the micro-plots in one block

had the same slope. Each treatment had equal amount of replicates and each treatment occurred once in a block resulting in a balanced design of experiment.

Soy resin used for this field trial consisted of 11.47% SF (w/w), 4.91% NB416 (w/w), 1.64% Toplin x-z linseed oil (w/w) and 81.96% water (w/w). The contents were mixed in a paint bucket using a drill machine with an impeller till the mixture was well mixed. A plastic template with 0.61 m x 0.61 m square hole was used for application of resin to plots so that the resin was sprayed only inside the plot. The resin was extruded using a sprayer (Spray-Pro hopper gun, Wallboard Tool Company, Long Beach, CA) and applied only in the area kept open by the template. Hydromulch was laid by hand on the plots.

The five treatments studied were CONTROL, SL, SH, SS and HYDRO as listed in Table 3.3. CONTROL treatment consisted of the micro-plot with the ryegrass seeds and no other material was applied. For SL treatment, SF-based resin was sprayed on the micro-plot for a period of 30 seconds resulting in a light layer. For SS treatment, a light layer of SF-based resin along with ryegrass seeds were sprayed using the sprayer for a period of 30 seconds. For SH treatment, SF-based resin was sprayed using the sprayer on the micro-plot for a period of 120 seconds resulting in formation of a heavy layer. For HYDRO treatment, hydromulch was applied on the micro-plots manually as required machinery for spraying of hydromulch was unavailable. Heavy rain and wind was observed in second week of the study and the first count of ryegrass shoots was taken on day 12, after the thunderstorms had stopped. Metal rings with 7.7 cm diameter were used to collect the shoot count on the micro-plots. Subset sampling of ryegrass count was done by randomly placing the metal ring on the micro-plot and counting the shoots inside the area of the metal ring. Shoot counts were measured on days 12, 16 and 21 after the start of the study. Heavy rains between day 9 and day 12 of the study resulted in grass growth and first reading of shoot counts was taken on

day 12. Counting of shoots was stopped after day 21 as the shoot counts and germination rate seemed to level off. Three readings were taken for each micro-plot at each of the time points.

Block 1	SL	SS	HYDRO	SH	CONTROL
Block 2	CONTROL	HYDRO	SS	SL	SH
Block 3	SH	SS	HYDRO	CONTROL	SL
Block 4	SS	SL	SH	CONTROL	HYDRO
Block 5	HYDRO	SS	SH	SL	CONTROL
Block 6	HYDRO	CONTROL	SH	SL	SS
Block 7	CONTROL	SS	SL	SH	HYDRO
Block 8	HYDRO	SS	CONTROL	SL	SS
Block 9	HYDRO	SH	CONTROL	SL	SS
Block 10	SS	SH	HYDRO	SL	CONTROL

Figure 3.7 Design of field trials

Table 3.3 Composition of treatments used for field trials in 3.8.3

1.	CONTROL	Plot with seeds
2.	SL	Plot with seeds covered by a light layer of SF resin
3.	SH	Plot with seeds covered by heavy layer of SF resin
4.	SS	Plot sprayed with soy resin containing seeds
5.	HYDRO	Plot with seeds covered with commercially available hydromulch

At the end of the trials (43 days), the grass was cut at ground level and analyzed for biomass. The grass was cut and put in brown paper bags, which were dried in an oven for 3 days at 60°C. After drying, the grass was weighed to record the

weight of biomass for each replicate. After analysis for biomass, the grasses were analyzed for nitrogen content at Department of Horticulture at Cornell University.

For shoot count analysis, a generalized mixed model was fit using SAS with ‘shoot count’ as the response variable. ‘Shoot count’ was assigned Poisson distribution due to the skewed nature of the data. Tukey HSD tests were conducted using SAS to test for analyzing treatment differences in the field study. For statistical analysis of biomass, a model using restricted maximum likelihood (REML) was fit with ‘logbiomass’ (logarithmic transformation of biomass) as the response variable, and ‘block’ and ‘treatment’ as predictor variables. ‘Block’ was assigned random attribute in the analysis. Biomass was converted into logarithmic form to ensure the normality required for fitting the model. For statistical analysis of nitrogen content, nitrogen content was adjusted for 50% carbon level as high correlation was observed between nitrogen content and carbon content. The adjusted nitrogen content was fitted using standard least squares in JMP to study the relationship of the response with treatments.

3.8.4 Greenhouse Trials for Evaluation of SF Resin on Seed Germination

The treatments used for greenhouse trials were same as that of the field trials. Greenhouse trials employed regulated conditions as compared to field trials which was dependent on natural weather. The design of greenhouse trials is shown in Figure 3.8. The design used in this study was an unbalanced randomized complete block design. Each block corresponds to a tray used in the greenhouse. The setup for the experiment consisted of an outer tray with no perforations containing an inner tray with perforations. The micro-plot cells were then placed in these trays with each tray able to hold 18 cells with each sell with dimensions 5 cm x 5 cm.

Block 1	Block 2	Block 3	Block 4	Block 5
HYDRO	HYDRO	HYDRO	CONTROL	CONTROL
SH	SH	CONTROL	CONTROL	HYDRO
SS	CONTROL	SH	SL	SL
SH	SL	CONTROL	HYDRO	SS
SS	SL	CONTROL	SH	SL
SH	SS	SS	SH	HYDRO
SS	HYDRO	SL	SH	CONTROL
SL	SH	CONTROL	CONTROL	CONTROL
SL	SL	SL	SH	SS
SS	SS	HYDRO	HYDRO	HYDRO
SS	SL	HYDRO	HYDRO	HYDRO
SL	SH	CONTROL	SH	HYDRO
SL	HYDRO	HYDRO	SH	SL
SL	SL	CONTROL	SS	CONTROL
SS	HYDRO	CONTROL	HYDRO	SS
Block 6	Block 7	Block 8	Block 9	Block 10
HYDRO	SL	SL	SS	CONTROL
SH	SH	SL	SS	CONTROL
SS	CONTROL	SS	SH	SH
HYDRO	SS	SH	SS	SH
SH	HYDRO	CONTROL	SS	SH
SL	SL	SH	CONTROL	HYDRO
SL	HYDRO	SH	HYDRO	SL
SH	SL	SS	CONTROL	CONTROL
SS	CONTROL	SS	SL	SL
CONTROL	SH	SH	HYDRO	SL
SL	CONTROL	CONTROL	SH	SH
CONTROL	SS	SS	SS	SL
CONTROL	SS	SS	HYDRO	SL
CONTROL	SS	SH	HYDRO	HYDRO
SS	SH	HYDRO	HYDRO	SL
HYDRO	SH	SL	CONTROL	SS

Figure 3.8 Design of greenhouse trials

In the experimental design, ten trays were used with each tray considered as a block. Each tray was filled with 16 cells to leave space for watering the cells through the 2 empty cells. Each treatment occurs at least once in each block but the number of replicates was not equal, resulting in an unbalanced completely randomized block design. The unbalanced nature was owed to the size of tray resulting in unequal replication in a single tray. The trays were watered periodically as required. The temperature was maintained between 79°F and 82°F over the course of this study. Relative humidity was not controlled, but it varied between 38% and 45%. Each cell was sown with 25 seeds except the SS compositions. In case of SS treatment, the seeds were incorporated in the resin and then sprayed. As a result, exact number of seeds in each micro-plot could not be verified to be 25. The grass count in each cell was measured on day 7, day 10, day 14, day 18 and day 23 in the greenhouse.

For statistical analysis of grass count, a generalized mixed model was fit using SAS with shoot count as the response variable. No transformation was needed as the residuals for shoot count exhibited normality which is a required condition for fitting the model. The predictor variables specified in the model were ‘block’, ‘treatment’, ‘days’, ‘block by treatment’ interaction and ‘days by treatment’ interaction. Tukey HSD tests were conducted to analyze for differences ($\alpha=0.05$) in response variable due to the predictors.

3.9 Soy Protein Resin Film Processing with Eco-Friendly Cross-linking Agents

Cross-linking increases the tensile strength of soy protein formulation, but the cross-linkers used like glutaraldehyde and glyoxal are not eco-friendly. In this research, rutin and quercetin which are plant-based polyphenols were used for cross-linking soy protein. SF was converted into a cross-linked resin form using rutin or quercetin which could be processed to form a film. Rutin or quercetin solution was

prepared by dissolving equi-molar amounts (according to amount amino groups in soy protein) of rutin or quercetin in predetermined amount of distilled water and 1:1 molar ratio of sodium hydroxide. This solution was then mixed with SF, glycerol (5% by weight of SF), a plasticizing agent which provided flexibility to the resin. Distilled water (1500% by weight of SF), was added to this mixture. The temperature and duration of the process were varied to study the effect on the tensile properties of the resin. Four different processes were used for preparing the cross-linked resins to study their effect on resin cross-linking and properties.

The first process denoted by 'A' is described as follows. The mixture containing SF, rutin/quercetin, glycerol and water was stirred using Kinematica Polymix stirrer for 120 minutes in a water bath maintained at 80°C. The pH of the mixture was adjusted to 8.4 by addition of 1 M NaOH after 10 minutes of stirring and pH was measured using pH meter. Ultra high pure oxygen (99.99%) was bubbled through the solution for 120 minutes. The mixture was poured on to Teflon[®] coated plates and allowed to dry to form film. The dry film was then transferred to the conditioning room maintained at 21°C and 65% RH.

In the second process denoted by 'B', the mixture was stirred for 40 minutes in a water bath maintained at room temperature. The pH of the mixture was adjusted to 11 by addition of 1 M NaOH before stirring. Ultra high pure oxygen was bubbled through the solution during stirring. Pouring and drying of the film was done the same way as described in the first process.

In the third process denoted by 'C', the mixture was stirred for 40 minutes in a water bath maintained at 80°C. The pH of the mixture was adjusted to 8.4 by addition of 1 M NaOH before stirring. Ultra high pure oxygen was bubbled through the solution during stirring. Pouring and drying of the film was done the same way as described in the first process.

In the fourth process denoted by 'D', the mixture was stirred for 40 minutes in a water bath maintained at 80°C and then stirred for 80 minutes in a water bath maintained at room temperature. The pH of the mixture was adjusted to 8.4 by addition of 1 M NaOH before stirring. Pouring and drying of the film was done the same way as described in the first process. Conditions in processes E and F were same as that of process D, but analytical grade rutin and quercetin were used in processes E and F respectively.

Soy protein when processed at higher temperatures for longer time durations, degrade and the film formed has poor mechanical properties. In this case, four different processes were studied to determine the optimum conditions to minimize soy protein degradation and maximum cross-linking possible.

3.10 Characterization of Cross-linked Resin with Eco-Friendly Cross-linking agents

This section describes the procedures followed to characterize the tensile properties of cross-linked resin and the molecular weight distribution using SDS-PAGE analysis.

3.10.1 Characterization of Tensile Properties

The characterization is identical to the process described in section 3.6. These tensile specimens (10 mm x 100 mm) were tested using Instron testing machine according to ASTM D 3039-89. The gauge length used for testing was 50 mm and the testing was performed at a strain rate of 100% per minute.

3.10.2. SDS-PAGE Analysis

The molecular weight distribution of soy protein was evaluated by Sodium Dodecyl Sulfate Polyacrylamide Gel Electrophoresis (SDS-PAGE). Soy Protein

Isolate (SPI) was used for SDS-PAGE as carbohydrates and lipids in SF were not required for the analysis and the protein would have had to be fractionated if SF was used for SDS-PAGE. For SDS-PAGE analysis, 300 mg of SPI was dissolved in 400 ml distilled water. The process parameters were varied because soy protein showed degradation when treated at higher temperatures for times greater than 2 hours. The parameters were varied to minimize soy protein degradation and to optimize cross-linking of soy protein with rutin or quercetin. The process parameters used were same as those for production of soy protein resin film production mentioned in section 3.9. For SDS-PAGE analysis, 1 ml of the solution was used. Soy protein was evaluated using SDS-PAGE to find the molecular weight distribution of the soy protein and the extent of cross-linking in soy protein. Soy protein from the reaction mixture produced very faint bands on the polyacrylamide gel. Soy protein from the reaction mixture was then concentrated by trichloroacetic acid (TCA) precipitation.

For TCA precipitation, 100% (w/v) Trichloroacetic acid was produced by dissolving 500 g TCA into 350 ml of distilled water and its temperature was maintained at room temperature^[95]. For precipitation, 1 volume of TCA was added to 4 volumes of protein sample from the reaction mixture which causes the protein to form a white fluffy precipitate. The mixture was then incubated for 10 min at 4°C and then centrifuged in an eppendorf centrifuge at 13,200 rpm for 6 min. Centrifugation leads to the precipitate forming a pellet on the walls of the tube. The supernatant liquid was removed leaving the protein pellet intact. The pellet was washed with 200 µl acetone and centrifuged in an eppendorf centrifuge at 13,200 rpm for 6 minutes. This step was repeated for total 2 washes of acetone. Acetone washes were carried out to remove any traces of TCA present in the pellet as residual TCA can interfere with SDS-PAGE analysis of the protein. The pellet was then dried by placing the tube in a Herat block maintained at 95°C for 5 to 10 min to drive off acetone. Residual acetone

can interfere with SDS-PAGE analysis and it was required to eliminate traces of acetone. Herat block consists of wells to keep the tubes at the desired temperature.

For SDS-PAGE, the protein pellet was mixed with 2X sample buffer and was boiled at 95°C for 10 min by placing it in a Herat block. Boiling with sample buffer denatures the protein and breaks secondary forces like H bonds in the protein pellet. The sample was then loaded onto the wells of polyacrylamide gel. The sample also contained low molecular weight dyes which move faster than protein molecules in gel electrophoresis. The movement of dyes gives an indication of the movement of protein. Proteins are invisible till they were stained. The gel was then operated at 200 V till the dyes reached the bottom of the gel. During electrophoresis, allowing the dyes to reach the bottom of the gel achieved maximum separation of different molecular weight bands. The time varied according to the samples and the time required for soy protein samples in this experiment was in the range of 45 to 50 minutes.

Glycinin was separated to analyze the effects of reaction on one protein instead of a mixture of proteins in soy protein. For separation of glycinin from soy protein, the following protocol was followed. The solution from the reaction mixture for preparation of soy protein resin was used. The pH was adjusted to 8.5 with 2N NaOH and stirred for 1 hour at 20°C. The insoluble residue was separated by centrifugation with a Beckman coulter centrifuge at 5000 rpm for 20 minutes. Sodium bisulfate (calculated to give 10mM SO₂) was added to the supernatant liquid. Glycinin was precipitated from solution by adjusting the pH to 6.4 with 2N HCl and storing overnight at 4°C. The cooled protein was centrifuged directly using a Beckman coulter centrifuge at 9800 rpm for 20 minutes. The precipitate obtained was glycinin and was used for SDS-PAGE analysis ^[96].

CHAPTER 4

RESULTS AND DISCUSSION

4.1 Fiber Characterization

This section discusses the results obtained for the tensile tests conducted on various SF-based fibers based on the compositions described in Chapter 3. Tensile stress at fracture (Tensile stress), tensile strain at fracture (Tensile strain) and Young's modulus or modulus (automatic) values were obtained from the tests and are shown in the tables and bar graphs along with the standard deviation bars.

4.1.1. Effect of Glycerol Content on SF-based Fibers

Experiments were conducted to find optimum glycerol content (% by weight of SF) for production of SF-based fibers. The composition with 0% glycerol was very brittle and could not be tested on Instron. Young's modulus also decreases with increase in glycerol content. The values of moisture contents are listed in Table 4.1.

Glycerol is used as a plasticizing agent in SF-based resins. As the glycerol content increases, the free volume of the polymer system also increases. There is also higher moisture absorption due to the hydroxyl groups present in glycerol. It has been shown by Nam and Netravali for SPC resin and by Lodha and Netravali for SPI resin [5, 21], that as glycerol content increases, tensile stress decreases and tensile strain increases due to the plasticizing effect. The mean tensile stress is higher for composition containing 5% glycerol compared to the composition containing 12.5% glycerol as shown in Figure 4.1. Thus, it can be concluded that tensile stress for composition containing 5% glycerol is significantly higher than that of composition containing 12.5% glycerol. Tensile stress and Young's Modulus decreased significantly with increase in glycerol content due to increase in free volume and

increased moisture absorption. Increase in glycerol as well as water content increases free volume that causes T_g to decrease, which makes the resin more flexible and increases tensile strain.

Table 4.1 Moisture contents of SF-based fibers with varying glycerol content

Glycerol content in SF-based fiber	Moisture content (%)
0%	13.9
5%	14.2
12.5%	15.0

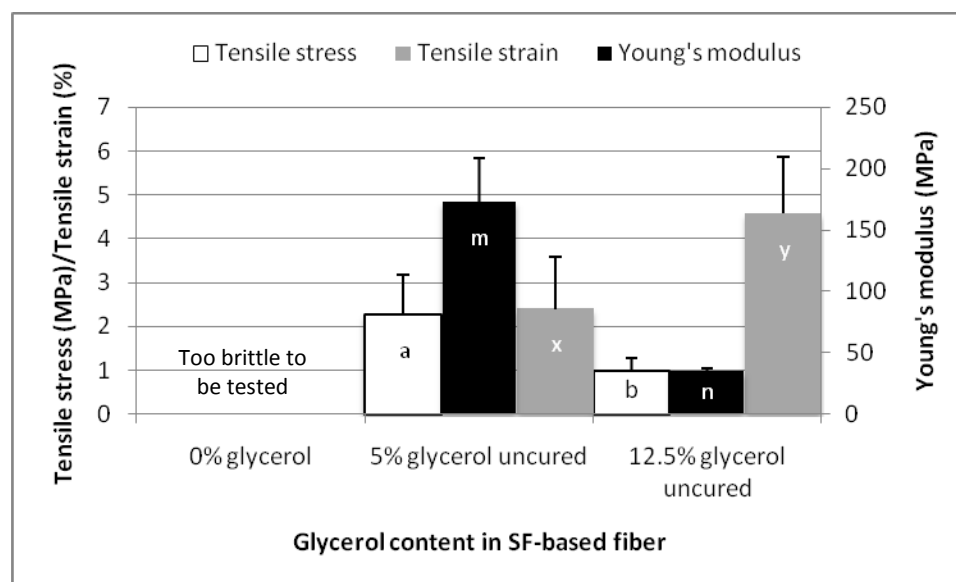


Figure 4.1 Mean and standard deviation of tensile stress, tensile strain and Young's modulus values of SF-based fibers modified with glycerol (Dissimilar letters within a tensile property indicate significant differences (p < 0.05))

For all further work, 5% glycerol (on the weight of SF) was chosen as the optimum glycerol content as the brittleness of fibers and decrease in strength had to be optimized. The control composition chosen for subsequent experiments, therefore, consisted of SF and distilled water in the ratio 1:2.3 and 5% glycerol (on the weight of SF).

4.1.2. Effect of Cellulo[®] Content on SF-based Fibers

Cellulo[®] is a cellulose-based filter aid which exists in the form of fibrils. Cellulo[®] was incorporated in the SF-based resin mixture and an attempt was made to orient Cellulo[®] during extrusion under pressure through the conical pipette tips. Orientation of these fibrils along the fiber axis was expected to increase the tensile properties of these fibers.

As the Cellulo[®] content increased, the moisture content increased from 14.2% for control to 15.3% for composition with 5% Cellulo[®] as seen in Table 4.2. The increase in moisture content can be attributed to the increase in hydroxyl groups available on the surface of Cellulo[®]. Tensile stress increased as seen in Figure 4.2, though not statistically significant, from control to composition with 2% Cellulo[®] and then decreased significantly for composition with 5% Cellulo[®]. Increase in Cellulo[®] content can result in reinforcement if the fibrils are well dispersed which increases the tensile stress as observed for composition with 2% Cellulo[®]. Further increase in Cellulo[®] content, however, results in aggregation and hence the reinforcing effect and hydrogen bonding of the aggregates is offset by their large dimensions which cause irregularity in the resin resulting in defects.

Table 4.2 Moisture contents of SF-based fibers with varying Cellulo[®] content

Cellulo [®] content in SF-based fiber	Moisture content (%)
0% (control)	14.2
2%	14.8
5%	15.3

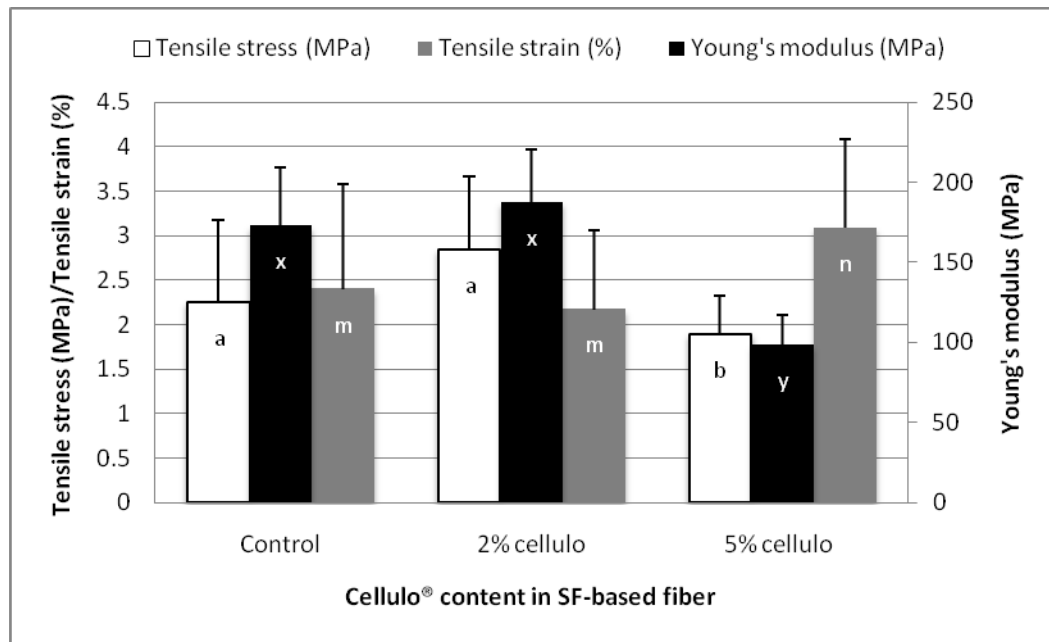


Figure 4.2 Mean and standard deviation of tensile stress, tensile strain and Young's modulus values of SF-based fibers modified with Cellulo[®] (Dissimilar letters within a tensile property indicate significant differences (p<0.05))

As the fibrils aggregate, resin cannot penetrate between them resulting in formation of defects or weak points. The aggregates, thus, behave as defects and cause the tensile stress to decrease significantly as observed for composition containing 5% Cellulo[®]. Tensile strain decreases as seen in Figure 4.2, though not statistically

significant, from control to composition with 2% Cellulo[®] due to the bonding between soy protein and Cellulo[®] which does not allow the polymer chains to flow easily under stress. Tensile strain, however, significantly increases for composition containing 5% Cellulo[®] and this is due to the aggregation of Cellulo[®]. Modulus increases, though not statistically significant, from control to composition with 2% Cellulo[®], indicating increase in stiffness due to reinforcing and hydrogen bonding of Cellulo[®] with soy protein. SF-based fibers with 5% Cellulo[®] shows significant decrease, thus, indicating lower stiffness due to aggregation of Cellulo[®].

4.1.3. Effect of Fitz Milled Grand Prairie (FMGP) Content on SF-based Fibers

FMGP was incorporated in SF-based resin so that the FMGP fibrils can impart strength due to the high aspect ratio of the fibrils. Tensile stress, as expected, increased with increase in FMGP content as can be seen in Figure 4.3 and that of composition with 5% FMGP was significantly greater than the rest. This can again be attributed to the increase in reinforcement and hydrogen bonding with increasing FMGP content that is well dispersed. Tensile strain increased with increase in FMGP content as seen in Figure 4.3. Tensile strain of compositions with 2% and 5% FMGP are significantly greater than control. As the content of FMGP increases, the dispersed FMGP fibrils probably act as crack bridging agents against cracks developing under stress. This crack bridging mechanism resists crack formation and expansion under applied stress and thus the specimen has to be strained more before it fractures. The orientation of fibrils in the resin occurs due to extrusion under pressure through long conical pipette tips. FMGP being a cellulose-based material attracts moisture due to -OH groups present in it and this moisture (Table 4.3) contributes as a plasticizer for the resin and thus decreases the stiffness of the fiber.

Table 4.3 Moisture contents of SF-based fibers with varying FMGP content

FMGP content in SF-based fiber	Moisture content (%)
0% (control)	14.2
2%	16.3
5%	15.3

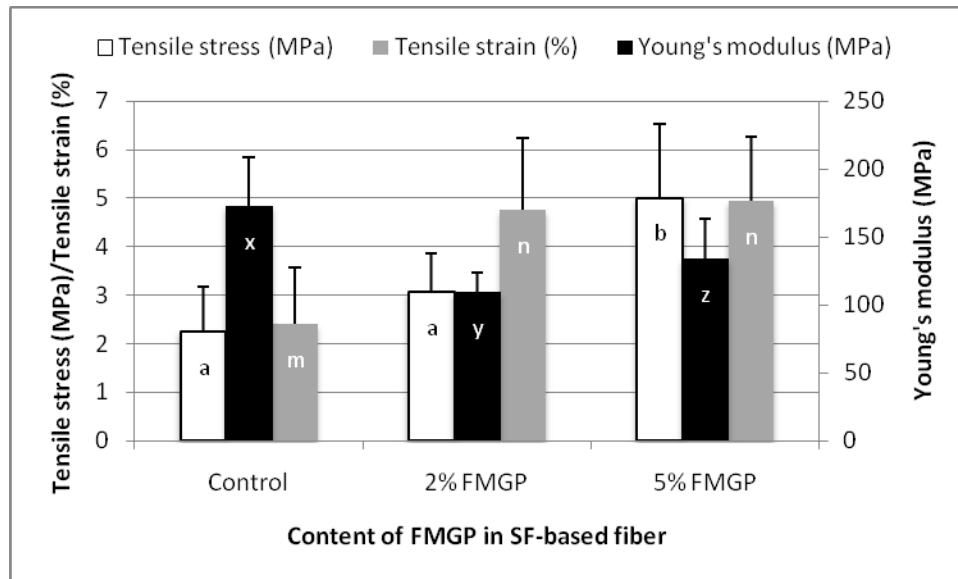


Figure 4.3 Mean and standard deviation of tensile stress, tensile strain and Young's modulus values of SF-based fibers modified with FMGP (Dissimilar letters within a tensile property indicate significant differences ($p < 0.05$))

Young's Modulus decreased significantly for composition with 2% FMGP as compared to control and this can be attributed to increase in moisture content. Modulus, however, increased significantly from composition with 2% FMGP to 5% FMGP which can be attributed to the increased reinforcement perhaps offsetting the negative effects of moisture. Both values, however, were lower than that obtained for the control fiber.

4.1.4. Effect of Micro-crystalline Cellulose (MCC) Content on SF-based Fibers

MCC contains nano-whiskers which tend to aggregate to form particles. MCC was incorporated in SF-based fibers to study its effect on the properties of fibers and the moisture contents of the fibers are listed in Table 4.4. Tensile stress and modulus of cured specimens were higher compared to uncured specimens of the same composition and tensile strain is lower for cured samples as compared to uncured samples of same composition as seen in Figure 4.4. In soy protein, dehydroalanine has been shown to react with lysine and cysteine to form lysinoalanine and lanthionine cross-links, respectively at higher temperatures [35, 36]. Also at higher temperatures, disulfide cross-linking of cysteine takes place. In addition, reaction of asparagine and lysine result in an amide-type of cross-link. The above mentioned reactions occur during the curing process of soy protein increasing the strength of the resin [37, 38]. As seen in Figure 4.4, for same MCC content, cured fibers exhibit higher tensile stress and lower tensile strain compared to the uncured fibers. In Figure 4.4, it is observed that modulus is higher for cured fibers as compared to uncured fibers for same MCC content. Thus, curing at higher temperatures results in cross-linking which causes increase in tensile stress and modulus, but decrease in tensile strain.

Table 4.4 Moisture contents of SF-based fibers with varying MCC content

MCC content in SF-based fiber	Moisture content (%)
0%	14.20
2% uncured	14.40
2% cured	14.43
10% uncured	14.61
10% cured	14.50

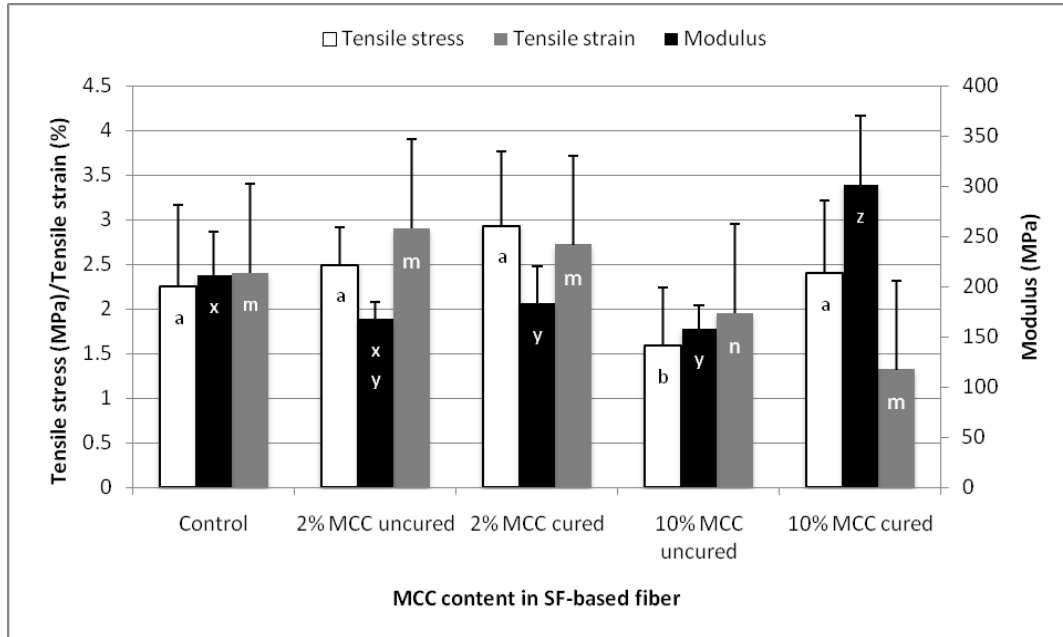


Figure 4.4 Mean and standard deviation of tensile stress, tensile strain and modulus values of SF-based fibers modified with MCC (Dissimilar letters within a tensile property indicate significant differences ($p < 0.05$))

The highly interactive nature of hydroxyl groups on the surface of MCC attracts moisture and causes it to self associate, and therefore, the dispersion is not uniform^[67]. MCC consists of nano-whiskers which tend to aggregate in particle form and these aggregates are of the order of 200 μm . Dispersed nano-whiskers have higher surface area and hence higher number of accessible polar groups which increase moisture content, but if they are aggregated, the resin cannot penetrate in between the MCC nano-whiskers forming weak points or defects. The moisture content (Table 4.4) does not change considerably with addition of MCC. At 2% MCC content, these aggregates offer reinforcement and hydrogen bonding to increase tensile stress. At 10% MCC content, the dispersion is probably poor and aggregates increase in size and behave as large defects and offer decreased hydrogen bonding resulting in decrease in

tensile strain and hence the tensile stress. Tensile strain is higher for up to 2% MCC content indicating crack bridging mechanism. However, at 10% MCC content bigger aggregate particles behave as defects, and the effect of crack bridging mechanism is very low resulting in decreased tensile strain. Modulus decreases for compositions with MCC except for the composition with 10% MCC cured. For uncured specimens with MCC, modulus decreases as the MCC particles behave as defects and do not increase the strength. Cross-linking in composition with 10% MCC cured causes the modulus to increase as it offsets the defective nature of higher aggregates of MCC.

4.1.5. Effect of micro-fibrillated cellulose (MFC) content on SF-based fibers

MFC contains cellulose fibrils which have high aspect ratio and were incorporated to increase the strength of SF-based fibers. Tensile stress gradually increased with increasing content of MFC as seen in Figure 4.5 and this can be primarily attributed to the high aspect ratio of MFC that results in reinforcement. MFC in well dispersed form in the resin will act as crack bridging agents against the cracks developed during straining. Composition with 10% MFC has significantly greater tensile stress than control. Modulus of fiber containing 10% MFC is significantly greater than the rest of the compositions as seen in Figure 4.6. Increase in tensile stress can be attributed to the orientation of linear fibrils along the fibril axis as well as high aspect ratio. The load applied is shared by the fibril network and the excellent mechanical properties of fibrils result in high modulus and tensile strain of the SF-based fiber when dispersed in the resin. Excellent interfacial adhesion due to high aspect ratio and hydrogen bonding on the interface of fibril and SF resin allows the load to be transferred from broken fibrils to the intact neighboring fibrils ^[97].

Table 4.5 Moisture contents of SF-based fibers with MFC (cured and uncured)

MFC content in SF-based fiber	Moisture content (%)
Control (0%)	14.2
0.5% uncured	13.8
0.5% cured	13.42
1% uncured	13.0
1% cured	13.0
2.5% uncured	15.2
2.5% cured	14.8
5% uncured	14.2
5% cured	13.9
10% uncured	13.8
10% cured	14.1

Tensile strain of composition with 0.5% MFC is significantly greater than the rest and can be attributed to crack bridging mechanism due to well dispersed MFC. Tensile strain decreases in composition with higher MFC content, except for the composition with 5% MFC cured and uncured as seen in Figure 4.5. Composition with 5% MFC both cured and uncured, have well dispersed MFC and therefore, show superior mechanical properties compared to other compositions which may not have well dispersed MFC. As MFC content increases, the fibril network in SF-based fiber probably reduces the extent of slippage under strain and hence, the tensile strain decreases. The highly crystalline nature of MFC does not allow it to absorb significant amount of moisture (Table 4.5) even though MFC is hydrophilic in nature. Cured fibers are expected to have higher tensile stress compared to uncured fibers, but the differences observed in Figure 4.5 are not significant.

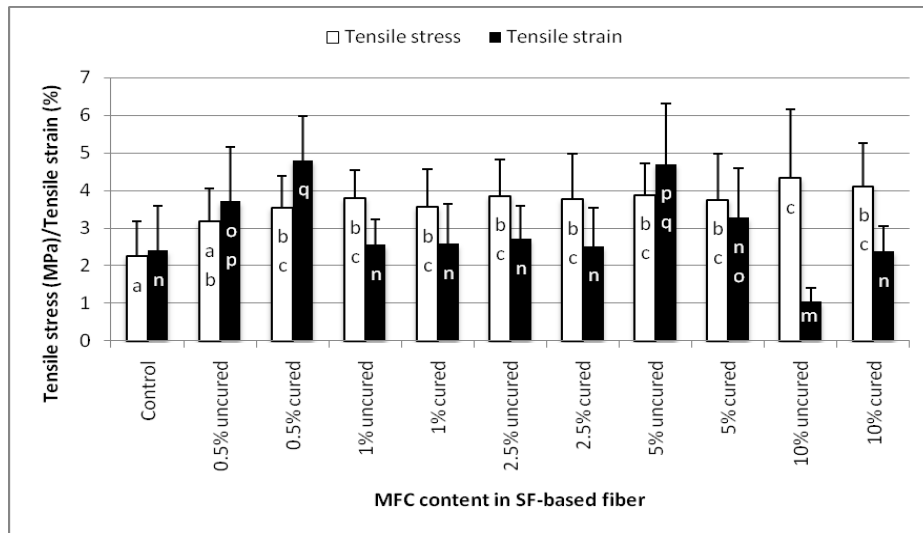


Figure 4.5 Mean and standard deviation of tensile stress and tensile strain values of SF-based fibers with MFC (Dissimilar letters within a tensile property indicate significant differences ($p < 0.05$))

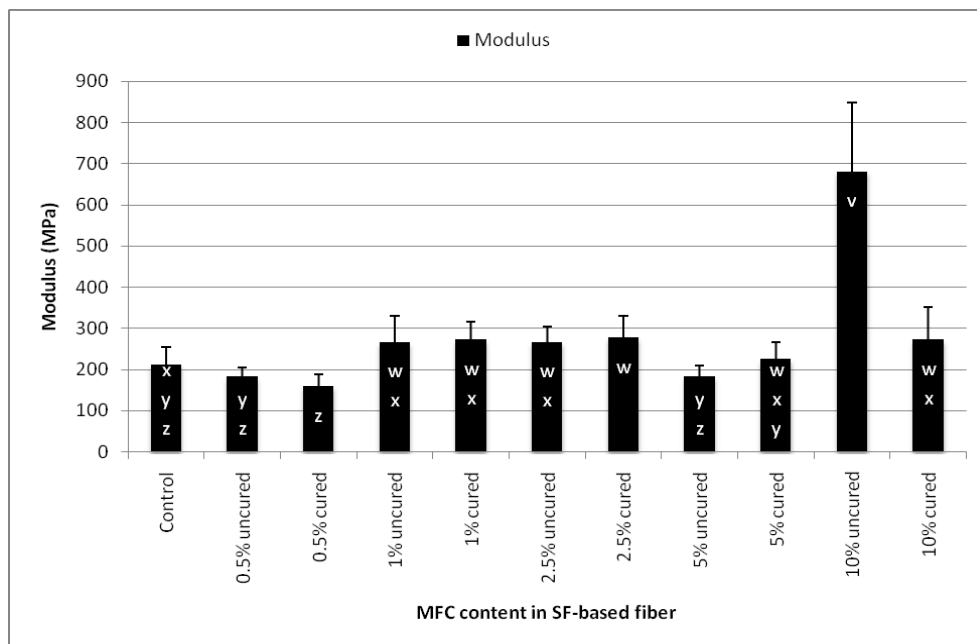


Figure 4.6 Mean and standard deviation of modulus of SF-based fibers with MFC (Dissimilar letters within a tensile property indicate significant differences ($p < 0.05$))

4.1.6. Effect of NB416 Fitz Milled Fiberized (NB416) Content on SF-based Fibers

NB416 similar to FMGP has fibrils with high aspect ratio and was incorporated to increase the strength of SF-based fibers. Moisture content increased for composition with 2% NB416 which is due to moisture absorption of well dispersed NB416 as seen in Table 4.6. Moisture content, however, decreased slightly for composition with 5% NB416. Tensile stress for composition with 5% NB416 was significantly higher than composition with 2% NB416 and control can be seen in Figure 4.7. NB416 fibers like MFC have high aspect ratio and when well dispersed, act as crack bridging agents against cracks developed during straining of the fiber. Increase in tensile stress can be attributed to the orientation of fibrillar structures along the fiber axis that act as reinforcing agents.

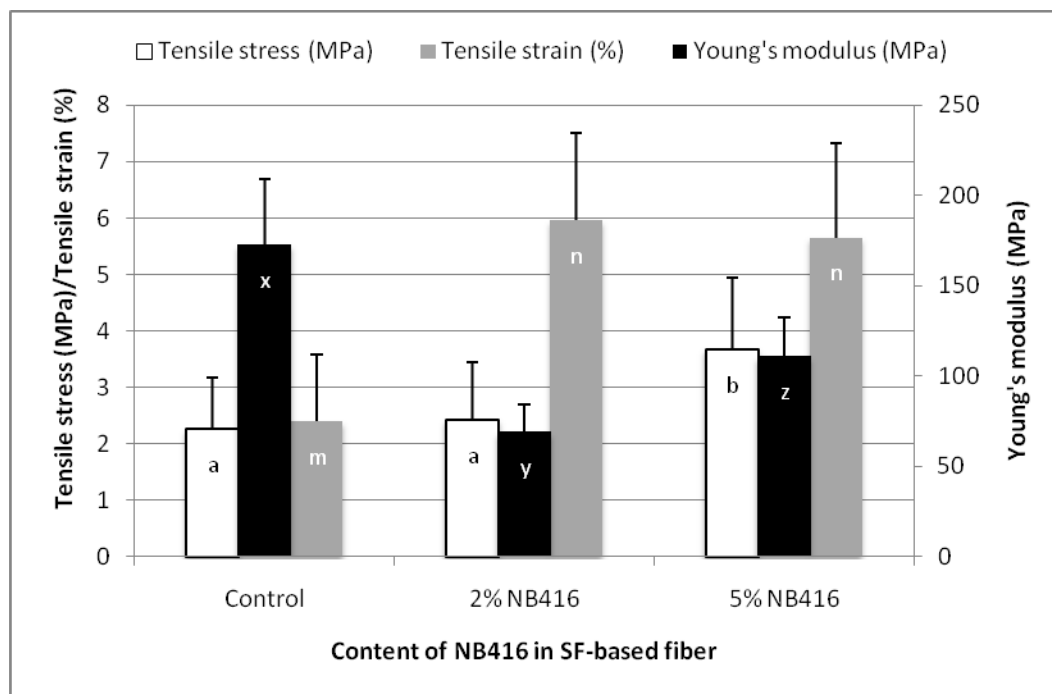


Figure 4.7 Mean and standard deviation of tensile stress, tensile strain and Young's modulus values of SF-based fibers modified with NB416 (Dissimilar letters within a tensile property indicate significant differences ($p < 0.05$))

Table 4.6 Moisture contents of SF-based fibers with varying NB416 content

NB416 content in SF-based fiber	Moisture content (%)
0% (control)	14.2
2%	15.6
5%	15.2

As seen in Figure 4.7, tensile strain values for compositions containing NB416 are significantly higher as compared to control. Increase in tensile strain can be attributed to increased moisture content due to the hydrophilic nature of the additive which acts as a plasticizer and crack bridging mechanism of the fibrils. Young's modulus decreases significantly for composition with 2% NB416 as compared to control and increases significantly for 5% NB416 when compared to composition with 2% NB416. Young's modulus decrease is considered to be due to plasticizing effect of water. However, increase in Young's modulus from composition with 2% NB416 to composition with 5% NB416 due to crack bridging mechanism and reinforcement due to NB416 fibrils.

4.1.7. Effect of Phytigel[®], Agar Agar and Guar Gum Addition on SF-based Fibers

The effect of gums on the SF-based fiber properties was characterized in this study. Addition of Phytigel[®], agar agar and guar gum did not increase the tensile stress, but increased the tensile strain as seen in Figure 4.8 and moisture content as seen in Table 4.7. Both Phytigel[®] and agar agar have been shown to increase mechanical properties of soy resin. However, the amounts needed of Phytigel[®] and agar agar are in the range of 20 to 40% [3, 49]. In this research only small amounts were added and, hence, significant effect could not be obtained.

Table 4.7 Moisture contents of SF-based fibers modified with Phytigel[®], agar agar and guar gum

Composition	Moisture content (%)
0% (control)	14.2
2.5% Phytigel [®] uncured	14.7
2.5% Phytigel [®] cured	14.63
2.5% agar agar uncured	14.96
2.5% agar agar cured	14.81
2% guar cured	15.1

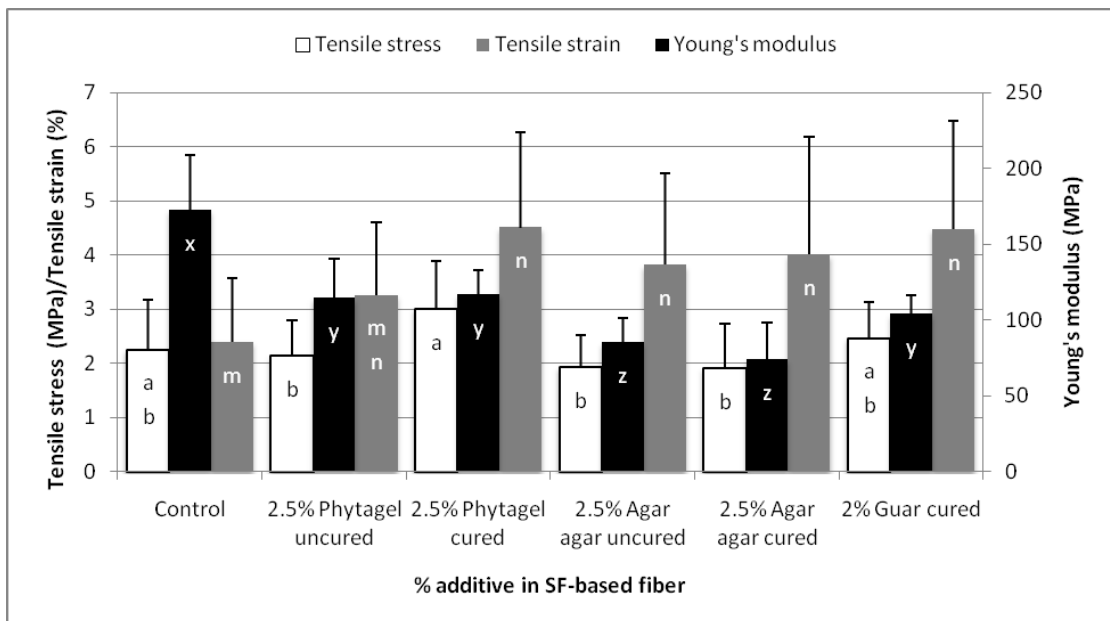


Figure 4.8 Mean and standard deviation of tensile stress, tensile strain and Young's modulus values of SF-based fibers modified with Phytigel[®], agar agar and guar gum (Dissimilar letters within a tensile property indicate significant differences ($p < 0.05$))

Increase in tensile stress of composition with 2.5% Phytigel[®] cured can be attributed to cross-linking due to extrusion at higher temperature. Tensile stress of compositions with 2.5% agar, both uncured and cured, were significantly lower than that of control. Decrease in tensile stress can be attributed to role of the amorphous gums as defects in SF-based fibers during straining of the fibers. Tensile strain of every composition except the one with 2.5% Phytigel[®] was significantly greater than that of control as seen in Figure 4.8. Increase in tensile strain can be contributed to the increase in free volume of the SF-based fiber due to addition of gums which has a plasticizing effect of the SF-based fibers. Young's modulus of every composition was significantly lower than that of control as seen in Figure 4.8. The gums are used as gelling agents ^[3, 97] and the polar groups, primarily hydroxyl groups, which attract water that plasticizes the SF-based resin, which negatively affects the Young's modulus. Decrease in Young's modulus can be attributed to the amorphous nature of the additives and increased moisture absorption.

4.2 Field Trials Evaluation

4.2.1 Preliminary Field Trials to Evaluate Soil Stabilization Effect of SF Fiber Mats

This section discusses the results of the field trials testing the formulations, CONTROL, CELLULO, MCC and MFC which were described in Table 3.1, for soil stabilization. The ryegrass count in micro-plots (measured after 4 weeks) is listed in Table 4.8. Tukey-Kramer test results presented in Figure 4.9 show that there are no significant differences in ryegrass count among treatments. It can be concluded that the effect of four treatments on ryegrass count which is a proxy measure for effect on soil erosion, is not significantly different among the treatments. Although the fiber mat withstood substantial rain and persisted to stay on the soil surface for 28 days (4 weeks), the shrinkage in fiber mats that occurred was sufficient to cause the fibers to

detach from the soil surface and to slowly creep down the incline, exposing the remaining soil and seeds. It was observed that there was greater emergence of grass in areas that remained covered by the fiber as the fibers acted as barriers against migrations of ryegrass seeds. However, the amount of grass was insufficient to cause a significant difference compared to untreated plots.

Table 4.8 Ryegrass seedling establishment as a percentage of number of seeds planted

Fiber formulation	Ryegrass establishment (mean proportion \pm sem)
CELLULO	59.6 \pm 4.6
CONTROL	48.0 \pm 6.6
MCC	68.4 \pm 9.7
MFC	48.8 \pm 1.1

Comparisons for all pairs using Tukey-Kramer HSD (Rye data)				
q*	Alpha			
2.86102	0.05			
Abs(Dif)-LSD	MCC	CELLULO	MFC	CONTROL
MCC	-0.13935	-0.09401	-0.03427	-0.02635
CELLULO	-0.09401	-0.13935	-0.07962	-0.07169
MFC	-0.03427	-0.07962	-0.13935	-0.13142
CONTROL	-0.02635	-0.07169	-0.13142	-0.13935
Positive values show pairs of means that are significantly different.				
Level	Mean			
MCC	A	0.62162800		
CELLULO	A	0.57628400		
MFC	A	0.51655200		
CONTROL	A	0.50862600		
Letter not connected by same letter are significantly different				

Figure 4.9 Results of Tukey-Kramer test for comparison of treatment means of ryegrass count

Table 4.9 presents the results of the fiber mat shrinkage study. It can be seen from Table 4.9 that the shrinkage was highest for MFC followed by MCC and CELLULO formulation had the least shrinkage. However, Tukey-Kramer test showed that the shrinkage was not significantly different among the formulations. These results are shown in Figure 4.10.

Table 4.9 SF-based fiber mat shrinkage as a percent of initial area covered by fibers

Fiber formulation	Shrinkage (mean % \pm sem)
CELLULO	38 \pm 2
MCC	47 \pm 4
MFC	48 \pm 4

Means Comparisons			
Comparisons for all pairs using Tukey-Kramer HSD (shrinkage)			
q*	Alpha		
2.70081	0.05		
Abs(Dif)-LSD			
	MFC	MCC	CELLULO
MFC	-0.13789	-0.13231	-0.05190
MCC	-0.13231	-0.13789	-0.05748
CELLULO	-0.05190	-0.05748	-0.15417
Positive values show pairs of means that are significantly different.			
Level	Mean		
MFC	A	0.47916000	
MCC	A	0.47358000	
CELLULO	A	0.38480000	
Levels not connected by same letter are significantly different.			

Figure 4.10 Results of Tukey-Kramer test for comparison of shrinkage means

4.2.2 Greenhouse Trials for Evaluation of Shrinkage of SF-based Fiber Mats

Three compositions were used for field trials, control, glutaraldehyde cross-linked SF-based fibers (GA) and glyoxal cross-linked SF-based fibers (GL). GA and

GL fibers were used for the greenhouse study because the study aimed at increasing the durability of the fiber mat. Other compositions like SF-based fibers with MFC had increased strength, but the moisture resistance did not increase. As a result, their life was not expected to improve substantially, and hence these fibers would not perform satisfactorily in rainy conditions. Cross-linked resins are expected to give reduced moisture absorption increased the life of the fiber mat. Cross-linked fibers may swell as they absorb moisture but once the water source is removed, they could dry without causing significant damage or disintegration.

The photographic images of the micro-plots are shown in Figures 4.11, 4.12 and 4.13. Figure 4.11 shows the images for control (SF with no cross-linker) micro-plot on day 1 and at the end of weeks 1, 4, 5, 6 and 7. Figure 4.12 shows the images for micro-plot of SF-based fibers cross-linked with glutaraldehyde (GA) on day 1 and at the end of weeks 1, 4, 5, 6 and 7. Figure 4.13 shows the images for micro-plot of SF-based fibers cross-linked with glyoxal (GL) on day 1 and at the end of weeks 1, 4, 5, 6 and 7. The micro-plots were observed every week for shrinkage. As seen from Figure 4.12 the GA fibers disintegrated after 28 days and the fiber mat area could not be recorded thereafter. SF-based fiber mats were observed to shrink in both dry and wet environments. Shrinkage of SF-based fiber mats is an important concern as any dimensional change is not favorable whatever the formulation is used for the application.

The SF-based fiber mats were subjected to wet environment after 28 days until 49 days. The GA composition fibers disintegrated on exposure to wet environment. There was no reading recorded for dimensions of GA composition fibers after 28 days and for all compositions after 49 days as all fiber mats degraded after 49 days.

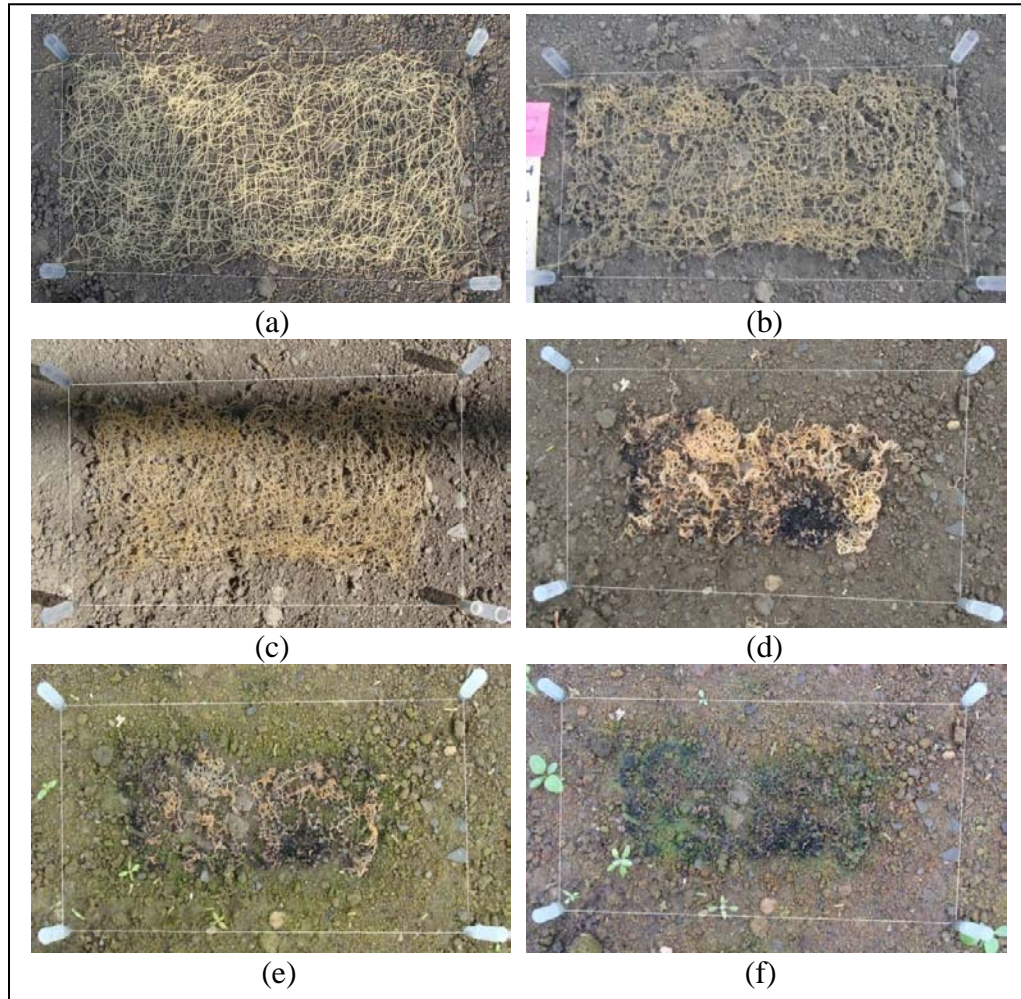


Figure 4.11 Photographic images of micro-plots of Control treatment on (a) day 1 just after extrusion; (b) week 1, dry condition; (c) week 4, dry condition; (d) week 5, wet condition; (e) week 6, wet condition and (f) week 7, wet condition

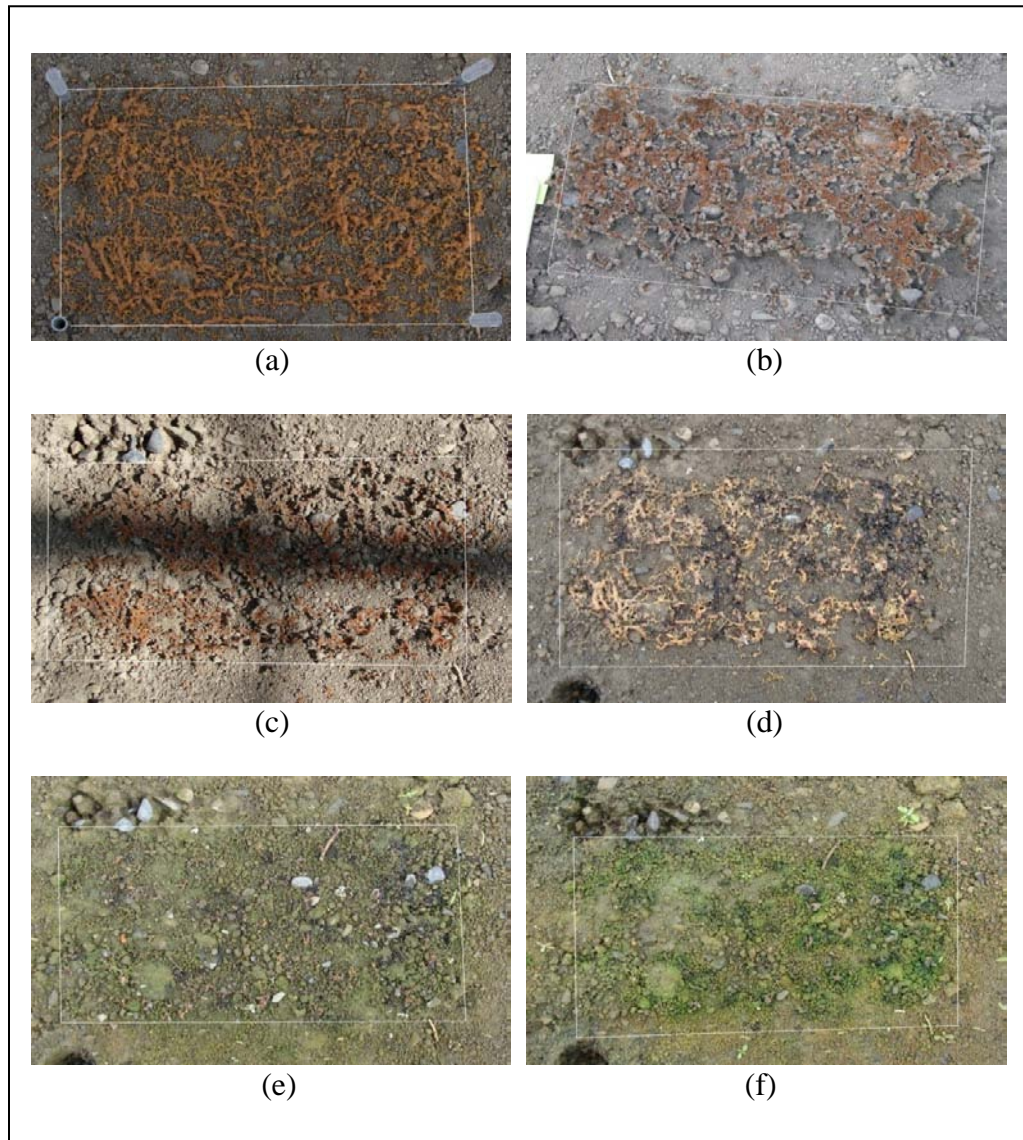


Figure 4.12 Photographic images of micro-plots with GA formulation on (a) day 1 just after extrusion; (b) week 1, dry condition; (c) week 4, dry condition; (d) week 5, wet condition; (e) week 6, wet condition and (f) week 7, wet condition

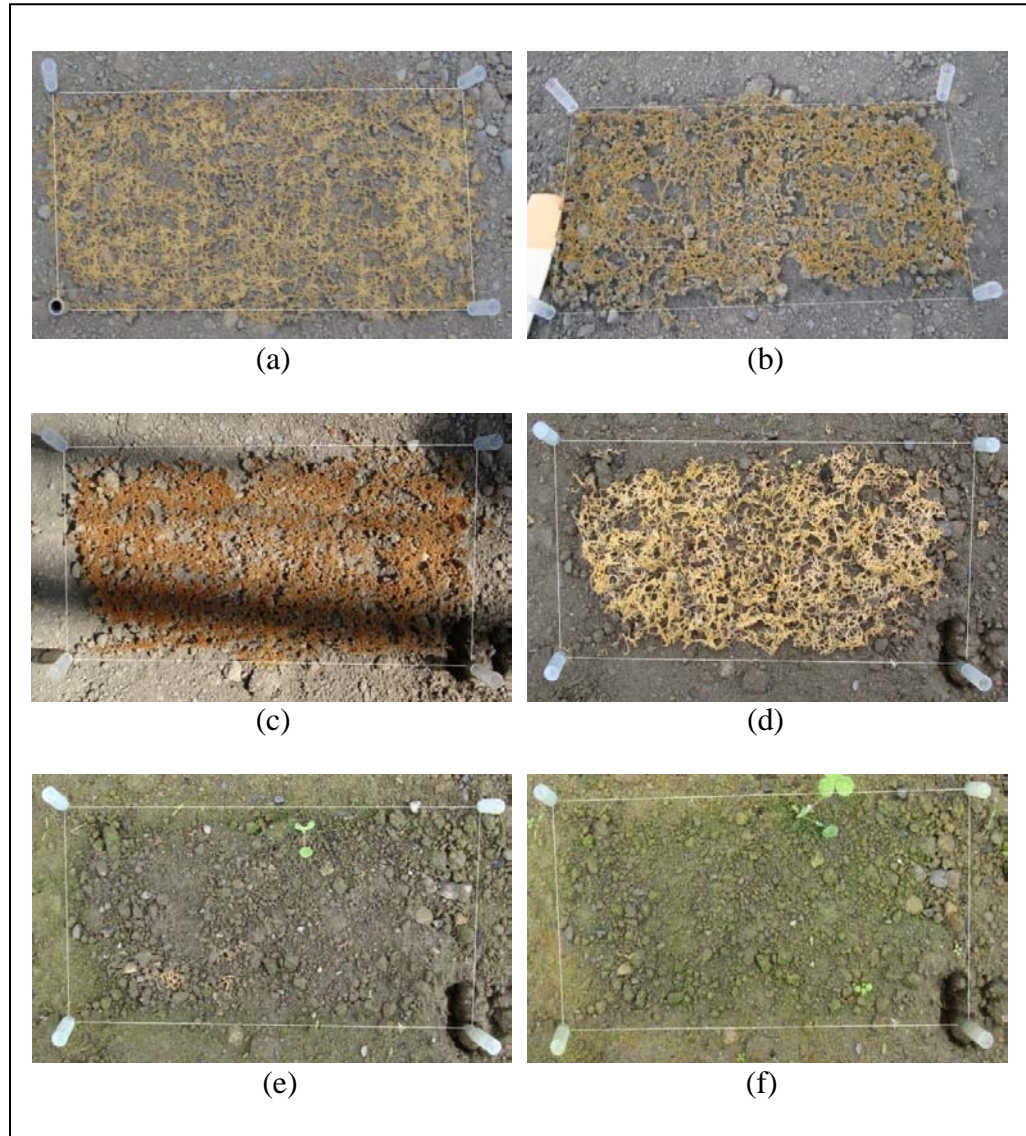


Figure 4.13 Photographic images of micro-plots with GL formulation on (a) day 1 just after extrusion; (b) week 1, dry condition; (c) week 4, dry condition; (d) week 5, wet condition; (e) week 6, wet condition and (f) week 7, wet condition

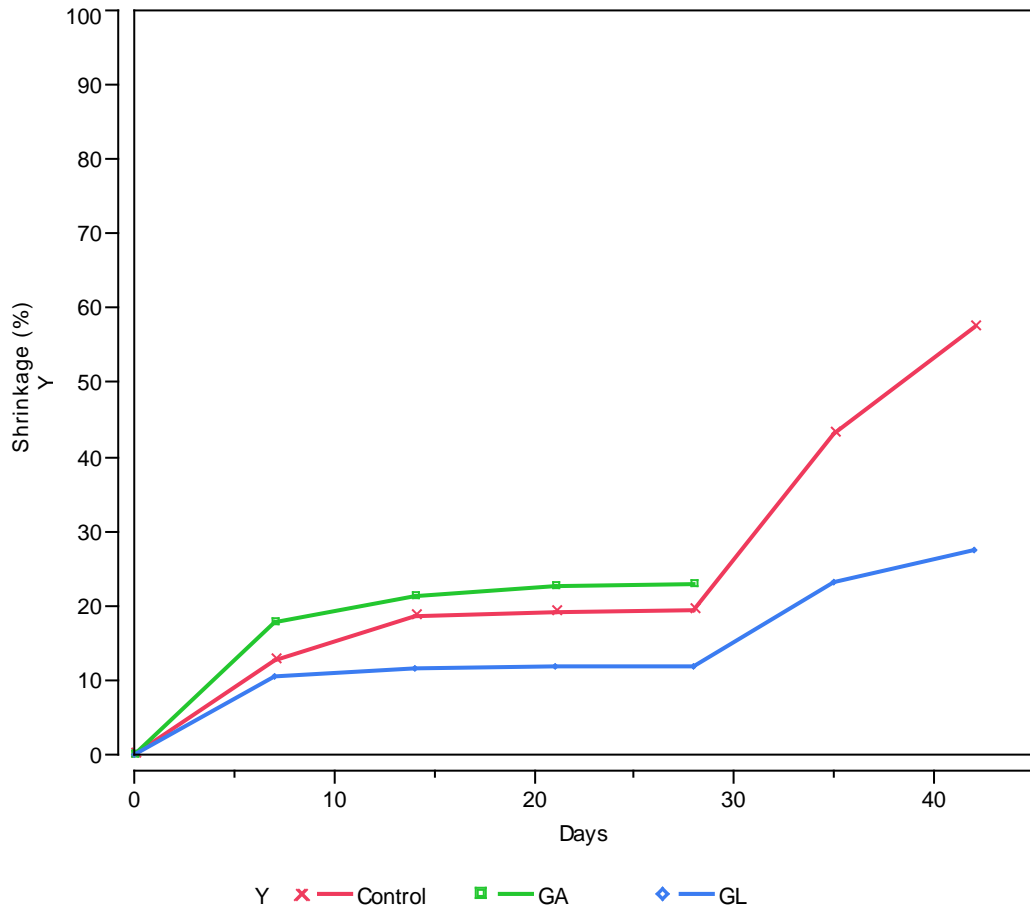


Figure 4.14 ‘Shrinkage’ by ‘days’ graph of SF-based fibers during field trials

The initial shrinkage is due to the evaporation of water used (230% on the weight of SF) in the resin to extrude fibers and the shrinkage appears to be uniform in length and width of the plot. GA fiber mats showed high initial shrinkage due to residual glutaraldehyde causing further cross-linking in the fibers as seen in Figure 4.12. Not all amine groups are available for cross-linking due to steric hindrance and therefore, residual glutaraldehyde is found after reaction. The area of GA fiber mats could not be calculated after 28 days as the fiber mat lost its structural integrity. GA fiber mats showed highest shrinkage initially and were greater than other two treatments in the dry environment. GA fiber mats developed brown color as seen in

Figure 4.12 which indicates the cross-linking reaction between glutaraldehyde and soy protein. GL fiber mats showed least amount of shrinkage during both dry and wet environments as seen in Figures 4.13 and 4.14. GL fiber mats also developed orange color as seen in Figure 4.13 indicating cross-linking reaction between glyoxal and soy protein. However, rate of cross-linking in GA fiber mats is faster as compared to GL fiber mats as observed from the faster change of color in GA fiber mats. Shrinkage in area of control fiber mats was intermediate as compared to the other two formulations; control and GA and the shrinkage increased rapidly in the wet environment. Dry condition was maintained up to 28 days and the maximum shrinkage observed was 22.85%. The shrinkage increased rapidly in wet condition and the fiber mats became soft and showed signs of biodegradation in wet condition ^[94]. Control fiber mats showed highest shrinkage at the end of experiment while GL fiber mats showed less shrinkage which can be attributed to the cross-linking of soy protein. GL fiber mats showed more dimensional stability as compared to control due to its cross-linked nature.

In the case of GA fiber mat, the reaction of glutaraldehyde is fast with soy protein and the reaction taking place after extrusion caused the mat to shrink due to increase in cross-link density. After the reaction in GA fiber mats, the evaporation of water caused the fiber mats to lose its structural integrity as the soy protein was already heavily cross-linked and evaporation of water caused the fiber to become brittle. In case of GL fiber mat, reaction of glyoxal is slow as compared to reaction glutaraldehyde with soy protein ^[50]. The slow reaction of glyoxal with soy protein and gradual evaporation of water meant that the fiber mat was not strained to dimensional stresses of enough magnitude, due to cross-linking and shrinking, to destroy the structural integrity of the GL fiber mat. In the case of control fiber mats, the shrinkage is primarily due to the evaporation of water and was not of enough magnitude to

destroy structural integrity of the fiber mat. In wet environment, all the fiber mats absorbed water and became soft. In case of GL fiber mats, the water absorption in wet environment as observed in Figure 4.13 is less as the mat is cross-linked and the amount of polar groups available for moisture absorption is low. GL fiber mats were completely biodegraded at the end of 49 days. In case of control fiber mat, the water absorption in wet environment is high as compared to GL fiber mat, as it contains larger number of polar groups for water absorption. All three fiber mats were completely biodegraded at the end of 49 days (7 weeks) proving the fully biodegradable nature of SF-based fibers as seen in Figures 4.11, 4.12 and 4.13.

4.2.3 Field Trials for Evaluation of SF-based Resin on Seed Germination and Soil Stabilization

The treatments used were CONTROL, SL, SH, SS and HYDRO and their arrangement is shown in Figure 4.15. Generalized mixed model was fitted to shoot count data as the response variable and the response was assigned Poisson distribution due to the skewed nature of the data. The fixed effects test results are listed in Table 4.10 and the tukey HSD test results for differences in shoot count are shown in Table 4.11.

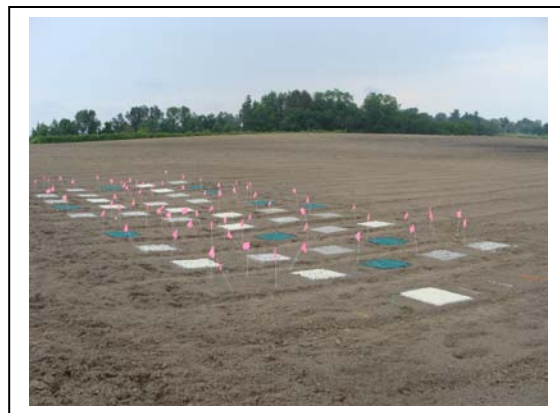


Figure 4.15 Arrangement of micro-plots for field trials described in section 3.8.3.

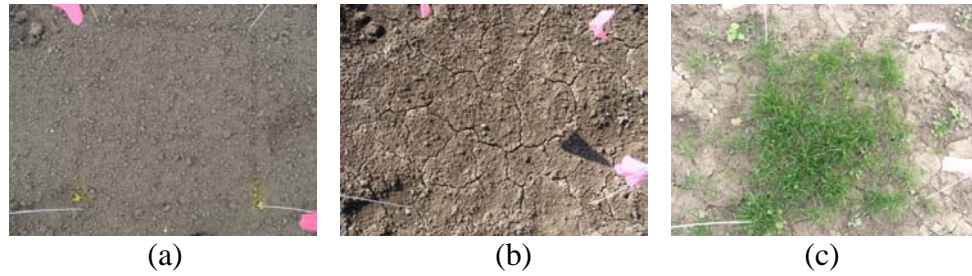


Figure 4.16 Photographic images of micro-plots for CONTROL on (a) day 1; (b) day 9 and (c) day 43

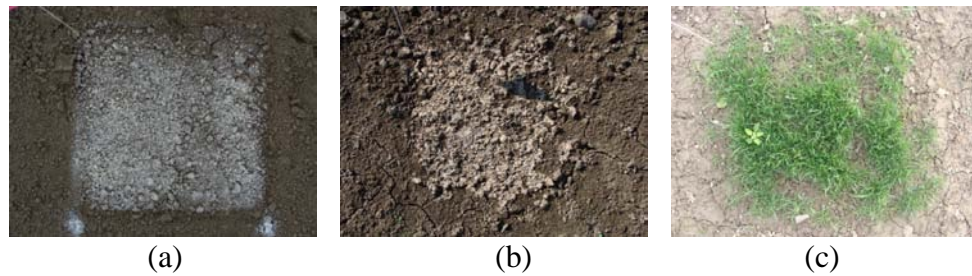


Figure 4.17 Photographic images of micro-plots for soy light (SL) treatment on (a) day 1; (b) day 9 and (c) day 43

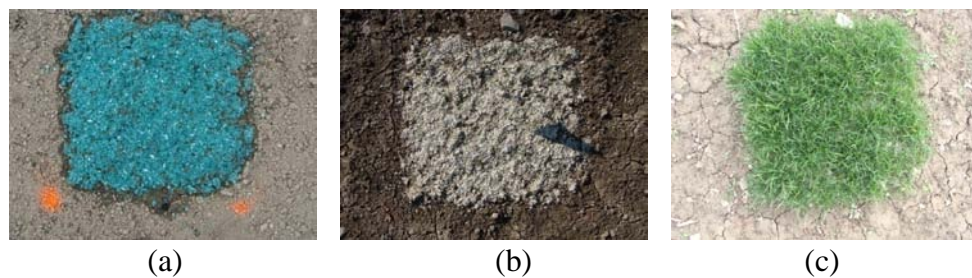


Figure 4.18 Photographic images of micro-plots for hydromulch (HYDRO) treatment on (a) day 1; (b) day 9 and (c) day 43

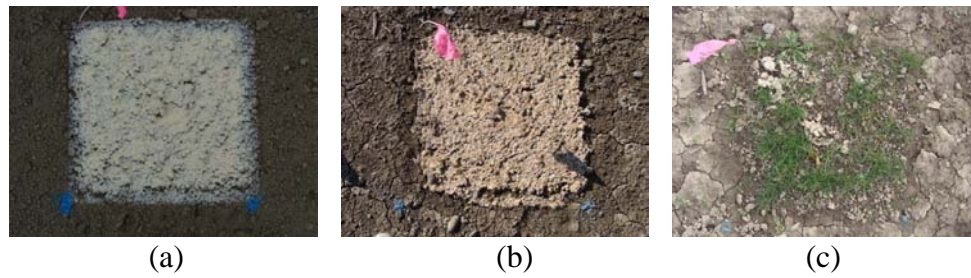


Figure 4.19 Photographic images of micro-plots for soy heavy (SH) treatment on (a) day 1; (b) day 9 and (c) day 43

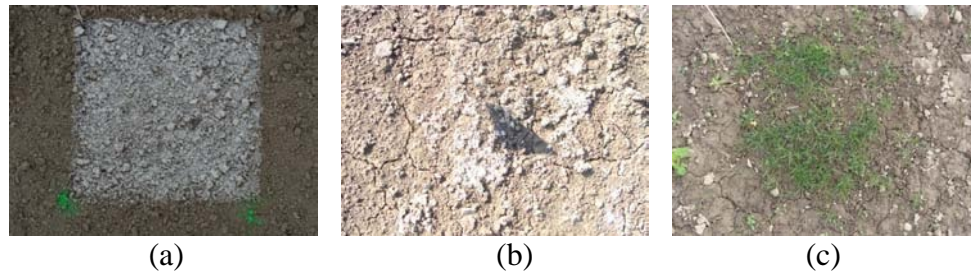


Figure 4.20 Photographic images of micro-plots for soy seed (SS) treatment on (a) day 1; (b) day 9 and (c) day 43

As seen in Table 4.10, the parameters ‘Days’, ‘Treatment’ and interaction ‘Days by Treatment’ have significant effects on shoot count. Figure 4.21 shows variation of ‘shoot count’ x ‘days’ for the five treatments used. From adjusted p-values in Table 4.11, it can be deduced that shoot counts for treatments SL and HYDRO are not significantly different, but both are significantly higher than for CONTROL. It can, therefore, be concluded that treatment SL, even though it was applied in light amount, is as effective for soil stabilization and crop protection, as treatment HYDRO which contains commercially available hydromulch. Hydromulch was applied manually due to lack of suitable equipment and larger amount of hydromulch was used than that would have been used for mechanical mode of application. There is no significant difference between SH and CONTROL according to Table 4.11.

Table 4.10 Fixed effect test from generalized mixed model for field trials

Type III Tests of Fixed Effects				
Effect	Num DF	Den DF	F Value	Pr > F
Treatment	4	36	28.97	<.0001
Days	2	390	250.88	<.0001
Days*Treatment	8	390	2.92	0.0035

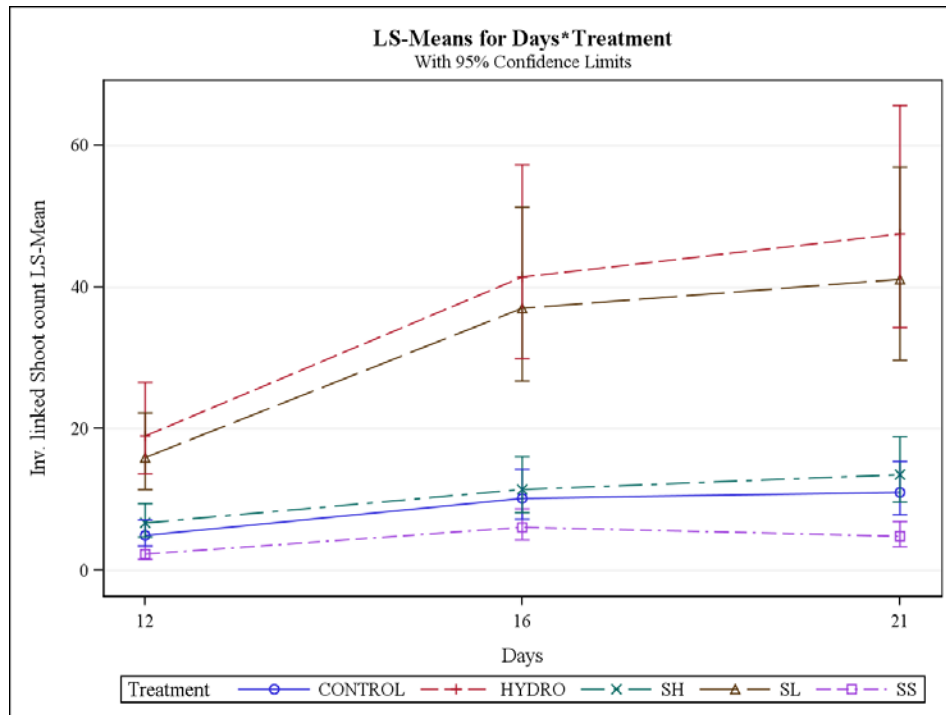


Figure 4.21 Plot showing 'shoot count' x 'days' for field trials in section 4.2.3

Table 4.11 Tukey HSD test results for shoot count difference among treatments

Treatment	Treatment	Estimate	Standard Error	DF	t Value	Pr > t	Adj P	Alpha
CONTROL	HYDRO	-1.4018	0.2301	36	-6.09	<.0001	<.0001	0.05
CONTROL	SH	-0.2062	0.2318	36	-0.89	0.3796	0.8989	0.05
CONTROL	SL	-1.2584	0.2302	36	-5.47	<.0001	<.0001	0.05
CONTROL	SS	0.6960	0.2365	36	2.94	0.0057	0.0422	0.05
HYDRO	SH	1.1956	0.2287	36	5.23	<.0001	<.0001	0.05
HYDRO	SL	0.1435	0.2271	36	0.63	0.5315	0.9689	0.05
HYDRO	SS	2.0978	0.2334	36	8.99	<.0001	<.0001	0.05
SH	SL	-1.0521	0.2289	36	-4.60	<.0001	0.0005	0.05
SH	SS	0.9022	0.2352	36	3.84	0.0005	0.0042	0.05
SL	SS	1.9544	0.2335	36	8.37	<.0001	<.0001	0.05

SH was tested for its weed suppression effect and suppressed growth of shoots on the applied area and the grasses grew only after biodegradation of SF-based resin. Hence, SH was satisfactory from the point of view of weed suppression. On the other hand, low shoot count in CONTROL was due to migration of ryegrass seeds from the micro-plot because of wind and rain. Heavy rains and wind were observed between day 9 and day 12 of the study which displaced ryegrass seeds, especially in CONTROL micro-plots, since the seeds were not covered by any material. Thus, statistical comparison between CONTROL and SH is not conclusive but the weed suppression effect of SH is evident from images in Figure 4.19. Shoot count for SS was significantly greater than that of CONTROL implying the satisfactory effect of SS on protection and support for ryegrass seeds. However, the shoot count for SS was lower than SL and this was due to fact that all the seeds in SS composition could not be sprayed with the sprayer and the actual number of ryegrass seeds on SS micro-plot was lower than 200. For SL and HYDRO, 200 ryegrass seeds were laid manually on the micro-plot and hence both had shoot counts that were significantly higher compared to SS. For SH treatment, shoot count was significantly lower than that for

both SL and HYDRO and this was predicted due to the weed suppression nature of SH treatment. SL and HYDRO treatments were used with an aim to provide support and aid growth of ryegrass seeds resulting in higher shoot counts compared to lower shoot counts of SH treatment which was used with aim of growth suppression.

Biomass was analyzed at the end of the field trials (43 days) to study the effect of treatments. A model using restricted maximum likelihood (REML) was fit with ‘logbiomass’ (logarithmic transformation of biomass weight to ensure normality is maintained) chosen as a response variable, and block and treatment as predictor variables. Block was assigned random attribute in the analysis. The tukey HSD test results are listed in Table 4.12. The biomass weights for the 5 treatments CONTROL, SL, SS, SH and HYDRO are listed in Table 4.13.

Table 4.12 Tukey HSD results for biomass means

Effect	Treatment	Treatment	Estimate	Standard Error	DF	t Value	Pr > t	Adj P
Treatment	CONTROL	HYDRO	-0.7809	0.1913	35	-4.08	0.0002	0.0022
Treatment	CONTROL	SH	-0.01968	0.1966	35	-0.10	0.9208	1.0000
Treatment	CONTROL	SL	-0.7423	0.1913	35	-3.88	0.0004	0.0038
Treatment	CONTROL	SS	0.2119	0.1869	35	1.13	0.2646	0.7877
Treatment	HYDRO	SH	0.7613	0.1966	35	3.87	0.0005	0.0039
Treatment	HYDRO	SL	0.03861	0.1913	35	0.20	0.8413	0.9996
Treatment	HYDRO	SS	0.9929	0.1869	35	5.31	<.0001	<.0001
Treatment	SH	SL	-0.7227	0.1966	35	-3.68	0.0008	0.0066
Treatment	SH	SS	0.2316	0.1923	35	1.20	0.2365	0.7488
Treatment	SL	SS	0.9543	0.1869	35	5.10	<.0001	0.0001

Table 4.13 Biomass weight data for Field Trials

Treatment	Biomass (g)		
	Mean	Standard deviation	Standard error mean
CONTROL	20.02	7.99	2.52
HYDRO	42.41	13.83	4.37
SH	24.97	15.96	5.04
SL	40.17	10.12	3.20
SS	13.70	4.00	1.26

From tukey HSD analysis in Table 4.12, it can be concluded that biomass of plots containing HYDRO, SL (soy light) are significantly higher than that of CONTROL. HYDRO treatment contains hydromulch which was able to retain water as it contains cellulose and provides satisfactory coverage facilitating germination and stopping the grass seeds from migrating. It also has to be taken into account that hydromulch was applied manually, in higher amounts than normal, and the higher shoot counts observed, thus, were a result of more hydromulch than used for conventional purpose. SL treatment was not able to retain water on surface as it was a light application of soy protein formulation, but provided satisfactory coverage to stop migration of seeds. CONTROL treatment did not have any applied treatment and the seeds migrated due to natural elements such as rain and wind occurring during the course of this experiment. It was verified by ryegrass growth outside the boundaries of micro-plots where no ryegrass seeds were sown. Plots containing SS treatment did not show good grass growth and the possible reason is that the number of seeds desired to be sprayed might not have extruded through the sprayer. Plots containing SH (soy heavy) treatment contained heavy application of SF and its potential use was for weed suppression. SH treatment gradually degraded over the course of this study (43 days) and then the grass seeds were able to germinate. The weed suppression effects of SH

treatment, however, cannot be concluded from the biomass study as the biomass was measured at the end of the study. Soy protein in SH treatment degraded during the study and the grass was able to grow and therefore, the weed suppression cannot be evaluated using the biomass study.

After evaluation of biomass, the grasses were analyzed for nitrogen content. Since nitrogen content and carbon content showed correlation, nitrogen content was adjusted for 50% carbon content and the means are listed in Table 4.14 along with standard deviations in parentheses. A model was fit with the adjusted nitrogen % as the response variable. The tukey HSD result for adjusted nitrogen % by treatments is shown in Figure 4.22. Treatment with SH shows significantly higher nitrogen content than with treatments SL, HYDRO and SS. It is not possible to conclude whether SH results in degradation of soy resulting in increase in nitrogen content as it does not differ significantly with CONTROL which has no treatment.

Table 4.14 Carbon %, Nitrogen % and adjusted nitrogen % of grasses from different treatments in field trials

Treatment	Mean carbon % (S.D.)	Mean nitrogen % (S.D.)	Mean adjusted nitrogen % (S.D.)
SH	42.78 (0.853)	4.73 (0.213)	5.53 (0.244)
CONTROL	43.00 (0.599)	4.71 (0.173)	5.47 (0.157)
SS	37.40 (4.384)	3.93 (0.48)	5.26 (0.180)
SL	42.39 (1.887)	4.49 (0.211)	5.30 (0.242)
HYDRO	43.34 (0.384)	4.34 (0.161)	5.01 (0.189)

LSMeans Differences Tukey HSD				
$\alpha=0.050$ $Q=2.84411$				
LSMean[i] By LSMean[j]				
Level				Least Sq Mean
SH	A			5.5330691
CONTROL	A	B		5.4778585
SL	A	B		5.3035047
SS		B	C	5.2633021
HYDRO			C	5.0145369

Levels not connected by same letter are significantly different.

Figure 4.22 Tukey HSD results for nitrogen content of grass in field trials

It is inconclusive whether soy protein degradation directly contributes to increase nitrogen content in ryegrass plant. Soy protein degradation returns nutrients to the soil but it is unclear whether the ryegrass absorbs nitrogen resulting from the process. Ryegrass from HYDRO micro-plots has lowest adjusted nitrogen content which could be due to absence of soy protein but it is inconclusive as CONTROL treatment also does not have soy protein but has the second highest adjusted nitrogen content.

4.2.4 Greenhouse Trials for Evaluation of SF Resin on Seed Germination

The results of greenhouse trials for evaluation of SF-based resins on seed germination under controlled conditions are discussed in this section. The photographs of typical block at different time points in the greenhouse study are shown in Figure 4.23. A generalized mixed model was fit with shoot count as the response variable (No transformation needed as residuals were normal after the model was fit) and ‘block’, ‘treatment’, ‘block x treatment’ interaction, ‘days’ and ‘days x treatment’ interaction as predictors.

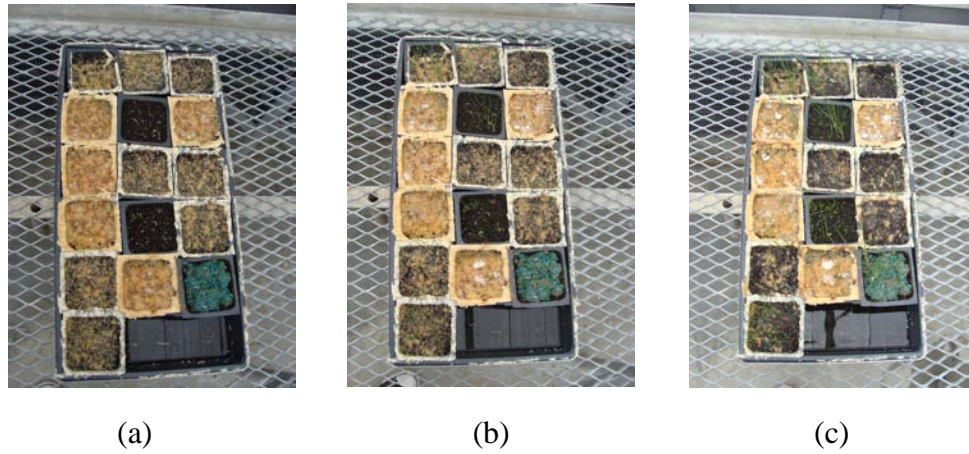


Figure 4.23 Image of a greenhouse tray (a typical block) on (a) day 1; (b) day 3 and (c) day 7

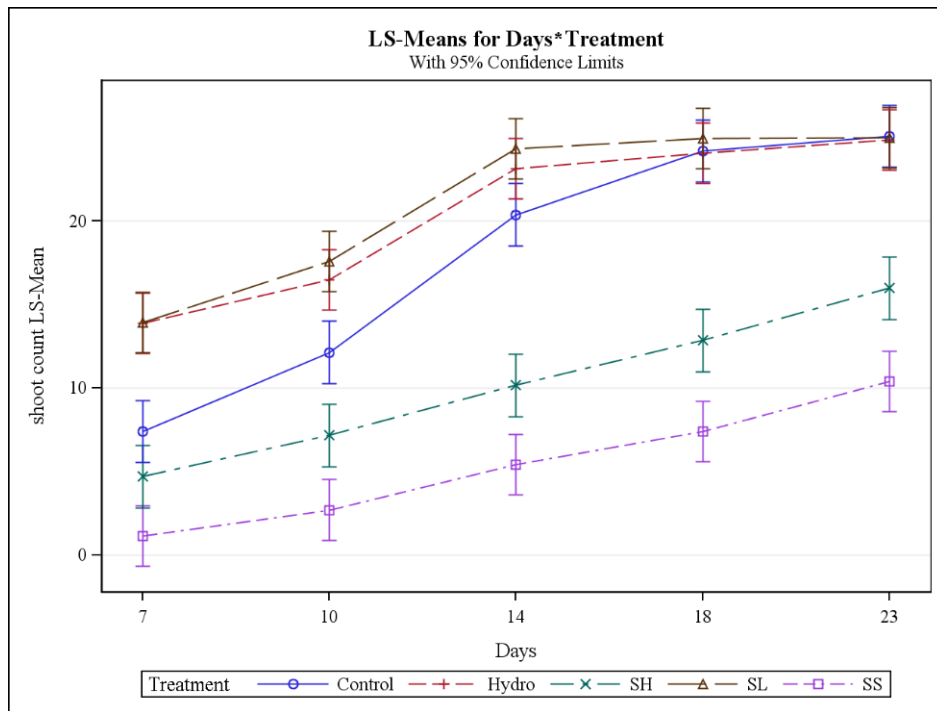


Figure 4.24 Graph showing 'shoot count' x 'days' grouped for each 'treatment' for greenhouse trials in section 4.2.4

Table 4.15 Fixed effects result for greenhouse trials

Type III Tests of Fixed Effects				
Effect	Num DF	Den DF	F Value	Pr > F
Treatment	4	34	90.14	<.0001
Days	4	732	469.34	<.0001
Days*Treatment	16	732	12.31	<.0001

Table 4.16 Tukey HSD for shoot count among treatments

Differences of Treatment Least Squares Means Adjustment for Multiple Comparisons: Tukey-Kramer							
Treatment	Treatment	Estimate	Standard Error	DF	t Value	Pr > t	Adj P
Control	Hydro	-2.6492	1.0421	34	-2.54	0.0157	0.1049
Control	SH	7.6646	1.0703	34	7.16	<.0001	<.0001
Control	SL	-3.3228	1.0458	34	-3.18	0.0032	0.0246
Control	SS	12.4218	1.0493	34	11.84	<.0001	<.0001
Hydro	SH	10.3138	1.0419	34	9.90	<.0001	<.0001
Hydro	SL	-0.6736	1.0169	34	-0.66	0.5121	0.9630
Hydro	SS	15.0710	1.0204	34	14.77	<.0001	<.0001
SH	SL	-10.9875	1.0443	34	-10.52	<.0001	<.0001
SH	SS	4.7572	1.0479	34	4.54	<.0001	0.0006
SL	SS	15.7447	1.0230	34	15.39	<.0001	<.0001

From Figure 4.24, it can be observed that shoot count for HYDRO and SL treatments increased from day 7 to day 14 and then levels off. Shoot count for SH treatment was initially low, but increased over the course of study (23 days) owing to the degradation of soy protein formulation. For CONTROL treatment, the shoot count increased steadily but was lower than SH, HYDRO and SL treatments. Shoot count for SS was lowest due to lower number of seeds present in the cells. It was found that the sprayer could not spray all the incorporated seeds in the micro-plot cell and hence, the total number of seeds in a cell containing SS treatment was lower than 25.

According to tukey HSD results from Table 4.16, it can be observed that the shoot count for SL and HYDRO treatments are significantly greater than that of CONTROL. SL and HYDRO are able to hold water and keep the cell moist resulting in faster germination rate and growth rate. There was no significant difference between shoot counts of SL and HYDRO treatments. It can, thus, be concluded that SL treatment is as effective as commercially available hydromulch used in HYDRO treatment for preventing soil erosion and aiding the growth of crops. Shoot count for SS treatment was significantly lower than the rest of the treatments. Shoot counts for HYDRO and SL treatments are significantly greater than that of SH as expected because SH was used for weed suppression contrary to the aims of using SL and HYDRO. From the shoot count growth profile in Figure 4.24, it can be seen that the shoot count increased with time and simultaneous degradation of soy protein formulation and all the seeds have grown by the end of the study. SH treatment, thus, can be used to manipulate the growth rate and germination rate of crops if desired. Shoot count for SH treatment was significantly higher than that of CONTROL and could be due to moisture holding capability of SH treatment which supports the seed and increases the germination rate of ryegrass seeds. The results of greenhouse trials are similar to that of field trials even though the parameters of temperature and relative humidity were regulated and natural elements of wind and rain were absent. This study confirms the scope for potential application of soy protein formulations to prevent soil erosion, protect seeds and improve germination conditions. Heavy application of soy protein formulation can be used to suppress weed or manipulate growth rate of crops as desired.

4.3 Characterization of Cross-linked Resin with Eco-friendly Cross-linking Agents

4.3.1 Tensile Properties

The tensile stress, tensile strain and Young's modulus values are shown in Figure 4.25. Statistical analyses were not carried out as the sample size was 7 for resin testing and normality of the data could not be established due to lower sample size. Resins prepared using B and D processes appear to have increased tensile properties. In processes B and D, the common step is precuring at 80°C for 40 minutes. It can be inferred that precuring at 80°C which results in unfolding of polypeptide chains and allows the orientation of polymer chains ^[19, 40], is required for achieving higher tensile stress and Young's modulus in SF-based resins. Resin prepared under C condition showed increased strain due to slipping of un-reacted polymer chains which is indicated due to presence of lower molecular weight bands in SDS-PAGE shown in section 4.3.2.

Resin produced using process A showed decreased tensile strength due to degradation of protein under those conditions involving longer times of the order of 120 minutes at a high temperature of 80°C. The degradation of proteins was observed in SDS-PAGE analysis (section 4.3.2) as the reaction product showed lower molecular weight bands suggesting cleavage of high molecular weight molecules. Resin from processes E and F showed comparatively increased tensile stress and Young's modulus values as compared to other processes and this can be attributed to use of analytical grade rutin and quercetin in processes E and F respectively. Processes A, B, C and D were carried out using rutin from dietary supplements and other additives in the dietary supplement might have behaved as defects in the resin resulting in lower tensile stress and Young's modulus. Decrease in tensile strain for processes E and F indicates possibility of higher cross-linking and absence of any plasticization effects of

additives in dietary supplements which might have been present in processes A, B, C and D

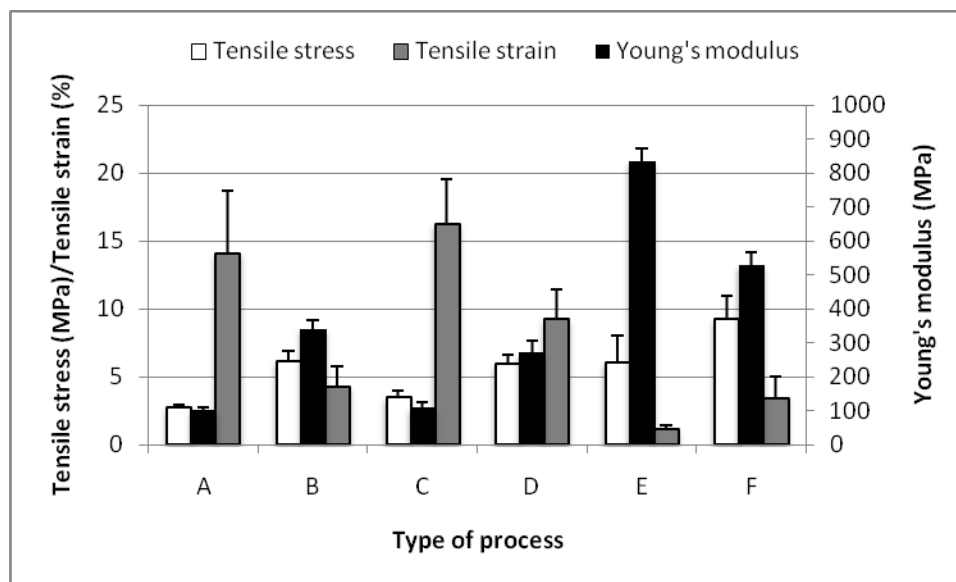


Figure 4.25 Mean and standard deviation of tensile stress, tensile strain and Young's modulus values of rutin and quercetin cross-linked SF-based resin using different process conditions

4.3.2. SDS-PAGE Analysis

Pure soy protein was analyzed using SDS-PAGE for distribution of proteins and the gel is shown in Figure 4.26 with the 10 lanes numbered. The clear portion and the hazy part of SPI solution (SPI in 0.3 M tris-HCl solution) were used for this analysis and the pure protein was separated using TCA precipitation. The molecular weight marker shows brighter bands at 20 kDa and 50 kDa. Each band in MW marker above 50 kDa corresponds to an increase of 10 kDa. Soy protein showed molecular weight of up to 120 kDa. The soy protein samples cross-linked with rutin and

quercetin were evaluated to study the protein molecule distribution on SDS-PAGE and these are shown in Figures 4.27 and 4.28 with the 12 lanes numbered.

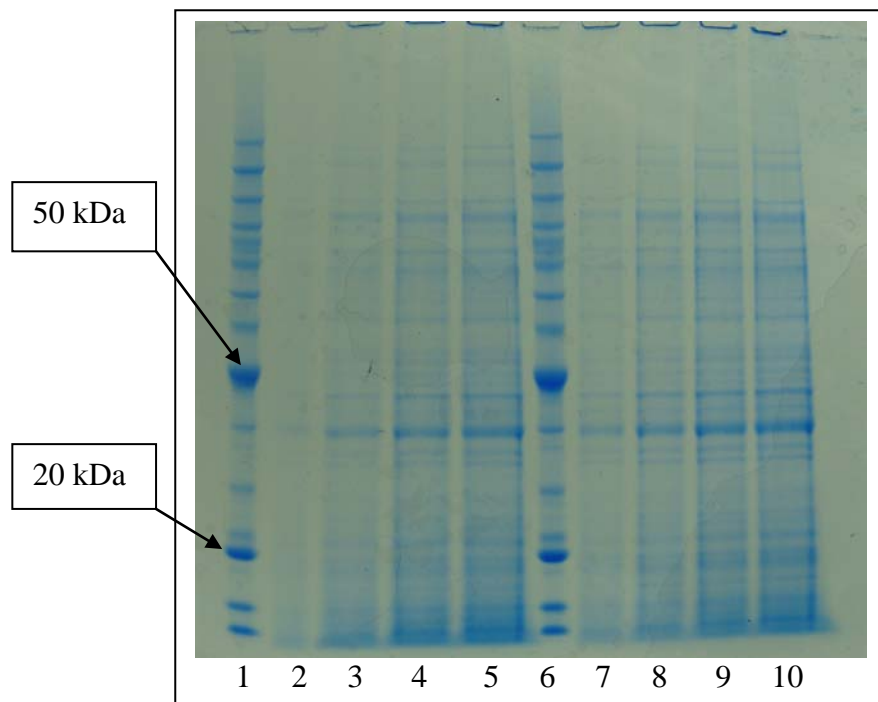


Figure 4.26 SDS-PAGE of unmodified soy protein showing molecular weight markers and soy protein profile

Table 4.17 Contents corresponding to lane numbers in Figures 4.26, 4.27 and 4.28

Lane	Contents of gel in Figure 4.44	Contents of gel in Figure 4.45	Contents of gel in Figure 4.46
1	MW Marker	MW Marker	MW Marker
2	SPI-5µl	SPI-10 µl	SPI-5 µl
3	SPI-10µl	SPI + Rutin (120 min 80°C)-10µl	SPI + Rutin (40 min 80°C + 80 min R.T.)-5 µl
4	SPI-15µl	SPI + Quercetin (120 min 80°C)-10µl	SPI + Quercetin (40 min 80°C + 80 min R.T.)-5 µl
5	SPI-20µl	SPI + Rutin (40 min 80°C)-10µl	SPI-20 µl
6	MW Marker	SPI + Rutin (40 min 80°C + 80 min R.T.)-10µl	SPI + Rutin (40 min 80°C + 80 min R.T.)-20 µl
7	SPI Hazy-5µl	SPI + Rutin (120 min R.T.)-10µl	SPI + Quercetin (40 min 80°C + 80 min R.T.)-20 µl
8	SPI Hazy-10µl	MW Marker	MW Marker
9	SPI Hazy-15µl	SPI-20µl	EMPTY
10	SPI Hazy-20µl	SPI + Rutin (120 min 80°C)-20µl	SPI-15 µl
11	--	SPI + Rutin (40 min 80°C)-20µl	SPI + Rutin (40 min 80°C + 80 min R.T.)-15 µl
12	--	SPI + Rutin (120 min R.T.)-20µl	SPI + Quercetin (40 min 80°C + 80 min R.T.)-15 µl

Each lane on the SDS-PAGE is loaded with a predetermined volume of desired solution and the compositions and their volumes corresponding to lanes 1 and 8 contain molecular weight markers and bands for 20 kDa and 50 kDa are indicated. Figures 4.26, 4.27 and 4.28 are listed in Table 4.17. In Figure 4.27, the bands around 25-30 kDa which is present in glycinin fraction of soy protein disappears in lane 11 and 12. Pure glycinin fraction of soy protein does not show bands above 120 kDa, but lanes 11 and 12 (rutin cross-linked soy protein) show staining above 120 kDa. However, the protein profile of rutin and quercetin (lane 4) cross-linked soy protein has smudgy appearance which could be attributed to residual chemicals from the cross-linking reaction. It could also have been due to the use of rutin and quercetin in the form of dietary supplements which could have other chemicals that interfere with SDS-PAGE analysis. The molecular weight distribution indicates that lower bands around 25-30 kDa have disappeared and appearance of higher molecular weight bands indicate a certain degree of cross-linking in soy protein due to reaction between soy protein and rutin.

In Figure 4.28, lane 1 contains the molecular weight marker and the bands for 20 kDa and 50 kDa are indicated. Lane 10 contains un-reacted soy protein and lower molecular weight bands for soy protein in lane 10 disappear in lane 11 and 12 which contain cross-linked soy protein. The lower molecular weight bands disappear in cross-linked soy protein and there is slight staining of high molecular weight bands in lanes 11 and 12 which might indicate higher molecular weight protein molecules due to cross-linking to lower molecular weight protein molecules. Lane 10 does not show any staining in high molecular weight region indicating absence of higher molecular weight protein molecules in un-reacted soy protein. Lanes 11 and 12 contain soy protein cross-linked with analytical grade rutin and quercetin respectively and the protein profile is comparatively sharp to gel in Figure 4.27.

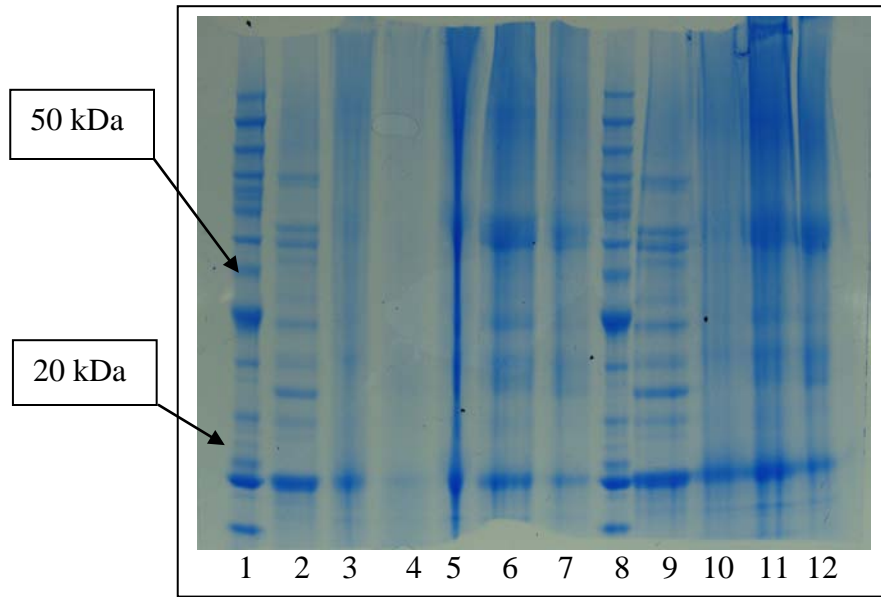


Figure 4.27 SDS-PAGE of unmodified and reacted soy proteins

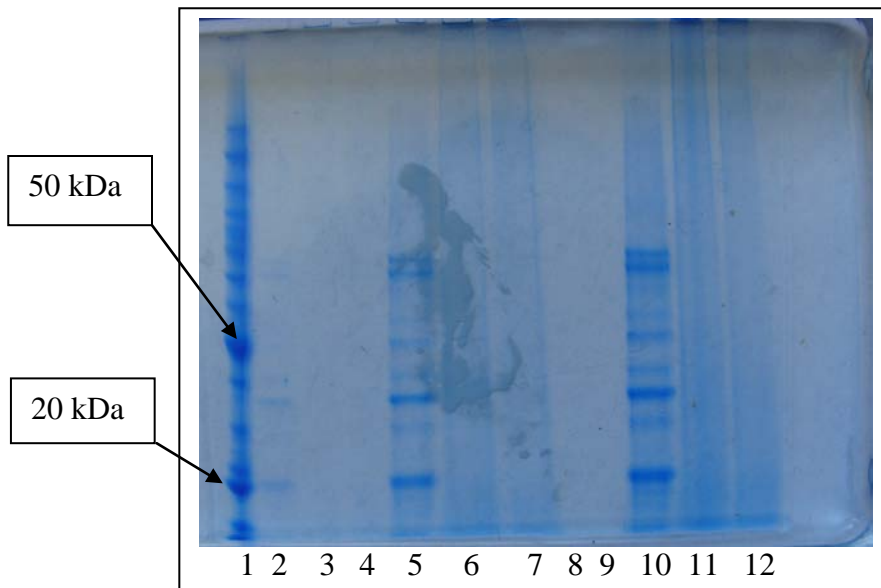


Figure 4.28 SDS-PAGE of unmodified and reacted soy proteins

4.4 Evaluation of Biodegradability of Soy Flour Resins

4.4.1. Weight Loss of SF-based Resin Films

This section discusses the behavior of three different types of specimens, control, glutaraldehyde cross-linked resin (GA) and rutin cross-linked resin in compost medium. The weight loss of specimens in compost medium is shown in Figure 4.29. The photographic images of control, GA and rutin cross-linked resins composted for 0, 30 and 60 days are shown in Figures 4.30 to 4.33. Effect of GA and rutin cross-linking of SF on biodegradability was characterized.

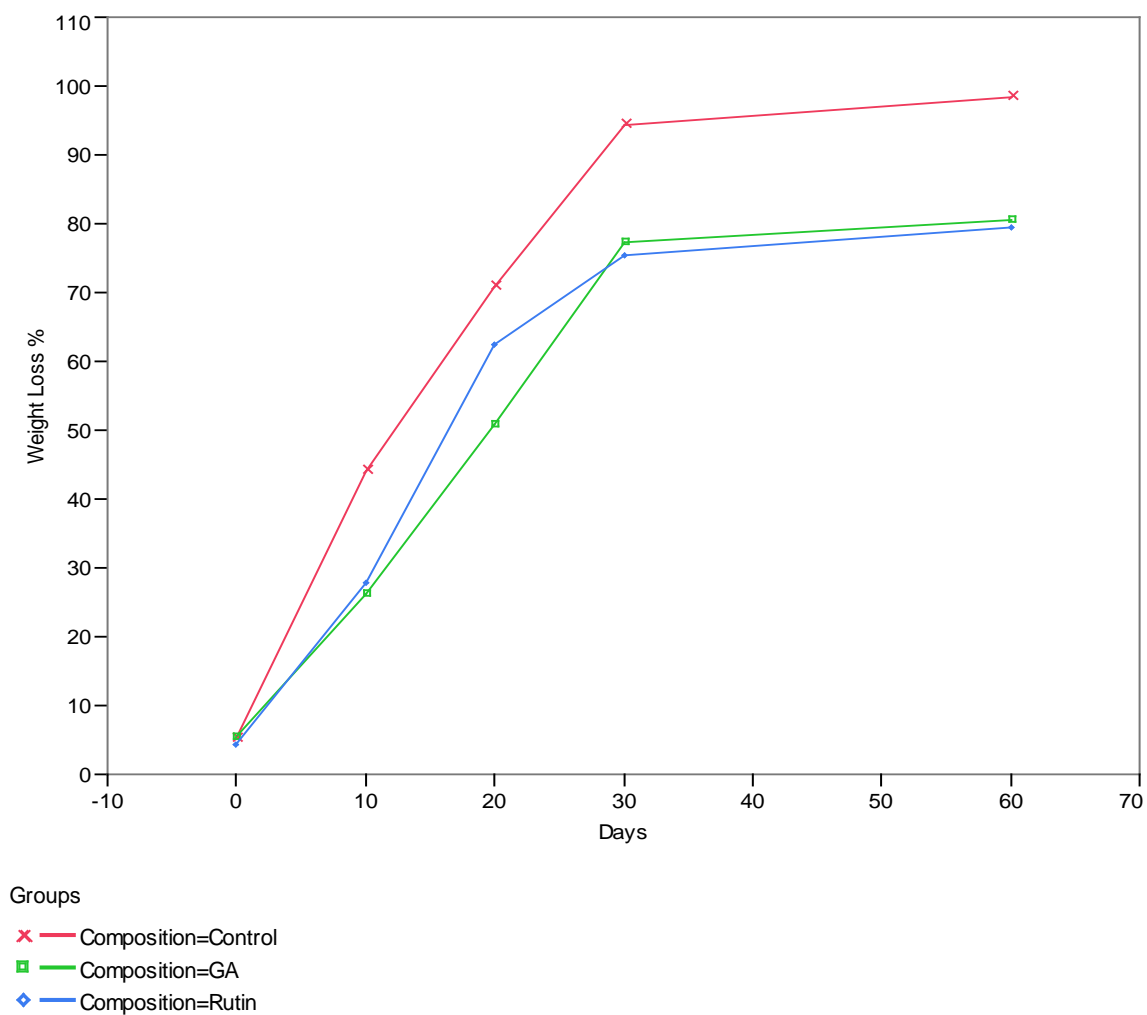


Figure 4.29 'Weight loss' x 'days' plot of compost specimens

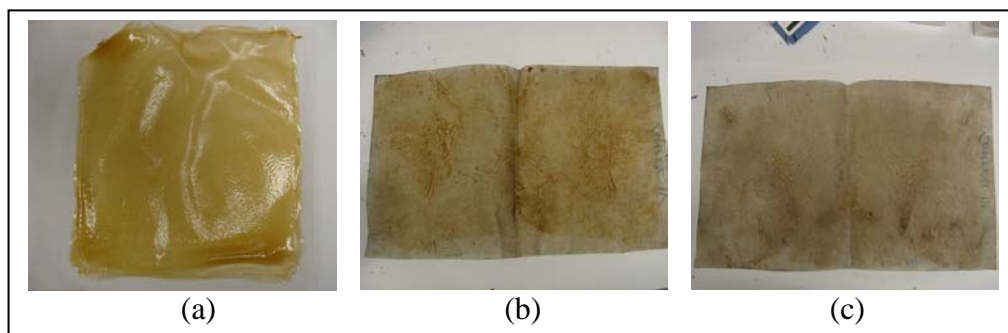


Figure 4.30 Photographic images of control specimen on (a) day 1; (b) day 30 and (c) day 60 of compost study

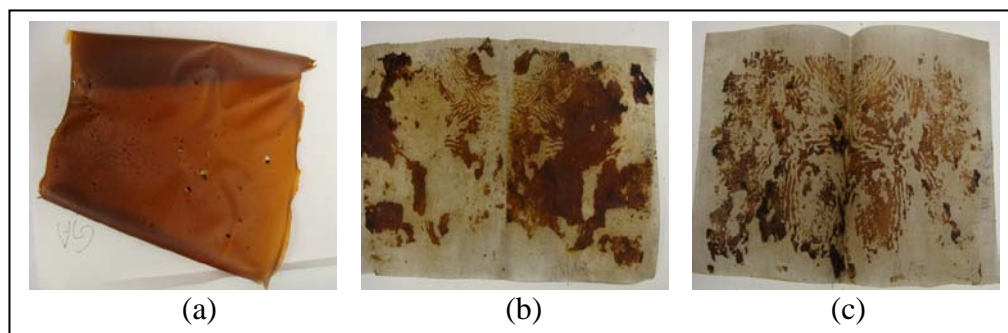


Figure 4.31 Photographic images of GA specimen on (a) day 1; (b) day 30 and (c) day 60 of compost study

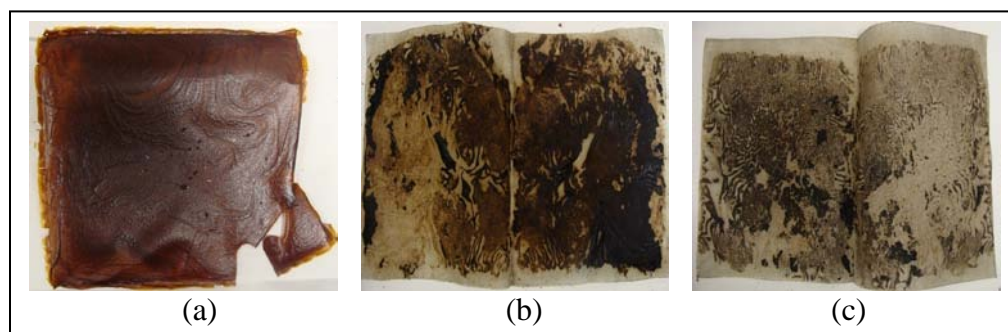


Figure 4.32 Photographic images of rutin specimen on (a) day 1; (b) day 30 and (c) day 60 of compost study

As seen in Figure 4.30, there is almost no trace of control specimen on the polypropylene bag at the end of 30 days of composting and there was no visible trace at the end of 60 days. On the other hand, glutaraldehyde cross-linked (GA) resin was degraded but not completely at the end of 30 days of composting as seen in Figure 4.31. At the end of 60 days of composting, GA resin was still found on the polypropylene bag. Similarly pieces of rutin cross-linked resin were found at the end of 30 days of composting sticking to the polypropylene bag as seen in Figure 4.32. There was progression of degradation of rutin cross-linked resin, but pieces of resin were found attached to the polypropylene bag at the end of 60 days of composting.

The control specimen lost half of its weight in first 10 days and lost 98% of its weight in 60 days. Glutaraldehyde modified resin (GA) and rutin cross-linked resin specimens lost about half of their weight in 20 days. The initial loss is due to leaching of glycerol. The degradation of resin samples is due to the activity of actinomycetes, fungi and mesophilic microorganisms^[40]. Cross-linking led to increased moisture resistance and low moisture absorption meant lower sites for attack by microorganisms^[40]. Therefore, cross-linked samples are attacked at a lower rate than control resin specimens. This is further supported by Figure 4.30 that shows no resin was left for control sample, but Figure 4.31 and 4.32 show that glutaraldehyde and rutin cross-linked SF-based resins were not completely degraded and part of the films still remained. It shows that cross-linking can increase the life of the resin. Rutin cross-linked resin showed weight loss behavior similar to GA samples supporting the earlier study of cross-linking of SF-resin using rutin. At the end of 60 days of composting, glutaraldehyde cross-linked specimen showed 80.45% weight loss and rutin cross-linked specimen showed 79.46% weight loss compared to 98.32% weight loss for control specimen.

4.4.2. ATR-FTIR Characterization

The chemical changes resulted on the surface due to composting was evaluated using ATR-FTIR. Pure glycerol FTIR spectrum (not shown) showed five absorption peaks corresponding to C-C and C-O groups in the wave number range of 800 cm^{-1} to 1150 cm^{-1} . The ATR-FTIR spectrum of control, GA and rutin specimens in Figures 4.33, 4.34 and 4.35 showed five peaks at 850 cm^{-1} , 900 cm^{-1} , 925 cm^{-1} , 1045 cm^{-1} and 1117 cm^{-1} with the first three peaks corresponding to C-C skeletal vibrations, fourth peak corresponding to C-O stretch at C^1 and C^2 and the fifth peak corresponding to C-O stretch at C^2 . The disappearance of these peaks in the spectra in all the three specimens indicates that glycerol has leached out during composting. The disappearance of peaks is supported by initial weight loss observed in the resins as shown in Figure 4.29.

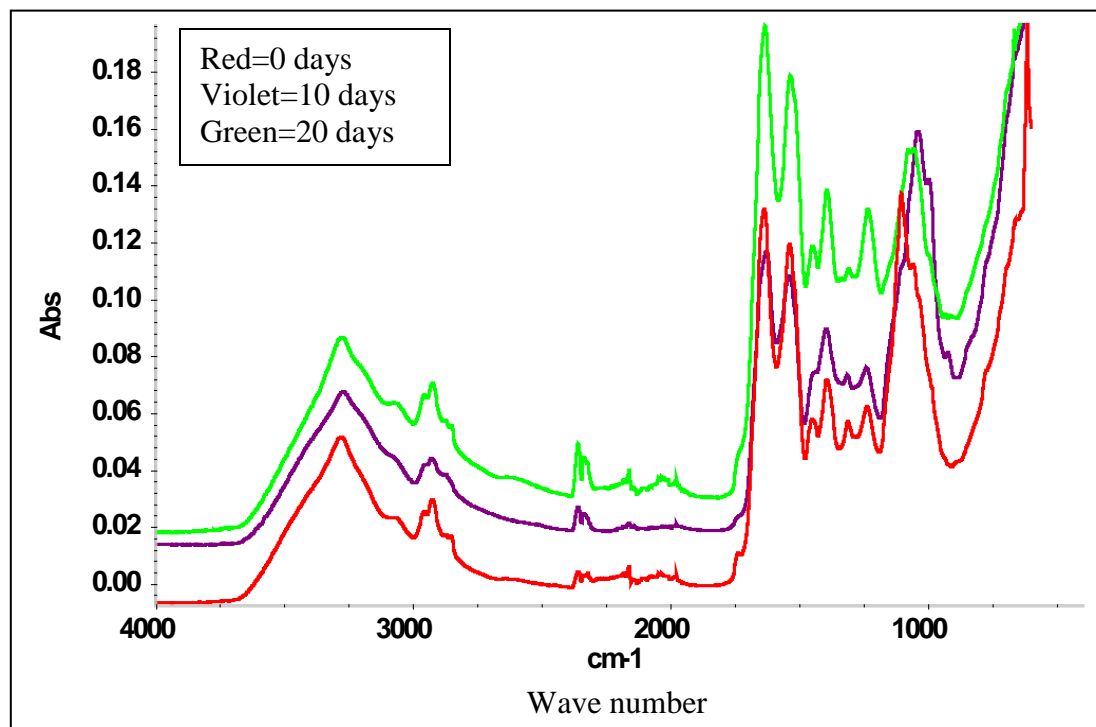


Figure 4.33 FTIR spectra of control specimens

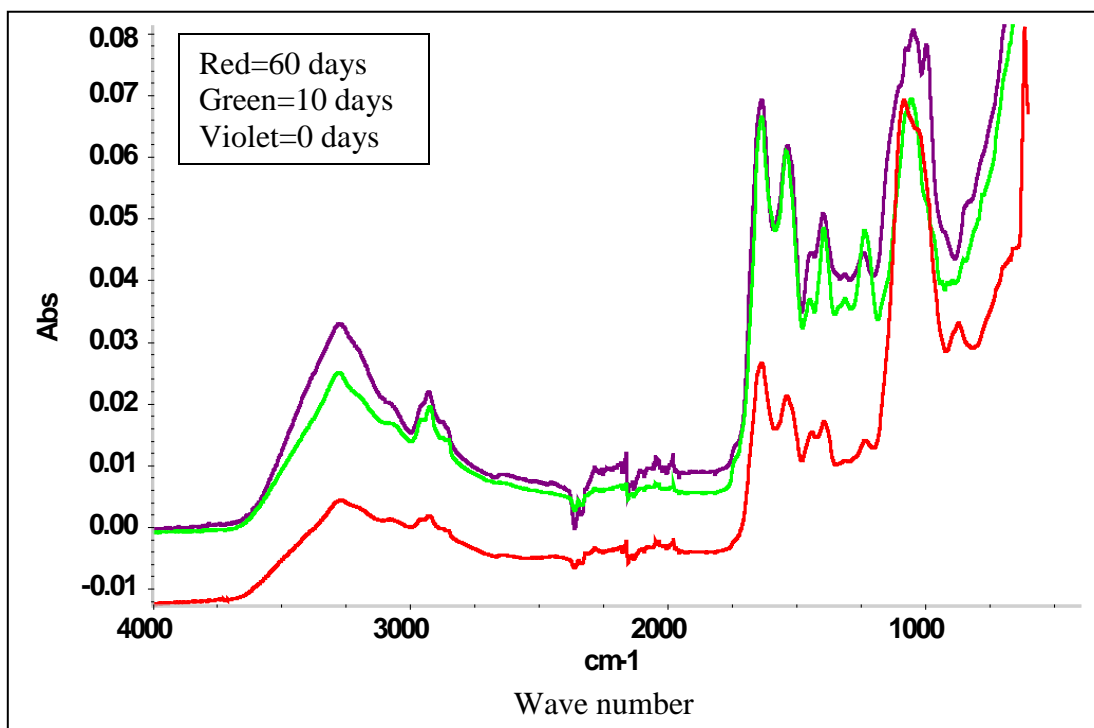


Figure 4.34 FTIR spectra of glutaraldehyde cross-linked soy protein resin specimens

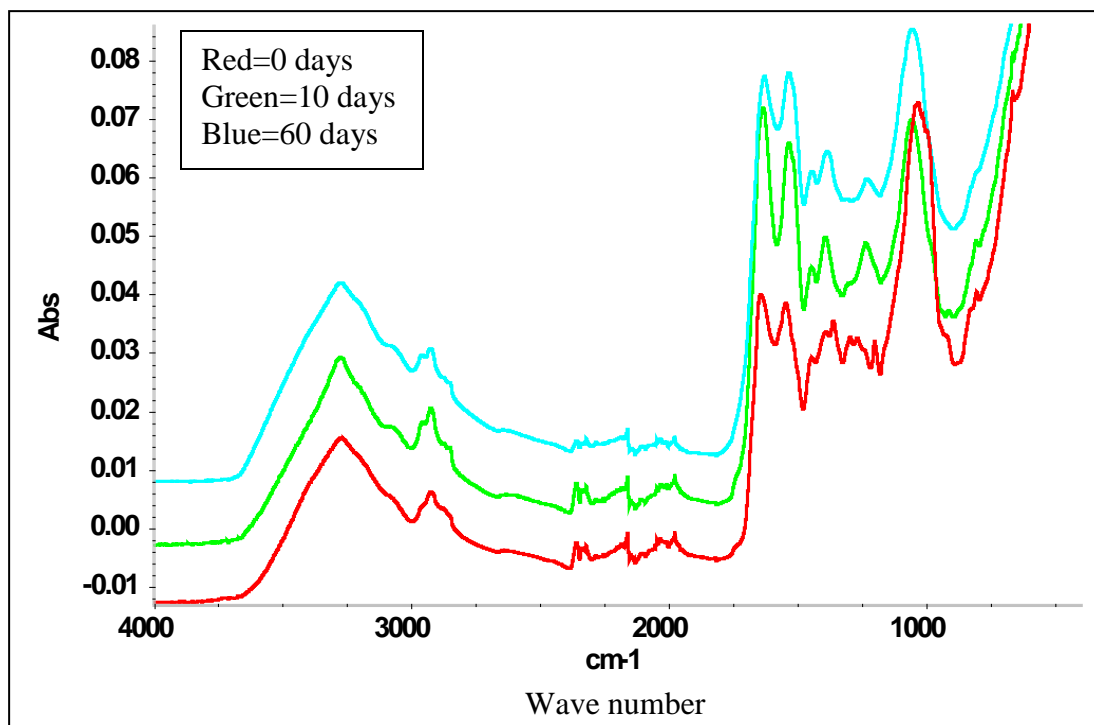


Figure 4.35 FTIR spectra of rutin cross-linked soy protein resin specimens

The ATR-FTIR spectra of all three specimens on 0 day showed two strong peaks in the 1480-1570 cm^{-1} and 1600-1700 cm^{-1} wave number range which correspond to the carbonyl groups in the amide linkages. The biodegraded resins showed reduction in the intensity of these two peaks and also in broad hydroxyl peak corresponding to water and amino groups in the 3200-3400 cm^{-1} range. Reduction in intensity suggests hydrolysis of amide linkages on the surface. The amide linkages could be cleaved under acidic conditions in composting conditions^[94]. In Figure 4.34, there is reduction in the intensity of two broad carbonyl peaks due to water and amine groups in the 3200 to 3400 cm^{-1} range. Reduction in intensity of these carbonyl peaks indicates hydrolysis of the amide linkages on the surface of the resin. The pH was acidic throughout this compost study. The presence of water in the compost system causes the byproducts to be leached out and therefore, not all byproducts can be retrieved with the resin sheet and do not show up on FTIR spectra.

CHAPTER 5

CONCLUSIONS

The objective of this research was to develop SF-based biodegradable fibers and resins for soil stabilization and crop protection and use eco-friendly cross-linkers to cross-link the soy protein. The conclusions drawn from the experimental and theoretical analyses are as follows:

1. Unmodified SF-based fibers showed tensile stress of 2.25 MPa, tensile strain of 2.4% and Young's modulus of 172.69 MPa.
2. SF-based fiber with diameter range 250-350 μm could be extruded using the fabricated lab scale extruder.
3. Incorporation on micro-fibrillated cellulose (MFC) increased the tensile properties of SF-based fibers. Orientation of fibrils during extrusion contributed to the increase in properties.
4. Field trials indicate that the SF-based fibers are completely biodegradable. SF-based fibers can be completely biodegraded in 3 weeks in wet environment. SF-based fibers are effective in adhering to soil and can be dimensionally stable.
5. Compost studies and SDS-PAGE analysis indicate that cross-linking has taken place due to reaction of rutin with polypeptide chains in soy protein. The behavior of rutin modified SF resin was similar to glutaraldehyde modified SF resin.
6. Field and greenhouse trials show that light application of SF composition containing NB416 fibers and linseed oil is useful in soil stabilization and crop protection and is comparable to the commercially available hydromulch.

7. Heavy application of SF composition with linseed oil and NB416 can be used for weed suppression and protection of seeds from natural elements like wind and rain.

The development of biodegradable fibers for soil stabilization is significant as it can replace non-biodegradable materials in application requiring similar strength as offered by the SF-based fibers. More research is required to increase the tensile properties of SF-based fibers and to tune them for other applications. Use of bioflavanoids (polyphenols) as eco-friendly cross-linking agents can be improved with further research. Preliminary tests for use of SF-based resin for crop protection and soil stabilization have shown great promise and with further research can be made more effective for use in fields and marginal lands.

REFERENCES

1. Huang SJ. Polymer waste management–biodegradation, incineration, and recycling. In: Albertsson AC, Huang SJ, editors. Degradable Polymers, Recycling, and Plastics Waste Management, New York: Marcel Dekker; 1995.
2. Peijs T. Composites turn green e-Polymers. 2002;T 002:2002,1-12.
3. Lodha P, Netravali AN. Characterization of phytigel® modified soy protein isolate resin and unidirectional flax yarn reinforced "green" composites. Polymer Composites. 2005;26(5):647-59.
4. Lodha P, Netravali AN. Characterization of stearic acid modified soy protein isolate resin and ramie fiber reinforced 'green' composites. Composites Sci Technol. 2005 6;65(7-8):1211-25.
5. Lodha P, Netravali AN. Characterization of interfacial and mechanical properties of "green" composites with soy protein isolate and ramie fiber J Mater Sci. 2002 09/01;37(17):3657-65.
6. Chabba S, Netravali A. Green composites part 1: Characterization of flax fabric and glutaraldehyde modified soy protein concentrate composites. J Mater Sci. 2005 12/17;40(23):6263-73.
7. Chabba S, Netravali A. Green composites part 2: Characterization of flax yarn and glutaraldehyde/poly(vinyl alcohol) modified soy protein concentrate composites. J Mater Sci. 2005 12/17;40(23):6275-82.

8. Nakagaito AN, Iwamoto S, Yano H. Bacterial cellulose: The ultimate nano-scalar cellulose morphology for the production of high-strength composites. *Appl Phys A*. 2005 01;80(1):93-7.
9. S. Nam. Environment-friendly 'Green' composites using ramie fibers and soy protein concentrate (SPC) polymer [dissertation]. Ithaca, NY: Cornell University; 2002.
10. Salmoral EM, Gonzalez ME, Mariscal MP, Medina LF. Comparison of chickpea and soy protein isolate and whole flour as biodegradable plastics. *Industrial Crops and Products*. 2000 3;11(2-3):227-36.
11. Rhim J, Gennadios A, Weller CL, Carole Cezeirat, Hanna MA. Soy protein isolate–dialdehyde starch films. *Industrial Crops and Products*. 1998 9;8(3):195-203.
12. Netravali AN, Chabba S. Composites get greener. *Materials Today*. 2003;6(4): 22-9.
13. Ramankutty N, Foley JA, Olejniczak NJ. People on the land: Changes in global population and croplands during the 20th century. *AMBIO: A Journal of the Human Environment*. 2002 /5/1;31(3):251-7.
14. Ramankutty N, Foley JA, Norman J, McSweeney K. The global distribution of cultivable lands: Current patterns and sensitivity to possible climate change. *Global Ecology & Biogeography*. 2002;11(5):377-92.
15. Soil management: Experimental basis for sustainability and environmental quality. Lal, R. Stewart, B. A. (Bobby Alton), 1932-, editor. Boca Raton: Lewis Publishers; 1995.

16. Tilman D, Cassman KG, Matson PA, Naylor R, Polasky S. Agricultural sustainability and intensive production practices. *Nature*. 2002 08/08;418(6898):671-7.
17. Matson PA, Naylor R, Ortiz-Monasterio I. Integration of environmental, agronomic, and economic aspects of fertilizer management. *Science*. 1998 April 3;280(5360):112-5.
18. Naylor RL. Energy and resource constraints on intensive agricultural production. *Annu Rev Energy Environ*. 1996 11/01;21(1):99-123.
19. Lodha P. Green composites with soy protein isolate resin and ramie fiber [dissertation]. Ithaca, NY: Cornell University; 2001.
20. Lodha P, Netravali AN. Thermal and mechanical properties of environment-friendly 'green' plastics from stearic acid modified-soy protein isolate. *Industrial Crops and Products*. 2005 1;21(1):49-64.
21. Nam S, Netravali AN. Characterization of ramie fiber/soy protein concentrate (SPC) resin interface. *Journal of Adhesion Science & Technology*. 2004;18(9):1063-76.
22. Paetau I. Biodegradable plastics made from soy protein [dissertation]. Ames, Iowa: Iowa State University; 1993.
23. Vaz CM, Mano JF, Fossen M, van Tuil RF, de Graaf LA, Reis RL, et al. Mechanical, dynamic-mechanical, and thermal properties of soy protein-based thermoplastics with potential biomedical applications. *Journal of Macromolecular Science, Part B: Physics*. 2002 [cited May 31, 2009];41(1):33-46.

24. Kumar R, Choudhary V, Mishra S, Varma IK, Mattiason B. Adhesives and plastics based on soy protein products. *Industrial Crops and Products*. 2002 11;16(3):155-72.
25. A.K. Bledzki, J. Gassan. Composites reinforced with cellulose based fibres. *Progress in Polymer Science*. May 1999;24:221,274(54).
26. H.P. Fink, P. Weigel, H.J. Purz, J. Ganster. Structure formation of regenerated cellulose materials from NMMO-solutions. *Progress in Polymer Science*. November 2001;26:1473,1524(52).
27. Lee SM, Cho D, Park WH, Lee SG, Han SO, Drzal LT. Novel silk/poly(butylene succinate) biocomposites: The effect of short fibre content on their mechanical and thermal properties. *Composites Sci Technol*. 2005 3;65(3-4):647-57.
28. Bond EB. Fiber spinning behavior of a 3-hydroxybutyrate/3-hydroxyhexanoate copolymer. *Macromolecular Symposia*. 2003;197(1):19-32.
29. Netravali AN, Xiaosong Huang, Mizuta KT. Advanced 'green' composites. ;16:269-82.
30. Endres JG. Soy protein products: Characteristics, nutritional aspects and utilization In: Endres JG, editor. Champaign, IL: AOCS Press; 2001. p. 4-18.
31. Liu K. Soybeans-chemistry, technology and utilization Liu K, editor. Florence, KY: International Thomson Publishing; 1997.
32. Lusas EW, Rhee KC. Soybean protein processing and utilization. In: Erickson DR, editor. Practical handbook of soybean processing and utilization. Champaign, IL: AOCS Press ; St. Louis, Mo. : United Soybean Board, c1995.; 1995. p. 584.

33. Food and agriculture organization of the united nations. Food energy – methods of analysis and conversion factors 2003. Report No.: 2003.
34. Ly YTP, Johnson LA, Jane J. Biopolymers from renewable resources. Kaplan DL, editor. New York: Springer; 1998.
35. Cheftel JC, Cuq JL, Lorient D. Food chemistry. Fennema OR, editor. New York: Dekker; 1985.
36. Creighton TE. Proteins: Structure and molecular properties. Creighton TE, editor. New York: Freeman; 1993.
37. Recent advances in polymers and composites. Mathur GN, Kandpal LD, Sen AK, editors. New Delhi, India: Allied Publishers; 2000.
38. Lodha P, Netravali AN. In: Proceedings of the international conference on composites engineering-7 Denver: ; 2000. p. 655.
39. Nam S. Environment-friendly "green" biodegradable composites using ramie fibers and soy protein concentrate (SPC) polymer [dissertation]. Ithaca, NY: Cornell University; 2002.
40. Lodha P. Fundamental approaches to improving performance of soy protein isolate based 'green' plastics and composites [dissertation]. Ithaca, NY: Cornell University; 2004.
41. Yamamoto Y. Engineered 'green' composites using kenaf and bamboo fibers with modified soy protein resin [dissertation]. Ithaca, NY: Cornell University; 2006.
42. Mo X, Sun X. Plasticization of soy protein polymer by polyol-based plasticizers. J Am Oil Chem Soc. 2002 02/01;79(2):197-202.

43. Wang S, Sue H-, Jane J. Effects of polyhydric alcohols on the mechanical properties of soy protein plastics. *Journal of Macromolecular Science, Part A: Pure and Applied Chemistry*. 1996 [cited June 22, 2009];33(5):557.
44. Monick JA. *Alcohols: Their chemistry, properties, and manufacture*. New York: Reinhold Book Corp.; 1968.
45. Chabba S, Matthews GF, Netravali AN. 'Green' composites using cross-linked soy flour and flax yarns. *Green Chem*. 2005;7(8):576-81.
46. Rhim JW, Gennadios A, Handa A, Weller CL, Hanna MA. Solubility, tensile, and color properties of modified soy protein isolate films†. *J Agric Food Chem*. 2000 10/01;48(10):4937-41.
47. Dicharry RM, Ye P, Saha G, Waxman E, Asandei AD, Parnas RS. Wheat Gluten–Thiolated poly(vinyl alcohol) blends with improved mechanical properties. *Biomacromolecules*. 2006;7(10):2837-44.
48. Yvonne M. Stuchell JMK,. Enzymatic treatments and thermal effects on edible soy protein films. *J Food Sci*. 1994;59(6):1332-7.
49. Huang X, Netravali AN. Characterization of nano-clay reinforced phytagel-modified soy protein concentrate resin. *Biomacromolecules*. 2006 10/01;7(10):2783-9.
50. Huang X. Preparation and investigation of soy protein based environment friendly plastics and composites [dissertation]. Ithaca, NY: Cornell University; 2007.
51. Rathi P. Soy protein based nanophase resins for green composites [dissertation]. Ithaca, NY: Cornell University; 2007.

52. Gan C, Latiff AA, Cheng L, Easa AM. Gelling of microbial transglutaminase cross-linked soy protein in the presence of ribose and sucrose. *Food Res Int.* 2009 12;42(10):1373-80.
53. Tanimoto SY, Kinsella JE. Enzymic modification of proteins: Effects of transglutaminase cross-linking on some physical properties of .beta.-lactoglobulin. *J Agric Food Chem.* 1988 03/01;36(2):281-5.
54. Gan C, Cheng L, Easa AM. Physicochemical properties and microstructures of soy protein isolate gels produced using combined cross-linking treatments of microbial transglutaminase and maillard cross-linking. *Food Res Int.* 2008 7;41(6):600-5.
55. Xi D, Yang C, Liu X, Chen M, Sun C, Xu Y. Graft polymerization of styrene on soy protein isolate. *J Appl Polym Sci.* 2005;98(3):1457-61.
56. Doner LW, Douds DD. Purification of commercial gellan to monovalent cation salts results in acute modification of solution and gel-forming properties. *Carbohydr Res.* 1995 8/25;273(2):225-33.
57. Banik RM, Kanari B, Upadhyay SN. Exopolysaccharide of the gellan family: Prospects and potential. *World Journal of Microbiology and Biotechnology.* 2000 07/01;16(5):407-14.
58. Chandrasekaran R, Thailambal VG. The influence of calcium ions, acetate and -glycerate groups on the gellan double-helix. *Carbohydr Polym.* 1990;12(4):431-42.
59. Nakajima K, Ikehara T, Nishi T. Observation of gellan gum by scanning tunneling microscopy. *Carbohydr Polym.* 1996 7;30(2-3):77-81.

60. Klemperner D, Sperling LH, Utracki LA. Interpenetrating polymer networks In: Sperling LH, editor. Interpenetrating polymer networks: an overview. Washington, DC: American Chemical Society; 1994. p. 3-38.
61. Chtourou H, Riedl B, Ait-Kadi A. Reinforcement of recycled polyolefins with wood fibers. *Journal of Reinforced Plastics and Composites*. 1992 April 1;11(4): 372-94.
62. V. Favier, J. Y. Cavaille, G. R. Canova, S.C. Shrivastava, . Mechanical percolation in cellulose whisker nanocomposites. *Polymer Engineering & Science*. 1997; 37(10): 1732-9.
63. Nakagaito AN, Yano H. Novel high-strength biocomposites based on microfibrillated cellulose having nano-order-unit web-like network structure. *Appl Phys A*. 2005 01;80(1):155-9.
64. Nakagaito AN, Yano H. The effect of morphological changes from pulp fiber towards nano-scale fibrillated cellulose on the mechanical properties of high-strength plant fiber based composites. *Appl Phys A*. 2004 03;78(4):547-52.
65. Okubo K, Fujii T, Yamashita N. Improvement of interfacial adhesion in bamboo polymer composite enhanced with micro-fibrillated cellulose. *JSME International Journal Series A Solid Mechanics and Material Engineering*. 2005;48(4):199-204.
66. Hao Y, Peng J, Li J, Zhai M, Wei G. An ionic liquid as reaction media for radiation-induced grafting of thermosensitive poly (N-isopropylacrylamide) onto microcrystalline cellulose. *Carbohydr Polym*. 2009 7/19;77(4):779-84.

67. Capadona JR, Shanmuganathan K, Trittschuh S, Seidel S, Rowan SJ, Weder C. Polymer nanocomposites with nanowhiskers isolated from microcrystalline cellulose. *Biomacromolecules*. 2009 04/13;10(4):712-6.
68. Cherblanc F, Boscus J, Bénet J. Electro-osmosis in gels: Application to agar-agar. *Comptes Rendus Mécanique*. 2008 10;336(10):782-7.
69. Wang W, Wang A. Preparation, characterization and properties of superabsorbent nanocomposites based on natural guar gum and modified rectorite. *Carbohydr Polym*. 2009 7/19;77(4):891-7.
70. Gupta S, Shah B, Sanyal B, Variyar PS, Sharma A. Role of initial apparent viscosity and moisture content on post irradiation rheological properties of guar gum. *Food Hydrocoll*. 2009 10;23(7):1785-91.
71. Zhu J, Yang X, Ahmad I, Jiang Y, Wang X, Wu L. Effect of guar gum on the rheological, thermal and textural properties of soybean β -conglycinin gel. *Int J Food Sci Tech*. 2009;44(7):1314-22.
72. Otaigbe J, Adams D. Bioabsorbable soy protein plastic composites: Effect of polyphosphate fillers on water absorption and mechanical properties. *Journal of Polymers and the Environment*. 1997 10/06;5(4):199-208.
73. Zhang J, Mungara P, Jane J. Mechanical and thermal properties of extruded soy protein sheets. *Polymer*. 2001 3;42(6):2569-78.
74. Zhong Z, Sun XS. Properties of soy protein isolate/polycaprolactone blends compatibilized by methylene diphenyl diisocyanate. *Polymer*. 2001 7;42(16):6961-9.
75. Mizuno A, Mitsuiki M, Motoki M. Effect of transglutaminase treatment on the glass transition of soy protein. *J Agric Food Chem*. 2000 08/01;48(8):3286-91.

76. Rhim JW, Lee JH, Kwak HS. Mechanical and water barrier properties of soy protein and clay mineral composite films. *Food Sci Biotechnol.* 2005;14:112-6.
77. Marquie C. Chemical reactions in cottonseed protein cross-linking by formaldehyde, glutaraldehyde, and glyoxal for the formation of protein films with enhanced mechanical properties. *J Agric Food Chem.* 2001 10/01;49(10):4676-81.
78. Vaz CM, de Graaf LA, Reis RL, Cunha AM. In vitro degradation behaviour of biodegradable soy plastics: Effects of crosslinking with glyoxal and thermal treatment. *Polym Degrad Stab.* 2003;81(1):65-74.
79. Strauss G, Gibson SM. Plant phenolics as cross-linkers of gelatin gels and gelatin-based coacervates for use as food ingredients. *Food Hydrocoll.* 2004 1;18(1):81-9.
80. Figueroa-Espinoza M, Morel M, Rouau X. Effect of lysine, tyrosine, cysteine, and glutathione on the oxidative cross-linking of feruloylated arabinoxylans by a fungal laccase. *J Agric Food Chem.* 1998 07/01;46(7):2583-9.
81. Figueroa-Espinoza MC, Morel M-, Surget A, Asther M, Moukha S, Sigoillot J-, et al. Attempt to cross-link feruloylated arabinoxylans and proteins with a fungal laccase. *Food Hydrocoll.* 1999 1/1;13(1):65-71.
82. Killham K. *Soil ecology.* Cambridge ; New York : Cambridge University Press, 1994.
83. Hart JF. Loss and abandonment of cleared farm land in the eastern united states. *Ann Assoc Am Geogr.* 1968;58(3):417-40.
84. Viswanadham BVS, König D. Centrifuge modeling of geotextile-reinforced slopes subjected to differential settlements. *Geotextiles Geomembranes.* 2009 4;27(2):77-88.

85. Chattopadhyay BC, Chakravarty S. Application of jute geotextiles as facilitator in drainage. *Geotextiles Geomembranes*. 2009 4;27(2):156-61.
86. Chattopadhyay BC, Chakravarty S. Containment of sulfate pollution in soil by natural geotextile from jute. *J Mat in Civ Engrg*. 2009 March 2009;21(3):128-32.
87. Smets T, Poesen J, Langhans C, Knapen A, Fullen MA. Concentrated flow erosion rates reduced through biological geotextiles. *Earth Surf Process Landforms*. 2009;34(4):493-502.
88. Vishnudas S, Savenije HHG, Van der Zaag P, Anil KR, Balan K. The protective and attractive covering of a vegetated embankment using coir geotextiles. *Hydrol Earth Syst Sci*. 2006;10:565-74.
89. Subaida EA, Chandrakaran S, Sankar N. Experimental investigations on tensile and pullout behaviour of woven coir geotextiles. *Geotextiles Geomembranes*. 2008 10;26(5):384-92.
90. Rawal A, Anandjiwala R. Comparative study between needlepunched nonwoven geotextile structures made from flax and polyester fibres. *Geotextiles Geomembranes*. 2007 2;25(1):61-5.
91. Verdu AM, Mas MT. Mulching as an alternative technique for weed management in mandarin orchard tree rows. *Agron.Sustain.Dev*. 2007 nov,;27(4):367-75.
92. Comis D. Cotton bests other spray-on erosion-control mulches. *Agricultural Research*. 2009:22-3.
93. Luo S, Netravali AN. A study of physical and mechanical properties of poly(hydroxybutyrate-co-hydroxyvalerate) during composting. *Polym Degrad Stab*. 2003;80(1):59-66.

94. Lodha P, Netravali AN. Effect of soy protein isolate resin modifications on their biodegradation in a compost medium. *Polym Degrad Stab.* 2005 3;87(3):465-77.
95. TCA protein precipitation protocol [homepage on the Internet]. . 2001. Available from: http://www.its.caltech.edu/~bjorker/Protocols/TCA_ppt_protocol.pdf.
96. Wu S, Murphy PA, Johnson LA, Reuber MA, Fratzke AR. Simplified process for soybean glycinin and β -conglycinin fractionation. *J Agric Food Chem.* 2000 07/01;48(7):2702-8.
97. Huang X, Netravali AN. Environmentally friendly green materials from plant-based resources: Modification of soy protein using gellan and Micro/Nano-fibrillated cellulose. *Journal of Macromolecular Science, Part A.* 2008 [cited April 14, 2009];45(11):899-906.